PROBABILISTIC METHODS FOR ASSESSING THE PERFORMANCE OF OFFSHORE PIPELINES CONDITION MONITORING SYSTEMS

by

©Alireda Ahmed Aljaroudi,

B.Sc. Eng., M.Sc. Eng., and M. Eng.

A Thesis Submitted to the
School of Graduate Studies
in Partial Fulfillment of the Requirements
for the Degree of

Doctor of Philosophy

Faculty of Engineering and Applied Science
Memorial University of Newfoundland

OCTOBER 2015

St. John's Newfoundland Canada

ABSTRACT

Oil and gas condition monitoring systems play a major role in maintaining the operability, integrity, and reliability of oil and gas infrastructure. A leak detection monitoring system (LDS) constitutes an important member of these systems. The main function of this system is to detect the occurrence and location of hydrocarbon leakages in a timely manner before the leaked products can cause a devastating effect on production, health, safety, and the environment. To ensure the continuity of operation and the safety of personnel as well as the environment, this system should be assessed on a regular basis. Traditionally, a deterministic approach is adopted to assess such systems. A deterministic assessment does not consider uncertainties or random variabilities that are inherent in the performance parameters. Thus, it produces results that may not characterize the actual situation of the system or its circumstances. To tackle this issue, it is proposed to use a probabilistic approach to assess the performance since it allows the incorporation of any uncertainties or random variabilities that may exist in the assessment. Hence, a quantifiable probability of failure can be estimated. Once the probability and consequences of failure become known, risk can be easily estimated.

A complete assessment of risk cannot by obtained without incorporating the probability of failure of the pipeline itself. The major research activities include, formulation of the LDS probability of detection and false detection for a single point along the oil and gas transport component; development of a probabilistic performance assessment scheme for the entire LDS along the oil and gas transport component using a limit-state approach; application

of probabilistic methods to determine the probability of failure and the remaining life of the oil and gas transport component and development of a risk-based assessment methodology to determine the risk associated with the simultaneous failure of the LDS and the oil and gas transport component (i.e., pipelines). These major research components establish the foundation for an overall evaluation scheme that can be used to provide an up-to-date assessment of the oil and gas transport components and the LDS. The outcome of the assessment can serve as a basis for a well-informed decision-making process that enables the decision makers to determine the best strategy for assessing and maintaining the integrity of the evaluated systems.

Dedicated to:

my parents, my wife, and my children

ACKNOWLEDGEMENTS

I would like to express my thanks and appreciation to Dr. Faisal Khan, Dr. Ayhan Akinturk, Dr. Mahmoud Haddara, and Dr. Premkumar Thodi for their excellent guidance and support throughout the course of this research. Their outstanding supervision and encouragement strongly contributed to the success of this research.

They were accommodating, committed, forthcoming, and most of all they were open-minded to new research ideas. Their ongoing support and guidance played a major role in going forward with this research, leading to a successful completion despite difficulties and challenges that have been encountered along the way. I also, would like to thank the examiners for their valuable and constructive feedback.

Thanks and words of appreciation go to the Faculty of Engineering and Applied Science and the library staff at Memorial University of Newfoundland for providing the required support and assistance throughout the research period.

Likewise, thanks and sincere appreciation go to Petroleum Research Newfoundland & Labrador (PRNL) and Research & Development Corporation (RDC) of Newfoundland and Labrador for their financial support, which significantly helped in moving forward with the research. Finally, special thanks go to all members of my family, friends, and colleagues for their support and encouragement.

TABLE OF CONTENTS

LIST OF TABLES

Table Title Page No.

LIST OF FIGURES

Figure **Title** **Page No.**

LIST OF ABBREVIATIONS AND ACRONYMS

API	:	American Petroleum Institute
ASME	:	American Society of Mechanical Engineers
BS	:	British Standards
BSS	:	Brillouin Stimulated Scattering
COV	:	Coefficient of Variance
CW	:	Continuous Wave
LDS	:	Leak Detection System
LSF	:	Limit State Function
NP	:	Noise Power
PD	:	Probability of Detection
PFA	:	Probability of False Alarm
PMD	:	Probability of Missed Detection
SNR	:	Signal-to-Noise Ratio
SMYS	:	Specified Minimum Yield Strength
UTS	:	Ultimate Tensile Strength

LIST OF ENGLISH SYMBOLS

A	:	Metal Loss Estimated Area
$A1$	:	Leak Opening Cross Section Area – m^2
A_{eff}	:	Effective Area of the Fiber
$A_i(T)$	:	Measured Defect Area at Time T – mm
$A_O(T)$	:	Original Area Before Defect Has Occurred – mm
C	:	Speed of Light (km/s) in Vacuum
C_{DP}	:	Cost of Deferred Production
C_{Eco}	:	Total Cost Associated with Economic Consequences
C_{Env}	:	Total Cost Associated with Environmental Consequences
C_{LP}	:	Cost of Lost Production
Cof	:	Consequences of Failure
C_{oil}	:	Oil Price ($/Barrel)
C_T	:	Total Cost Associated with the Consequences of Failure
d	:	Location of the Temperature Change
$d(T)$	:	Measured Corrosion Depth at a Given Time T
d_c	:	Critical Corrosion Depth
$d_i(T)$	:	Measured Defect Depth at Time T – mm
$d_i(T_1)$	:	Estimated Cumulative Depth of Defect Corrosion *i* at the End of Interval 1 – mm
$d_i(T_n)$	:	Estimated Cumulative Depth of Defect Corrosion *i* at the End of Interval *n* – mm
d_o	:	Estimated Initial Corrosion Depth

d_{rate}	:	Corrosion Annual Growth Rate (mm/year)
$dP/_{d\varepsilon}$	:	Strain Coefficient (mW/με)
$dP/_{dT}$	:	Temperature Coefficient (mW/^{o}C)
g_B	:	Gain
L	:	Load Imposed on the System
$L\,(T)$	:	Measured Corrosion Length at a Given Time T
L_{eff}	:	Effective Length of the Fiber
$L_i(T)$	:	Measured Defect Length at Time T – mm
L_o	:	Estimated Initial Corrosion Length
L_{rate}	:	Corrosion Length Rate
M	:	Folias Factor
N	:	Total Number of Simulation Trials
N_f	:	Number of Simulation Trials when LSF Becomes Less than Zero
$P_{B(measured)}$	:	Measured Brillouin Power
P_b	:	Burst Pressure
P_{CW}	:	Input Probe Power
P_f	:	Pressure Failure
$P_{fi}(T)$	:	Pressure Failure for Defect i at Time T – MPa
P_o	:	Operating Pressure of the Pipeline Segment – (N/m^2)
Pof	:	Probability of Failure
$Pof_i(T)$	:	Probability of Failure for Segment i
$Pof_n(T)$	:	Probability of Failure for Segment n

Pof_{Bursti}	:	Burst Failure Probability at a Flaw i
Pof_{Corri}	:	Corrosion Failure Probability at a Flaw i
Pof_{Ti}	:	Total Probability of Failure (Pof_T) at Each Time Interval for Each Flaw i
Pof_T	:	Total Probability of Failure
$Pof_{T\,(PL)}$	:	Overall Probability of Failure for the Entire Pipeline for All Flaws at a Given Time
P_P	:	Pulse Power
P_R	:	Reference Power
P_s	:	External Pressure Surrounding the Leaking Spot – (N/m^2)
P_{TX}	:	Pulse Transmission Time
Q	:	Leak Rate – Kg/s
Q_{DP}	:	Quantity of Deferred Production in Barrels/hour
Q_{LP}	:	Quantity of Lost Production in Barrels/hour
Q_T	:	Size of Oil Spill in Tonnes
R	:	Capacity (Resistance) of the System
$R.T$	:	Response Time
t	:	Pipe Wall Thickness, mm
T	:	Time
T_{DP}	:	Time Duration of the Deferred Production
t_F	:	Fiber Optic Cable Response Time
Th_a	:	Achievable Threshold
Th_s	:	Specified Minimum Detectable Change in Temperature

T_{LP}	:	Time Duration of the Lost Production in Hours
t_M	:	Measurement Time
$t_{operating}$	:	Operating Response Time at a Given Time
t_P	:	Processing Time
$t_{specified}$	:	Maximum Specified Response Time
$T - T_o$	:	Time Difference for the Two Measurements
V_a	:	Acoustic Velocity
Xth	:	Threshold Temperature Change
Z	:	Performance Function

LIST OF GREEK SYMBOLS

α_{ε}	:	Strain Coefficient Expressed in MHz/με
$\alpha_{Operating}$	:	Operating Temperature Change at a Given Time T
$\alpha_{Specified}$	:	Minimum Detectable Change in Temperature
α_{T}	:	Temperature Coefficient Expressed in MHz/ºC
δT	:	Minimum Detectable Temperature
β	:	Reliability Index
δT	:	Minimum Detectable Temperature Change
Δd	:	Difference in mm between the Current and the Previous Flaw Depth Measurement
$\Delta \varepsilon$	:	Strain Change
ΔL	:	Difference in mm between the Current and the Previous Corrosion Length Measurement
Δt	:	Traveled Time
ΔT	:	Difference in Time between the Current and the Previous Measurement
$\Delta T_{measured}$	:	Measured Temperature Change
ΔT_{1}	:	Time Interval 1
ΔT_{n}	:	Last Time Interval
Δv_{B}	:	Brillouin Spectral Width
Δz	:	Fiber Optic Cable Length in Kilometers

λ	:	Wavelength of the Incident Light
μ_C	:	Mean of the Capacity of the System
μ_L	:	Mean of the Load
μ_R	:	Mean of the Resistance (Capacity)
μ_Z	:	Mean of the LSF
v_B	:	Brillouin Frequency Shift
v_o	:	Reference Brillouin Frequency at No Strain and at the Ambient Temperature – MHz
ρ	:	Liquid Density – Kg/m^3
σ_L	:	Standard Deviation of the Load
σ_R	:	Standard Deviation of Resistance (Capacity)
σ_y	:	Specified Minimum Yield Strength
σ_Z	:	Standard Deviation of the LSF

CHAPTER 1
INTRODUCTION

1.1 INTRODUCTION

As industrial systems age, they will eventually degrade in performance leading to partial or complete failure. Failure of a system may adversely affect its production, the environment, and the reputation of its owner. The consequences of such failure may include loss of production and environmental damage. More importantly, safety of operators and credibility of the company might be jeopardized. All of these consequences may entail financial losses and liabilities.

To maintain competitiveness and survivability in the market, companies must adopt the best and most effective approach to assess the integrity of their assets in a timely and structured fashion using the best available tools. Companies must strive to maintain optimum performance of their assets and minimize consequences of their failures. Among the critical industrial infrastructures are oil and gas transport systems. The conditions of these systems must be monitored regularly to ensure that their integrity is maintained and that there is no risk to the environment. Being underwater, such systems may pose threats to the surrounding habitats if the system fails to function in a safe manner.

One of the most important tools used for monitoring pipelines is the Leak Detection System (LDS). Selecting an appropriate LDS to work in harsh and aggressive environments, such as underwater, is a very challenging task.

All the factors that influence the LDS operation performance including environmental impact, impact of the auxiliary systems, probabilistic nature of the factors, sensitivity of the measuring components, and variability and fluctuation in measurements must be considered in selecting the best LDS for subsea operation.

The performance of the LDS and its associated components should be assessed regularly to determine if the system is safe to operate. Based on the outcome of the assessment, a decision can be made if the whole system or a component of the system needs to be repaired, upgraded, or replaced.

Current practices use deterministic approaches for assessing the performance of these systems. A deterministic approach does not consider the random variability and uncertainty associated with the degradation and the assessment models. The deterministic assessment may provide conservative results in the event the upper limits of the performance parameters are used or an underestimated outcome in the event the lower limits are used. A deterministic approach may also produce partial assessments that may not truly characterize the actual condition of the system, which may eventually lead to poor

decisions. To deal with these issues, a probability-based approach should be implemented to assess the performance of the LDS. Adopting this approach allows the incorporation of uncertainties and random variability into the assessment. Thus, a quantifiable probability of failure can be estimated.

Similarly, the performance assessment of the LDS in conjunction with a probabilistic assessment of the oil and gas transport component should also be used. There are codes and standards that can be used to assess corroded pipelines, but these codes and standards are based on deterministic methods and exclude condition monitoring systems such as LDS from the assessment and only focus on pipelines. In order to provide a reliable and inclusive assessment of the integrity of the pipeline and its LDS, a probabilistic approach, by providing joint probabilistic assessment, should be used. Adopting this approach will provide a realistic assessment that better describes the actual condition of the system being evaluated. Additionally, it will enable evaluators to correctly determine if the systems are operating in a safe and reliable manner.

1.2 LDS FAILURE

Generally, the key factors that affect the performance of a leak detection system are missed detection and false detection. The system may reveal that a leak is happening somewhere along the pipeline when in fact there is no leak present (this is termed a false detection or

false alarm). Likewise, the system may not declare a leak is happening when in fact it is present (this is termed a missed detection). Missed or false detections may not completely place the system out of service; however, they cause the system to fail partially. In either case, whether there is total or partial failure, the performance of the system will be in jeopardy. Once we know of these failures and are able to calculate the probability of their occurrences and their consequences, we can evaluate the risk and its impact on the environment and production.

1.3 PIPELINE FAILURE

Pipeline failure events consist of a leak or rupture of the pipe; the failure modes are the degradation mechanisms, i.e., corrosion, cracks, or other flaws. Uncertainty in the collected inspection data, pipeline geometry, pipeline material properties, and operating characteristics present a great challenge to the analysis. A probability-based assessment approach should be adopted as it is the best suited to deal with uncertainty, where a quantifiable value of the probability of failure can be estimated (Lindley, 1982). Probabilistic methods can be used for assessing the current and future ability of pipelines to support operational demand without jeopardizing safety and reliability. Based on the outcome of the assessment, the pipeline fitness for service as well as the remaining life can be determined.

The probability of failure is estimated by probabilistic modeling in terms of the failure modes where uncertainty is included in the estimation. The Monte Carlo simulation method is used to evaluate the probabilistic characteristics of the random variables and then determine the probability of failure, either by sample statistics or by counting methods (Haldar & Mahadevan, 2000).

1.4 RISK ASSESSMENT

Two fundamental components establish the risk assessment, as illustrated in Figure 1.1: the probability and consequences of failure for both the pipeline and the LDS.

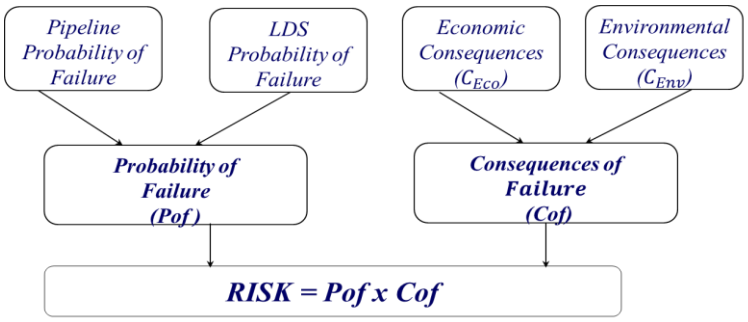

Figure 1-1 Failure and Its Consequences

The figure indicates that in order to know the risk, the probability of failure (*Pof*) and consequences of failure (*Cof*), which incorporate environmental as well as economic consequences, should be known beforehand. The pipeline fails to operate safely due to rupture or leakage caused by excessive corrosion or cracking. Obviously, the leaked product will damage the surrounding environment and the problem becomes worse if the

LDS fails to detect this failure in time. The LDS failure and the pipeline failure events are independent, and as such the probability of their occurrence at the same time is the product of both probabilities.

1.5 RESEARCH SCOPE AND OBJECTIVES

This research explores, investigates, and establishes a probabilistic assessment framework for oil and gas pipeline condition monitoring systems. Engineering probabilistic methods, concepts of signal detection theory, and concepts of distributed fiber optic sensing will be applied and adopted as appropriate. The scope of the research is broken down into four major tasks that represent the building blocks for the overall framework.

1. Formulation of the probability of detection and false detection for fiber-optic-based LDS.
2. Development of a probabilistic performance assessment scheme for fiber-optic-based LDS.
3. Application of probabilistic methods for assessing the integrity and determining the probability of failure as well as the remaining life of oil and gas transport components (i.e., pipelines).
4. Development of a risk-based assessment methodology to determine the risk associated with the simultaneous failure of the LDS and the oil and gas transport components (i.e., pipelines).

1.6 RESEARCH ASSUMPTIONS

The research is based on the following general assumptions:

- Power signal and noise power signal are assumed to follow normal distribution.
- The mean of the noise power signal is assumed to be zero.
- The time required to process the data contained in the signal by the system are assumed to follow normal distribution.
- The power represents the true temperature measurements and noise represents the measurement error.
- The probability of detection, probability of delayed detection, or probability of false alarm is computed as per-single LDS segment.
- The threshold represents the minimum detectable temperature change that can be detected by the LDS. It is assumed that it is a given parameter as part of the specification of the system. If this parameter is not given, then the probability of false detection (probability of false alarm) should be a given parameter as per the specification.
- The capacity as well as the load of the limit state functions addressed in the research are assumed to be random.
- The fiber-optic response time to temperature change is in the nanoseconds range and can be ignored.

- The failure of the entire LDS along the pipeline is assumed to be a series system and the failure of each LDS segment is independent.
- The failure of the LDS is the event that it misses the detection of an actual leak.

1.7 RATIONALE

LDS is one of the critical condition monitoring systems of the entire oil and gas infrastructure. The failure of the LDS to detect an actual oil or gas leak, whether sudden or gradual, has drastic effects on the environment, production, as well as safety, and jeopardizes the survivability of the operating company in the market. Similarly, the incorrect declaration of a leak by the LDS, i.e., providing a false alarm, will result in deploying all the necessary equipment and personnel to the pipeline site that is thought to be leaking, which will result in great losses in time and money. This is the reason for focusing on the LDS.

There are various types of LDS that use different technologies, but one of these technologies that is gaining wide acceptance in the industry is the fiber-optic leak detection system. This emerging and promising technology has great potential for oil and gas condition monitoring applications. It is the most suited for underwater applications due to the ease of installation and reliable sensing capabilities. This technology relies on distributed sensing techniques, where the fiber optic cable acts as a large sensor that

provides sensing capabilities in a timely and cost-effective manner. Moreover, increased temperature accuracy and spatial resolution are achieved when using this technology. It is immune to electromagnetic interference, unaffected by corrosion, and easier to install along or on the pipeline.

Current codes and standards, industry practices, and literature exclude condition monitoring systems from the assessment process. At every instant of time, each defect point along the pipeline is subject to two undesirable events: the pressure failure that may take place causing a leak or rupture due to the weakness of the defective point to resist the internal pressure (load) imposed on it; and the inability of the LDS to detect the leakage at the defective point. Therefore, to achieve a comprehensive and precise assessment, the LDS and the pipeline should be evaluated jointly.

An integrated probabilistic approach for assessing the integrity of a corroded oil and gas pipeline and LDS should be developed. This is a joint probability of failure function for both the pipeline and the LDS. It encompasses the failure pressure and the detection failure only and does not include the false detection (false alarm). The probability of false alarm is evaluated separately since the consequences of detection failure are different from the consequences of false alarm. It should be noted that the detection failure will only occur if a leak is present along the pipeline, whereas false detection occurs when a leak is not present.

In light of the above, the focus of the scope will be on a condition monitoring system that monitors and reports hydrocarbon leakage only. The scope will be limited to fiber-optic-based LDS. Among the different fiber-optic distributed sensing techniques, the scope will be limited to what is called Brillouin Optical Domain Analysis (BOTDA) (Soto, Bolognini, & Pasquale, 2011).

1.8 ORGANIZATION OF THE THESIS

Chapter 2 summarizes the literature review and presents background information related to the research. Chapter 3 discusses the formulation and analysis of the probability of detection and false detection for fiber-optic-based LDS. The emphasis is on the LDS at a single segment of the pipeline and is not for the entire LDS along the pipeline. Chapter 4 presents a probabilistic performance assessment scheme based on limit state approach for the entire fiber-optic LDS along the pipeline. The threshold and the probability of false alarm (PFA) (the outcome of chapter 3) are used to perform the assessment. The probabilistic assessment outcome includes the probability of failure for the entire LDS along the pipeline. The probability of failure encompasses detection failure and false detection. Detection failure is the combination of missed detection and delayed detection. Essentially, it determines the overall probability of failure of the entire LDS along the pipeline. Chapter 5 presents a methodology for assessing the condition of corroded

pipelines by calculating the pipeline probability of failure using limit state approach and pressure failure models, as recommended by internationally recognized codes and standards. The outcome of the assessment can be used to determine the pipeline fitness for service and its remaining life. Chapter 6 presents an integrated risk assessment approach of the pipeline failure due to burst and LDS failure due to missed detection. The outcome of chapters 3 and 5 are used to conduct the risk-based assessment. This approach can be used to predict and quantify the future financial impact in the event a pipeline and condition monitoring system (i.e., LDS) fail. The assessment provides the expected level of risk expressed in monetary value. Chapter 7 provides a risk-based assessment methodology to assess the simultaneous failure of the LDS and the pipeline due to leakage and rupture. Chapter 8 provides summary and concluding remarks and chapter 9 summarizes the research contributions and recommendations for future research.

CHAPTER 2
LITERATURE REVIEW

The literature review focuses on the monitoring function of subsea oil and gas infrastructure. Mainly, there are four monitoring functions that fall under the category of integrity monitoring processes. These are the monitoring functions for downhole (equipment that is used in the well), wellhead gathering/manifold, seabed processing/pumping, and transportation pipeline (Ogwude, 2003). The research will focus on the monitoring function for transporting oil and gas pipelines, which is the leak detection function.

The following paragraphs summarize the latest work that has been accomplished in the area of leak detection. Only common leak detection techniques are discussed. This chapter starts by providing a description of generic reporting systems (in section 2.1), followed by information about common LDS (sections 2.2-2.4). Finally, section 2.5 discusses fiber-optic distributed sensing, and section 2.6 provides an overview of failure modeling using limit state functions.

2.1 INTEGRITY MONITORING AND REPORTING

A generic system that performs an integrity monitoring and reporting function is illustrated in Figure 1. The monitoring and sensing functions are performed by the sensors attached to the object. The data collection is then performed jointly by the sensors, which convey

the data to the communications network, which sends the data to the control room to be analyzed in order to determine if a leak has occurred or not.

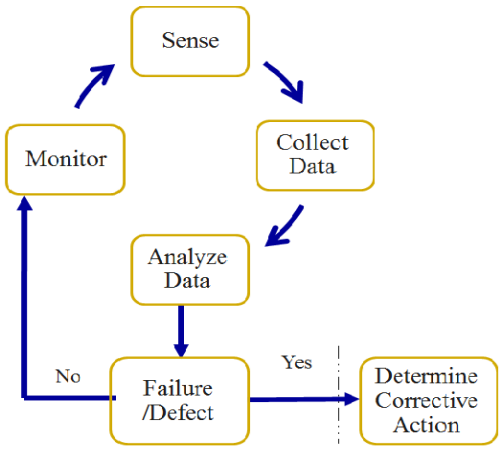

Figure 2-1: Generic Monitoring and Reporting System

A more detailed representation of the diagram shown in Figure 2.1 is depicted in Figure 2.2. The system mainly consists of three subsystems that perform the monitoring, reporting, data analysis, and decision-making functions. The leak detectors perform the monitoring function; the fiber-optic or wireless communications systems perform the reporting function; software applications residing in the main computer at the land or offshore processing facility perform the data analysis and decision-making function.

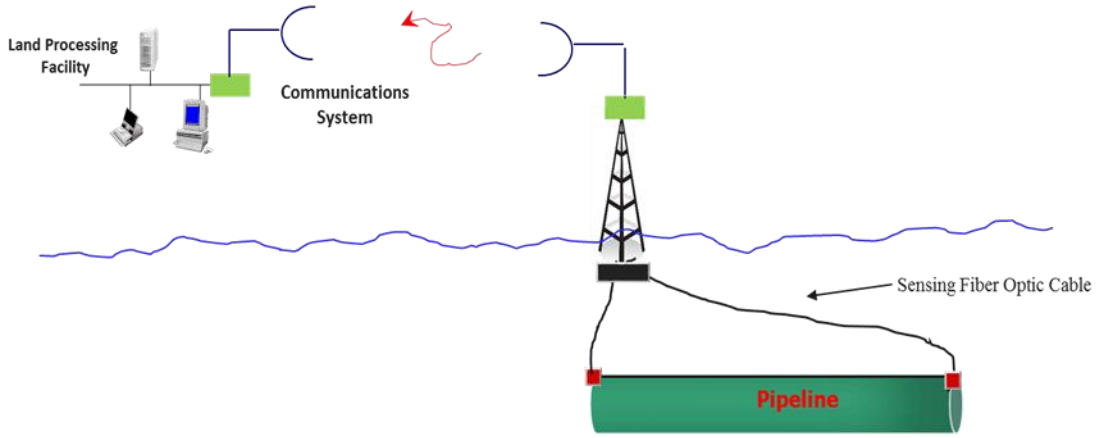

Figure 2-2: Typical Leak Monitoring and Reporting System

2.2 COMMON LEAK DETECTION TECHNIQUES

Commonly used leak detection methods include pressure monitoring, volume balance, negative pressure wave, model-based, fiber-optic, statistical, and transient methods. In the literature, leak detection methods are classified by either internal or external, or hardware-based or software-based methods. The following classification will consist of internal- and external-based methods. One of the promising external-based methods is the fiber-optic sensing, which will be discussed separately.

2.3 INTERNAL LEAK DETECTION METHODS

***Pressure Point Analysis* (*PPA*)**

The pressure point analysis technique performs monitoring function by comparing the pipeline pressure at predetermined points with a statistical trend established for prior pressure measurements (Akib, Saad, & Asirvadam, 2011; Wan et al., 2012). The main advantage of this method is that leaks can be detected easily, while the major drawback is that the leaks cannot be located easily. Furthermore, performance is poor in multiphase flowlines, transient conditions, slack lines, etc.

One method that falls under this category is the FFT-based Algorithm Improvements for Detecting Leakage in Pipelines. Lay-Ekuakille, Vedramin and Trotta (2009) applied this method on a group of pipes placed in a zigzag manner, where several valves were installed and five leak points were established along the pipe. The frequency versus amplitude curves can be used to determine if a leak has occurred or not. The valves of the pipes were opened and then closed during the testing to simulate the drop in pressure; these pressure drops or discrepancies indicate the existence of a leak. The experiment was implemented in a stress-free environment, i.e. the pipeline was not buried or placed in an underwater environment. It is not clear if the plots provided can locate or quantify the leaks. There was no mention of the minimum detectable leak rate.

Volume Balance / Mass Balance

The volume balance method works by balancing the volume of the fluid at the inlet with that of the outlet against the mass inventory of the pipeline; any deviation would indicate a leak. The volume or the mass of the fluid can be approximated by calculating the state of variables, temperature, pressure, and flow rate. This method has the ability to detect leaks resulting from progressive crack or corrosion growth and leaks that are accidental. This system requires flow meters at the downstream and upstream of the pipeline in addition to pressure and temperature sensors located in between. The main advantages of this method are the accurate prediction of the leak flow rate, the ability to detect progressive leaks, and that it is a proven technology. It performs very well in oil lines and can detect large leaks easily. This method takes longer time to detect and does not accurately locate a leak. It does not perform very well in detecting small crude oil leaks. Moreover, it does not perform very well in gas pipelines. The longer detection time, if looked at from a different perspective, becomes an advantage of the system, as the longer response time will give assurances that there is in fact a leak, which will in the end prevent false detection (Martins & Seleghim, 2010).

Negative Pressure Wave

Negative pressure method detects sudden leaks that may result from accidental impacts caused by an object or from abrupt pipeline failure due to neglected cracks or corrosion. Upon the occurrence of a leak, two negative pressure waves will travel from the leak

location in opposite directions with the speed of sound of the fluid towards the ends of the pipeline or pipeline segment. The leak location can be determined by calculating and comparing the time of arrival of the two waves at each end. This method is fairly simple and does not require complex mathematical models for predicting a leak. The main advantage of this method is the accurate and quick prediction of the leak and its position. The main disadvantage is the inability to detect progressive leaks (Martins & Seleghim, 2010; Ge, Wang, & Ye, 2008).

Hierarchical Leak Detection and Localization Methods

Hierarchical leak detection and localization methods for gas pipelines are based on wavelet transforms and multi-classifier Support Vector Machine (SVM) (Wan et al., 2012). This method is implemented by applying a bilinear search method to determine the optimal parameters and sigmoid function to convert the results obtained from the recognition done by the SVM to probability estimates. For locating the leak, the principle of time difference of arrival is used. Essentially, the purpose for using the wavelet transform is to remove noise and dispersion from the propagating signal along the pipe; then the signal is broken down into smaller portions to obtain the characteristics of the leak. Concerning the method developed under this research, it is not clear if the pipeline was tested under water, buried, or aboveground. The proposed method adopts so many mathematical and analytical tools that make the use of this method complicated and time consuming. There is therefore a

need to develop a technique that minimizes the time and effort in performing the detection and analyses of leaks, should they occur, to make it more attractive and worth considering.

Expert System Methods

Xu et al. (2007) studied belief-rule-based expert system to detect and quantify pipeline leaks. The system used different pipeline operating conditions, and based on the pipeline operation pattern the leaks can be detected. The belief-rule-based expert system was based on the mass-balance method. When a leak develops along the pipeline, the pressure will change and adopt certain patterns that are different from normal operation patterns. Experts can determine the patterns for each situation, leak or no leak. Along the way, relationships were established between the leak sizes and the pipeline pressure measurements and flow rates. These relationships are essential components for the belief-rule-based system. The method requires prior knowledge about the pipeline's normal operation to establish these relationships between pressure, flow rates, and leak sizes. Human judgments are subjective and could lead to erroneous information. It is not clear if the pipeline was underground or buried.

Real Time Transient Methods (RTTM)

RTTM works by using conservation of mass, conservation of momentum and energy principles, and the equation of state for the fluid. Sensors located along the pipeline measure flow, pressure, density, and temperature. The measurement data are sent to the

processing computer for analysis and any deviation between the measured values and the predicted values indicates that a leak is happening. This method requires a lot of instrumentation to collect data in real time and is expensive to implement as it is complicated and requires extensive training. The next few paragraphs discuss the advances related to transient method. Leak detection based on this method can detect leaks accurately up to and below 1% and performs extremely well in large and long pipelines.

Model-based pipeline monitoring uses hyperbolic partial differential equations to detect oil and gas pipeline leaks (Hauge, Aamo, & Godhavn, 2009). The system consisted of a Luenberges observer and Heuristic update laws. The system considered only the inlet and outlet of the pipe as data collection points, and the data of concern were the flow rate and pressure. The Luenberges observer relies on flow condition by using hyperbolic differential equations to describe the flow condition.

Heuristic update laws were used for adjustment of the leak time varying parameters. The model was verified by simulation and proved to be capable of detecting, locating, and quantifying pipeline leaks under transient conditions. The assumption was that a leak is a time-varying incident because leaks vary during shutdown of the pipe (therefore a leak is not constant).

The lumped parameters model was used for detecting and locating leaks along the pipe using static and dynamic behaviors of the flow (Daneti, 2010). The developed model was verified experimentally where the measuring points located at an interval of 0.3 meters along a 12.8-meter pipe. The received signal plus noise originating from leak points were analyzed using a Matlab Simulink environment.

Leak detection in pipes using transient flow and genetic algorithm is a method that can detect leaks coming out from a water pipeline (Kim, Miyazaki, & Tsukamoto, 2008). Under this method, the transient pressure analyses along with the genetic algorithm were used to determine the location of a leak. The work carried out in this paper was based on the assumption that the leak in the pipe contributes to the attenuation of the transient pressure waves. A case study was presented for a 100-meter pipe with three conditions: one leak, two leaks, one leak and noise. The friction factor played a major role in determining the leak location. It was concluded from the case study that a linear relationship existed between the friction factor and the leak location. Moreover, leak detection with noisy signals was also possible where the noise was modeled with zero mean and random deviation of ± 0.5 m added to the reference pressure.

Leak detection in pipe networks using coded transients is one of the methods used to detect and locate leaks, where a linear analytical solution was developed and Fourier series solution applied as an analytical method (Wang, Simpson, & Lambert, 2006). The work

resulted in what is called coded transients. The authors studied the influence of leaks on transient events. A reduction in the amplitude of the signal would indicate the existence of a leak. A comparison study was done between the Method of Characteristic (MOC) and the developed analytical solution, resulted in accurate results for the two conditions (no leak and leak). Also, it was shown that the leaks influenced only the amplitude of resonant transients, and the amplitude was expressed as a function of frequency. The whole study resulted in developing a method to detect, locate, and quantify the leak.

Leak detection in pipes by frequency response method using step excitation is another method based on transient analysis that takes pressure variation into consideration in the analysis to determine if a leak has occurred along the pipe (Mpesha, Chaudhry, Kahn, & Gassman, 2002). The frequency responses were analyzed using Fast Fourier Transforms to detect, locate, and quantify leaks. The analysis was performed by comparing the frequency responses of no leak with that of a leak. Different piping systems and different configurations with different number of leaks were experimented with (one leak, multiple leaks, parallel piping system, branched piping system with one leak, and multiple leaks were tested). The experiment was conducted by taking the pressure and discharge readings as the valve was opened and closed gradually to simulate the leak situation, which is a change of the behavior of the pipes' operating conditions. The no-leak signals showed only primary amplitude peaks while the leak signals showed additional secondary amplitude peaks to indicate that a leak had occurred. The difference between the two responses in

terms of amplitude was used to determine the location of the leak. The experiment was conducted in open-air environment and the plots presented several smaller peaks, which might be confused with leak signals.

The challenge for internal LDS is mainly the detection of small chronic leaks at start up, shut down, valve closures, transient flow, slack lines, etc.

2.4 EXTERNAL LEAK DETECTION METHODS

Acoustic Emission

Acoustic emission technique for detecting and locating leaks was experimentally investigated by Xiang, Fang, and Lu (2011). The leak was observed by variation in pressure while the location of the leak was determined by using wavelet transforms. A leak can be determined based on the signal shape and variations. Wavelet transforms used to de-noise the signal and cross-correlation method were used to determine the location of the signal. It is not clear from the paper if the experiment was conducted in a lab environment or in the field. There is no indication if the pipeline was buried, above ground, or underwater.

Fiber Optic Leak Detection Methods

The fiber optic method identifies leaks when a change in temperature of the surrounding environment takes place or when a micro bend in the cable occurs.

2.5 FIBER OPTIC DISTRIBUTED SENSING

Fiber optic distributed sensing is one of the promising technologies that can perform continuous sensing along the entire length of the monitored object, i.e., pipeline. By using fiber optic distributed sensing technology, the vibration, strain, and temperature changes along the monitored object can be detected. Strain occurring on a pipeline can indicate the existence of cracks, and detecting it in advance will provide ample time to perform corrective action before the crack can cause structural failure that may lead to a leak and eventually oil spill, causing environmental damage. The same fiber optic cable used for sensing can be used to support pipeline telecommunications requirements along the pipeline via another dedicated fiber strand (Bao & Chen, 2012).

Leaked crude oil will increase the temperature of the surrounding area; this increase in temperature will cause scattering of the light wave to indicate the occurrence of a leak as indicated in Figure 2.3 (Nikles, 2009).

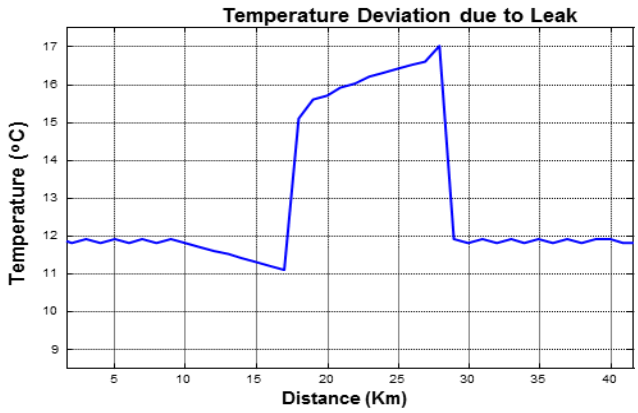

Figure 2-3: Distance versus Temperature for Leaking Oil Pipeline

Leaked gasses will decrease the temperature of the surrounding area as indicated in Figure 2.4 resulting in alarm indicating a gas leak (Nikles, 2009).

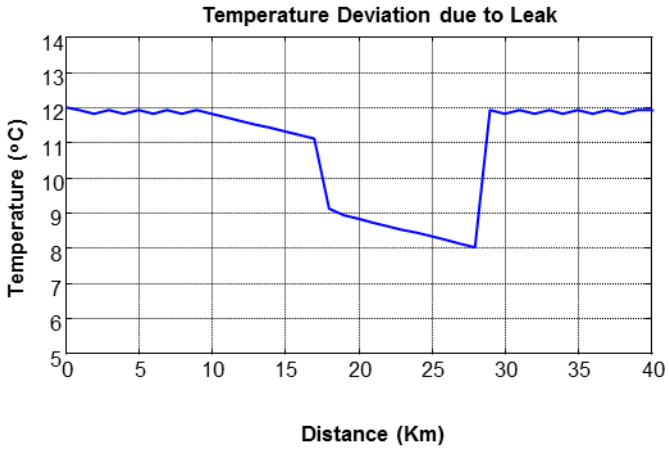

Figure 2-4: Distance versus Temperature for Leaking Gas Pipeline

2.5.1 Distributed Sensing

Implementing point sensing will require hundreds if not thousands of sensors to be mounted on the pipeline to be monitored, which makes such an endeavor difficult to implement and costly (and at times impossible). On the other hand, distributed sensing enables the fiber optic cable to function as a sensor providing sensing capabilities in a timely and cost-effective manner. Moreover, increased temperature accuracy and spatial resolution are achieved. When an optical laser propagates through the fiber, it gets scattered back in three different spectral forms with different frequencies:

1. Rayleigh
2. Raman
3. Brillouin scattering

The thing that distinguishes one form of scattering from the other is the wavelength characteristic (shown in Figure 2.5). Rayleigh scattering remains at the same wavelength as the source light and the other two scatterings shift for a certain wavelength. All three have been employed in the distributed sensing technology.

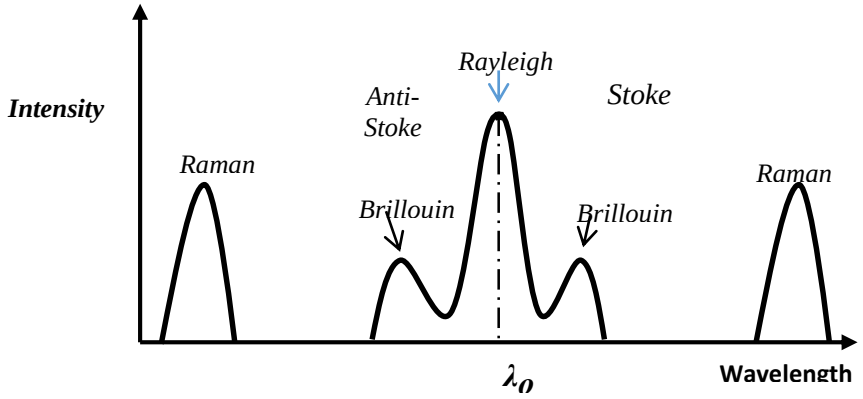

Figure 2-5: Scattering Spectrum

Rayleigh scattering is linear and used for distributed acoustic sensing; it is called elastic scattering because the scattering does not experience any frequency change. It is created due to the interaction of the photon particles that were emitted by the source with the molecules of the fiber materials (Bao & Chen, 2012).

The other two scattering mechanisms are nonlinear and are called inelastic as they experience frequency change, where the scattered power is expressed as a fraction of the incident power. The spectrum to the right side of Rayleigh is called stoke spectrum, and the one on the other side is called anti-stoke peak. As Figure 2.5 indicates, the Raman spectrum consists of two components: the temperature-dependent anti-stoke Raman component and the temperature-independent stoke Raman component. The Raman scattering can be used for temperature sensing where ratio of the stoke and anti-stoke light

intensity is used for determining the temperature at the point where the light is scattered back to the source.

Brillouin scattering is used to sense strain and temperature changes, which can be determined from changes in the wavelength. The scattering occurs when the laser (the incident light) interacts with the phonons and incident laser light is split into scattered photon (light particles) and phonon (acoustic or vibration energy). The scattered light creates wavelength shift or frequency shift, which can be used to measure local strain or temperature changes.

2.5.2 TECHNOLOGIES

Distributed Temperature Sensing (DTS)

Raman and Brillouin scattering can be used to sense and detect temperature change. During a leak incident, the temperature of the local region surrounding the leak will change and from time of arrival of the backscattered light the location of the leak can be determined. The change of light intensity will indicate a change of temperature for systems that are based on Raman scattering. While in the case of a Brillouin-based system, a change of frequency or wavelength will indicate a change of temperature and strain.

Brillouin-based systems are more favorable than Raman-based systems for long-haul pipelines because the light can go longer distances without the need for regenerating or

amplifying the signal. Moreover, Brillouin-based sensing can sense temperature and strain at the same time.

Distributed Acoustic Sensing (DAS)

DAS is used to detect acoustic emissions in which the fiber optic will detect the vibration along the pipeline. If this vibration event is distinct and different than the normal low-level vibration activities and related to a leak, the sensing cable will detect it and trigger an alarm. This technology uses Rayleigh band to detect change of acoustic energy by the change of the signal intensity. It can be used to detect leaks, sabotage activities, and any other disruption activities, since the only element that is monitored is the sound coming from the pipe (Eisler & Lanan, 2012).

Distributed Strain Sensing (DSS)

The extent of strain and the change of temperature of the area around the pipe can be determined by using the Brillouin backscattered light from where the frequency change has occurred. Brillouin-based scattering has the advantage over other methods for its ability to perform sensing and detection of longer-range pipes. It has the ability to measure temperature and strain with high sensitivity and accuracy. The measurement here is based on Brillouin; the temperature and strain measurements can be determined from the frequency shift of the Brillouin band, which is different from the Raman case where the measurement is based on the power measurements.

Other Brillouin-sensing-based techniques cited in the literature that can provide temperature and strain sensing include Differential Pulse-Width Pair Brillouin Optical Time Domain Analysis (DPP-BOTDA); Brillouin Optical Time Domain Reflectometry (BOTDR) (Bao & Chen, 2012; Li et al., 2008); and Brillouin Grating (Song, Zou, He, & Hotate, 2008). These methods have different sensing range, measurement time, temperature and strain accuracies, and spatial resolution. Of these techniques, DPP-BOTDA performs the best in terms of sensing range and accuracy.

2.5.3 OVERVIEW OF DISTRIBUTED SENSING AND FIBER- OPTIC- BASED LDS

Fiber optic distributed sensing can perform continuous sensing along the monitored object, which enables the system to provide early warnings of any abnormalities that may occur. One of the technologies based on distributed fiber optic sensing is the fiber-optic-based LDS. One of the distributed sensing techniques is the Brillouin Optical Time Domain Analysis (BOTDA), (Soto et al., Bolognini, and Pasquale, 2011), which is the focus of this research. It is widely used by the industry for condition monitoring and reporting.

2.6 MODELING FAILURE

The parameters that influence the performance of the system during operation vary from time to time. The capacity is a design parameter that dictates the system's ability to deliver

and it is assumed to be probabilistic. Using the same argument, the load of the system is also assumed to be probabilistic.

$$P(\ Failure) = P(C < L) \tag{2.4}$$

Where L is the load and C is the capacity or resistance of the system. Equation. 2.4 expresses the fact that the probability of failure is a conditional probability and encompasses all possible combinations of $L = x$ and $C < L$; x is a specified limit value that the load should not exceed, (Nowak and & Collins, (2000)).

CHAPTER 3
FORMULATION OF THE PROBABILITY OF DETECTION AND FALSE DETECTION FOR LEAK DETECTION SYSTEMS

Ensuring the integrity of subsea process components is one of the primary business objectives of the oil and gas industry. Leak detection system (LDS) is one type of systems that is used to safeguard reliability of a pipeline. Different types of LDS use different technologies for detecting and locating leaks in pipelines. Fiber optic based LDS is gaining wide acceptance by the industry and has great potential for subsea pipeline applications.

It is the most suited for underwater applications due to the ease of installation and reliable sensing capabilities. Having pipelines underwater in the deep sea presents a great challenge and a potential threat to the environment and operation. Thus, there is a need to have a reliable and effective system to provide assurances that the monitored subsea pipeline is safe and functioning as per operating conditions. Two important performance parameters that are of concern to operators are the probability of detection (PD) and probability of false alarm (PFA).

There is no established method for evaluating the PD and PFA for a fiber-optic-based LDS. False detection results in excessive expenditure and unnecessary mobilization of equipment and personnel to the site that is thought to be leaking. On the other hand, missed

detection results in environmental and financial liabilities and unfavorable impacts on reputation.

The main objective of this chapter is to formulate the PD and PFA for a fiber optic distributed sensing technique used for leak detection. This is accomplished by adopting some concepts from signal detection theory (SDT) and engineering probabilistic methods. Once the threshold becomes known, the PFA can be determined by expressing the PFA in terms of the threshold. In addition, PD can be determined in terms of the PFA. The emphasis of this chapter is on the LDS at a single segment of the pipeline and not for the entire LDS along the pipeline. Fiber optic distributed sensing techniques and some concepts from signal detection theory are used to formulate the PFA and the threshold. Matlab is the programing tool used to perform the analysis.

3.1 LEAK DETECTION SYSTEMS

One of the key monitoring systems for subsea pipelines is the LDS. Its performance should be assessed regularly to ensure that its operability and functionality as well as its reliability are maintained at all times and more importantly to ensure that it does not miss detection of or falsely detect a pipeline leak. The consequences of such an incorrect diagnosis may pose a threat to the environment or production. Based on the outcome of the assessment, a

decision should be made if the whole or part of the system needs to be repaired, upgraded, or replaced.

Missed detection and false detection are key factors that generally affect the performance of a subsea LDS. The system may declare the occurrence of a leak when in fact a leak is not present. Similarly, the system may not reveal that a leak is happening when in fact it is happening. The latter scenario is termed a missed detection, and the former is termed a false detection or false alarm. Missed or false detection may not completely place the system out of service; however, they cause the system to fail partially. In either case, whether we have total or partial failure, the performance of the system will be in jeopardy. Once we know these failures and are able to calculate the probability of their occurrences and their consequences, we can evaluate the risk and its impact on the environment and production.

Regardless of which leak detection method is used, the characteristics of the received signal are what allow us to determine the status of the pipeline. All leak detection methods or systems have one common task: to detect and declare if a leak has or has not occurred and, based on the characteristics of the received signal, determine the quantity and location of the hydrocarbon leak.

3.2 FIBER-OPTIC-BASED LDS

One of the most promising condition-monitoring technologies is the fiber optic distributed sensing, which can perform ongoing sensing along the entire length of the monitored structure. The fiber optic components act as a sensor, providing sensing and prior warning capabilities in real time and on a continuous basis. By using distributed fiber optic sensing technology, the vibration, strain, and temperature changes along the monitored object can be detected. Strain occurring on a pipeline may give indication of the existence of cracks, and detecting them in advance will enable maintenance personnel to perform corrective actions in a timely manner. Applying this technology will prevent structural failure that could lead to a leak and eventually to an oil spill. The same fiber optic cable used for sensing can be used to support the pipeline's telecommunications requirements along the pipeline via another dedicated fiber strand.

Generally, oil is transported through pipes at a temperature that is higher than its surroundings. In the event a leak happens, the temperature of the surroundings will increase, causing a portion of the light wave to scatter back to the source, indicating the occurrence of a leak (Nikles, 2009). On the other hand, when a gas pipeline starts leaking, the released gas will cool down the surrounding area resulting in a cooler temperature than the normal temperature. As a result, the sensing cable will trigger an alarm indicating a leak (Nikles, 2009). The LDS system based on this technology performs multiple scans for

every measurement at a predefined time interval. Then the average is computed to determine the mean value of the measurement and this value will be the measured temperature. The result will include a plot showing distance versus temperature and any change along the path can be noticed very easily on the plot.

This technology can provide accurate information in real time about the status of the monitored structure, which can significantly enhance the decision-making about what mitigation actions should be considered in the event a risk or safety issue becomes imminent.

3.2.1 Scattering

When optical laser light propagates through the fiber, it gets scattered in three different spectral forms. They include Rayleigh, Raman, and Brillouin as indicated in Figure 3.1 (Ulrich & Lehrmann, 2008).

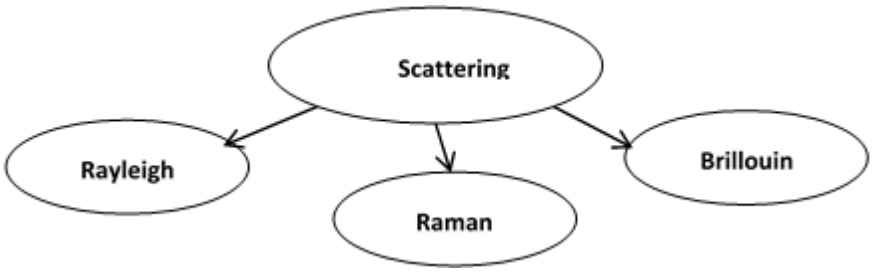

Figure 3-1: Scattering Mechanisms

The scattering is created due to impurities or changes of composition and interaction of the laser light with molecules of the fiber.

The Raman-based technique can achieve sensing up to 37 km, with measurement time of < 3 min and temperature accuracy of 3 ºC, and measures temperature changes only (Bai & Chen, 2012; Park et al., 2008). The Brillouin scattering-based technique has the ability to sense temperature and strain changes along the fiber optic cable. The wavelength of the reflected wave is closely related to the changes of the surrounding temperature and strain of the fiber optic cable (Walk & Frings, 2010). This technique can achieve less than 1-m spatial resolution, 1-min measuring time, and 2 ºC temperature resolution, and up to 50 km sensing range (Bao & Chen, 2012). The range can be extended by using fiber optic amplifiers. The reported strain accuracy is approximately 10 micro strains (Bao et al., 2001). As stated above, the Brillouin scattering-based technique outperforms the Raman-based technique, as it can achieve longer sensing range, improved accuracy, less measuring time, and can measure both temperature and strain. Therefore, the focus of this research is on the Brillouin-based sensing.

3.2.1.1 Brillouin Scattering

Brillouin scattering is caused by the fluctuations of the refractive index of the fiber. These fluctuations take place due to the variations of fiber composition, pressure, temperature, or density (Agrawal, 2001).

The process is called inelastic because a transfer of energy between the incident light, photons, and the molecules of the fiber takes place. If the energy is transferred from the photons to the fiber material, then the backscattered light is downshifted in frequency. In this case, photons lose energy. Conversely, if energy is transferred from the fiber material (the silica glass) to the photons, then the backscattered light is upshifted in frequency. Here, photons gain energy and the frequency becomes higher. The shift in frequency is called the Brillouin frequency shift and is given by Agrawal (2001):

$$v_B = \frac{2nV_a}{\lambda} \tag{3.1}$$

Where v_B is the Brillouin frequency shift, V_a is the acoustic velocity of the phonons, n is the refractive index of the fiber, and λ *is* the wavelength of the incident light.

3.2.2 Distributed Brillouin Sensing Techniques

Several techniques are used for distributed Brillouin sensing. They include Brillouin Optical Time Domain Reflectometry (BOTDR), Brillouin Optical Time Domain Analysis (BOTDA), Brillouin Optical Frequency Domain Analysis (BOFDA), Brillouin Optical Correlation Domain Analysis (BOCDA), and Brillouin Echo Distributed Sensing (BEDS) (Soto et al., 2001). This thesis focuses on the BOTDA technique because it is one of the most commonly used monitoring techniques by the industry.

3.2.2.1 Brillouin Optical Time Domain Analysis (BOTDA)

BOTDA works by launching lasers in two opposite directions; one is pulsed and the other one is continuous. The frequency difference for the two lasers can be used to measure strain and temperature along the fiber (Bao & Chen, 2012).

Figure 3-2: Illustration of a Simplified BOTDA System

v_1 is the pulsed laser or the pump signal; and v_2 is the continuous wave (CW), also called the probe signal. In this configuration, the power of the probe signal is transferred to the

pump pulse, resulting in an increase in the intensity of the pulse as it travels along the fiber. This then yields a better signal-to-noise ratio (SNR) and hence longer sensing range can be achieved (Bao et al., 1995; Belal, 2011). This configuration is referred to as Brillouin stimulated scattering (BSS).

The Brillouin frequency shift is dependent on material temperature and strain. The Brillouin scattering may lose or gain energy; the energy loss is called a Stokes process and energy gain is called an anti-Stokes process. To enhance the interaction between the incident light (the pump signal) and the Stokes, a probe laser is launched at the opposite side of the fiber (Horiguchi & Tateda, 1989; Smith, 1999a). For the first laser a square pulse is used, as this is usually used for timing control because the square pulses are of equal duration. Every pulse sent will have the same time duration. The spatial resolution, which is the smallest length of the monitored object whose temperature change can be determined, can be calculated from the pulse width (see Equation 3.2).

$$\Delta z = \frac{c\tau}{2n} \tag{3.2}$$

Where c is the speed of light in vacuum, n is the fiber optic cable refractive index, and τ is the pulse width. There exists a linear relationship between the frequency shift and the

changes of temperature and strain (Smith, 1999b; Bao et al., 2001; Brown, 2006). The frequency shift can be expressed as follows:

$$v_B - v_o = \alpha_\varepsilon \Delta\varepsilon + \alpha_T \Delta T_{temp} \quad (3.3)$$

Where v_o is the reference Brillouin frequency at no strain and at ambient temperature MHz; α_ε is the strain coefficient expressed in MHz/με; α_T is the temperature coefficient expressed in MHz/°C; ΔT_{temp} is the temperature change, which is the difference between the measured temperature and the ambient or reference temperature; and Δε is the strain change. The strain measurement is referred to as a micro strain (με). If a fiber optic cable has an original length of 1 meter and due to stress is stretched to 1.000007 meters, then the strain becomes seven micro strains (7 μm).

Sensing is possible from the frequency shift, but the challenge is that the shift is dependent on both strain and temperature. From the frequency shift, it is impossible to determine which change has occurred. Temperature is the determining factor for the presence or non-presence of a leak. To address this challenge, the fiber optic cable is held in close proximity to the pipe, as shown in Figure 3.3.

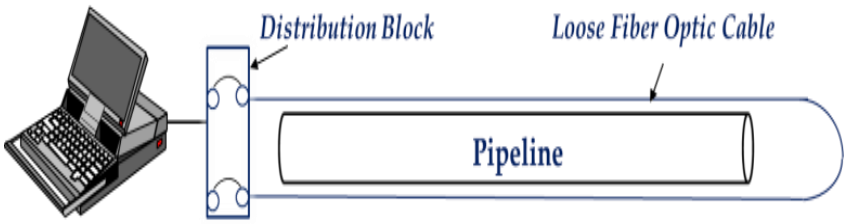

Figure 3-3: Configuration for Temperature and Strain Detection

The loose fiber is used to monitor the temperature change only, assuming zero strain since the fiber is held loose and not attached to the pipeline, Equation 3.3 can be re-written as:

$$v_B - v_o = \alpha_T \Delta T_{temp} \tag{3.4}$$

Figure 3.4 uses Equation 3.4 to illustrate the linear relationship between the Brillouin frequency shift and the temperature for a system that has a reference frequency (v_o) of 14650 MHz measured at the ambient temperature with a rate of change of 1.4 MHz/^{o}C.

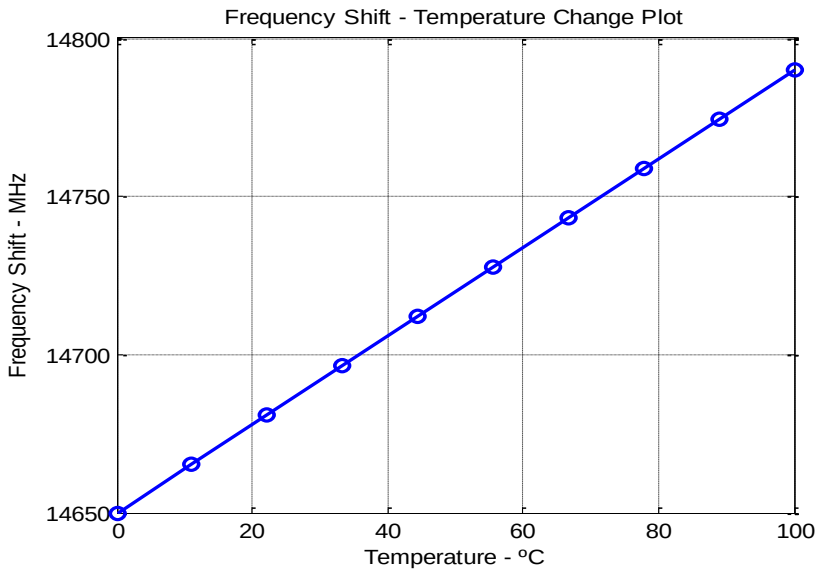

Figure 3-4: Brillouin Frequency Shift versus Temperature

The Brillouin peak power can be expressed as (Smith, 1999b):

$$P_B = P_{CW}\, e^{(-\alpha L)} \left[1 - \exp\left(-g_B P_P \frac{L_{eff}}{A_{eff}}\right)\right] \tag{3.5}$$

Where P_{CW} is the input probe power, P_P is the pulse power, g_B is the gain, L_{eff} and A_{eff} are the effective length and effective area of the fiber, respectively. The Brillouin peak power has a positive relation to the temperature. As the temperature increases, the Brillouin peak power increases. On the other hand, it is inversely related to strain. As strain increases, the

Brillouin peak power decreases (Parker et al., 1998; Smith, 1999b). The Brillouin peak power has a dependence on temperature and strain (Wait & Newson, 1996; Smith, 1999b).

$$P_B = P_R + \frac{dP}{dT}\,\Delta T_{temp} + \frac{dP}{d\varepsilon}\Delta\varepsilon \tag{3.6}$$

Where $\frac{dP}{dT}$ is the temperature coefficient (mW/ºC), and $\frac{dP}{d\varepsilon}$ is the strain coefficient (mW/με). Referring to Figure 3.3, the fiber is laid near the pipeline, assuming zero strain; the Brillouin peak power P_B can be expressed as:

$$P_B = P_R + \frac{dP}{dT}\,\Delta T_{temp} \tag{3.7}$$

Either Equation 3.7 or Equation 3.4 can be used to determine the temperature change. The location of the temperature change can be determined using Equation 3.8.

$$d = \frac{C\Delta t}{2n} \tag{3.8}$$

d is the location of the temperature change, *c* is the speed of light, *n* is the fiber optic cable refractive index, and Δt is time traveled.

3.3 PROBABILITY OF FALSE ALARM (PFA)

PFA is the probability of declaring a leak when in fact no leak is present. Whenever noise power exceeds a predefined noise power, a false alarm is declared. Stated differently, the PFA is described as the likelihood that the LDS will falsely detect a leak when none exists. The PFA is expressed in terms of the threshold, which is the minimum detectable temperature change. Any measured signal level below the established threshold will be considered as a noise signal and does not contain any true power.

Within the framework of signal detection theory, the mean and standard deviation of the noise are random. Noise is modeled as a normal distribution with zero mean (μ) and standard deviation (σ): $N(0, \sigma)$. A false alarm occurs whenever the noise power exceeds the predefined noise power (Wickens, 2002). Figure 3.5 illustrates the noise power's varying levels over time and the threshold; the threshold has been set to be at a value of two. This is the maximum acceptable noise power (σ^2). Any departure of the noise power from the baseline (the threshold power) will signal an alarm indicating false detection. In fact, the signal is mainly a noise signal that is increased in amplitude and has exceeded the threshold value due to excessive noise generated by the equipment, frequencies interfering with the monitoring equipment, or other external factors. Using Monte Carlo simulation the results are shown in Figure 3.5.

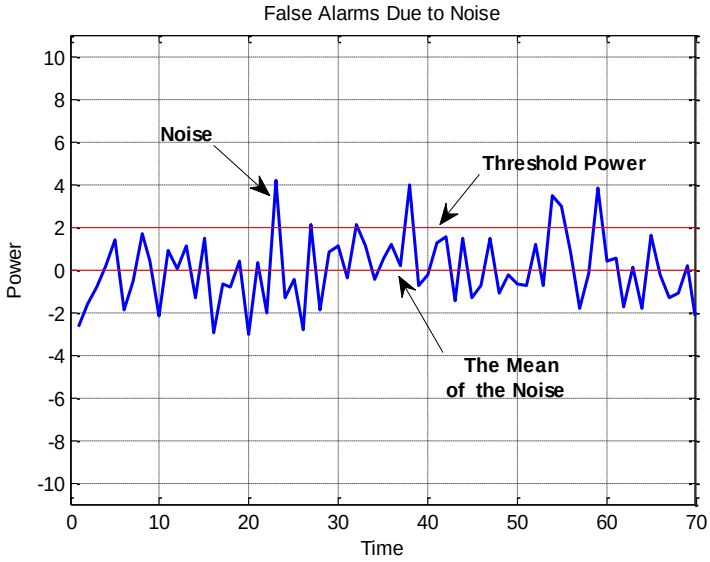

Figure 3-5: Illustration of Noise Signal

Every signal has two elements, power and noise, that respectively correspond to measured temperature and error, as indicted in Equations 3.9–3.14. The noise affects the final accuracy of estimated ΔT_{temp}.

3.3.1 Power Signal and Temperature Relationship

The signal-to noise-ratio is defined as:

$$SNR = \frac{\mu^2}{\sigma^2} \tag{3.9}$$

The variance corresponds to the noise power or measurement error and the square of the mean corresponds to the power amplitude or measurement. Referring to Equation 3.7, the

power has a noise term that results in error in the measurement of temperature – *Measured power signal = Power + Noise:*

$$P_B = P_{B(measured)} + NP \tag{3.10}$$

Where $P_{B(measured)}$ is the measured Brillouin peak power and *NP* is the noise power. Both the $P_{B(measured)}$ and *NP* are measured at a given point in time. After obtaining the values of the measured power, the temperature change can be determined.

$$\Delta T = \Delta T_{measured} + \varepsilon \tag{3.11}$$

Where ε is a random measurement error that corresponds to noise in the signal with a mean of 0 and variance σ^2. The Brillouin peak power P_B in Equation 3.7 is the measured Brillouin power. Substituting Equation 3.7 into Equation 3.11, ΔT can be expressed as:

$$\Delta T_{temp} = \frac{P_{B(measured)} - P_o}{dP/dT} + \varepsilon \tag{3.12}$$

Using Equation 3.10 and Equation 3.11, the temperature change (ΔT_{temp}) is given as:

$$\Delta T_{temp} = \frac{P_{B(measured)} - P_R}{dP/dT} + \frac{NP}{dP/dT} \tag{3.12.1}$$

Where P_R is the reference power taken at the reference temperature change (this is not to be confused with the threshold temperature change) and $^{dP}/_{dT}$ is the temperature coefficient (mW/ºC). The first term in Equation 3.12.1 corresponds to measured temperature and the second term corresponds to measurement error (ε). Mainly, the measured temperature change is obtained from a set of *n* measurements, $\Delta T_1, \Delta T_{2\ldots} \Delta T_n$ expressed as:

$$\Delta T_{measured} = \frac{\Delta T_1 + \Delta T_2 + \cdots \ \Delta T_n}{n} \tag{3.13}$$

$$\Delta T_{temp} = \Delta T_{measured} \pm \frac{\sigma}{\sqrt{n}} \tag{3.14}$$

Where $\Delta T_{measured}$ is the measured temperature change, σ is the standard deviation of the measurement error, and *n* is the number of samples or the number of measurements. The system performs a number of scans, and each scan measures the temperature of the monitored pipeline and records the temperature at each point along the pipeline. At the end of the scanning, the averages of measured temperatures as well as the variance of measurement errors are taken.

3.3.2 Probability Density Function of the Noise Signal

Figure 3.6 depicts the probability density for noise power. As shown in the figure, the shaded area on the right represents the failure region. This is the probability that the noise power (measurement error) exceeds the predetermined threshold. The threshold represents the minimum power level or the minimum detectable temperature change.

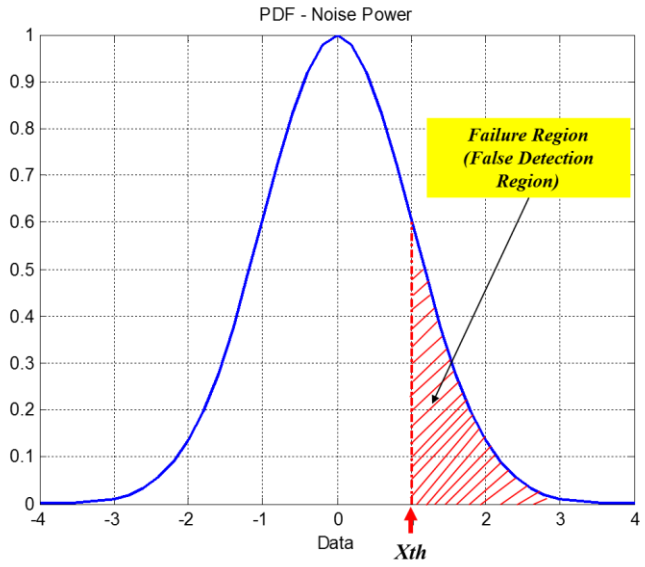

Figure 3-6: Amplitude Distribution of the Noise Power Signal

The PFA is expressed in terms of the threshold and the noise power level (σ^2). The threshold will be either the lowest detectable power or the lowest detectable temperature change. The main task of the system is to detect if the received signal power level has exceeded the threshold. Therefore, to determine the PFA, the threshold and the number of data samples need to be determined. Assuming that the noise power level (σ^2) is known

from previously recorded data for a large population, then the noise level for the sample of interest is σ^2/n, the standard deviation is $(\sigma/\sqrt{n})$, where n is the number of data samples. There is a PFA for every threshold value. The mean of the noise signal is zero because the summation of the amplitudes of the noise power is zero. This is because the noise power signal levels vary and, as a result, the summation of the different signal levels becomes zero. When the measured signal level is greater than the threshold change, a false alarm will be declared. Let us define $X_{th,}$ as the threshold power; then the probability of false alarm becomes:

$$PFA = \frac{1}{\sqrt{\frac{2\pi\sigma^2}{n}}} \int_{Xth}^{\infty} e^{\frac{-X^2}{2\sigma^2/n}} \, dX \tag{3.15}$$

Integrating Equation 3.15 yields:

$$PFA = \frac{1}{2}\left[1 - erf\left(\frac{Xth}{\sqrt{\frac{2\sigma^2}{n}}}\right)\right] \tag{3.16}$$

Where *erf* is the error function. The threshold power is calculated as:

$$Xth = \sqrt{\frac{2\sigma^2}{n}}\, erf^{-1}(1 - 2PFA) \tag{3.17}$$

Where erf^{-1} is the inverse of the error function, Xth is the threshold, σ^2 is the noise power, *n* is the number of measurements, and *PFA* is the probability of false alarm. Figure 3.17 illustrates the PFA for various threshold power values for a system that has a bandwidth (ΔV_B) of 25 MHz and a temperature coefficient (α_T) of 1.52 MHz/ºC. The figure reveals that as the threshold value increases the PFA decreases.

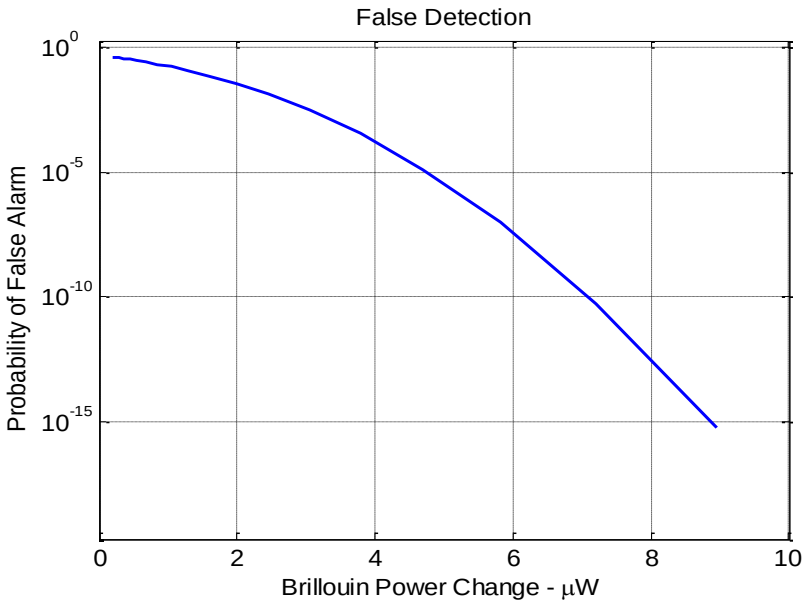

Figure 3-7: PFA for Various Changing Levels of Power

Figure 3.7 is re-plotted in Figure 3.8 to show the temperature change. This is for a system that has the same input data as indicated above and a temperature coefficient (*dP/dT*) of 0.9 mW/ºC.

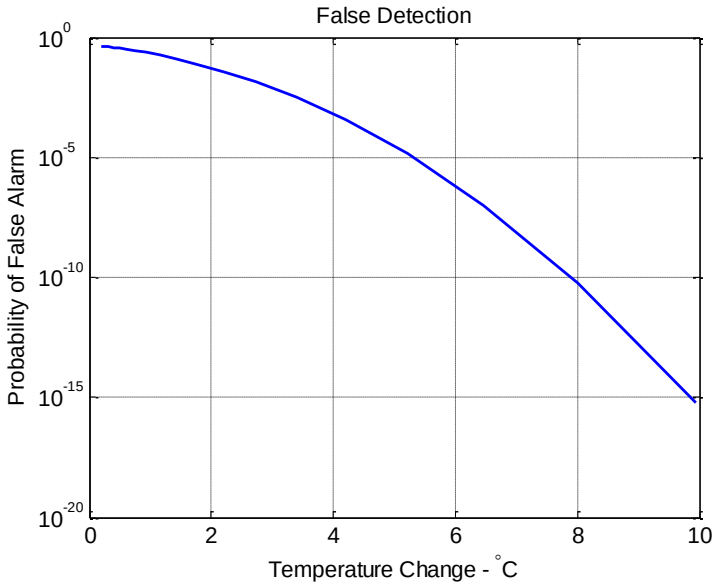

Figure 3-8: PFA for Various Temperature Values

3.3.3 Minimum Detectable Temperature by Fiber-Optic-Based LDS

The minimum detectable Brillouin frequency shift (δV_B) *as* a function of SNR is expressed in Equation 3.18 (Horiguchi et al., 1992).

$$\delta V_B = \frac{\Delta V_B}{\sqrt{2}(SNR)^{0.25}} \tag{3.18}$$

ΔV_B is the Brillouin spectral width of the Brillouin input signal and *SNR* is the signal to noise ratio. Using Equation 3.18 and Equation 3.4 and assuming zero strain, the minimum detectable temperature change δT can be expressed as 3.19 (Horiguchi et al., 1992):

$$\delta T = \frac{\Delta V_B}{\sqrt{2}\alpha_T (SNR)^{0.25}} \tag{3.19}$$

Where α_T is the temperature change coefficient expressed as MHz/ºC, and δV_B is the difference between the reference Brillouin frequency and the measured Brillouin frequency shift ($v_B - v_o$), as indicated in Equations 3.3 and 3.4.

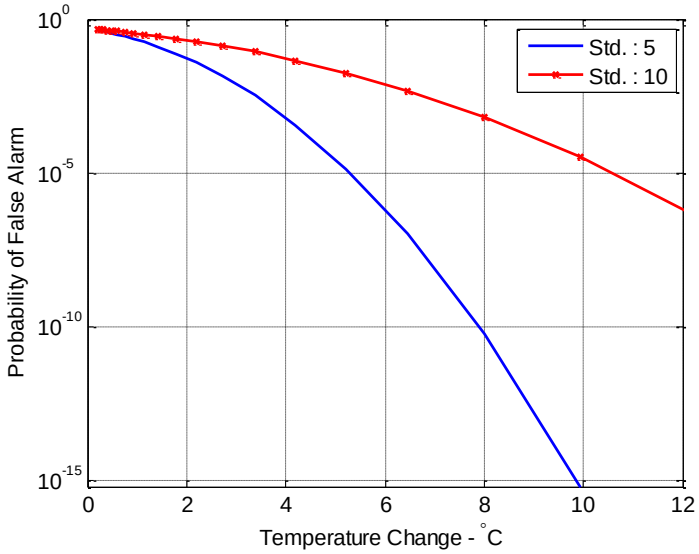

Figure 3-9: PFA for Various Temperatures Using Different Standard Deviation Values

For a system with α_T = 1.52 MHz/ºC, *SNR* = 21.18 dB, ΔV_B = 25 MHz, δT = 3.44 ºC, this is the minimum temperature change that can be detected by the system. From this, the minimum detectable peak power can be estimated using Equation 3.7. Assuming that the Brillouin reference power is 128 µW at a reference temperature of 5 ºC, with a power-

temperature coefficient 0.9 µW/ºC, the power threshold can be estimated to be 131.1 µW and the threshold power change to be 3.1 µW. The variance of measurement has an effect on the PFA, as indicated in Figures 3.9 (shown on logarithmic scale) and 3.10 (shown on linear scale); as the variance of the measurement increases the PFA increases. Basically, these two Figures illustrate the PFA versus temperature change using two different standard deviations of the measurements. As the figures reveal that the increase in the standard deviation leads to higher PFA.

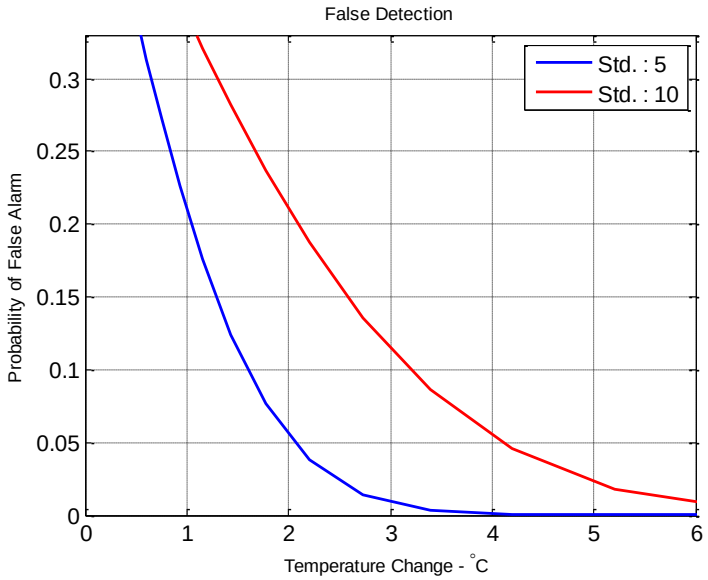

Figure 3-10: PFA for Various Temperatures Using Different Standard Deviation Values

Figure 3.11 illustartes PD versus PFA for different number of measurement samples, as the Figure indicates that a set that has 1000 samples of measurements at a PD value of 1 has a PFA value of 0.2133. At the same PD value of 1, a set of 100 samples of

measurements has higher PFA value of 0.3031. This indicates that the increase or decrease in the number of samples affects the PFA and PD. This is illustrated in these two Figures that as the size of the sample increases the PFA decreases.

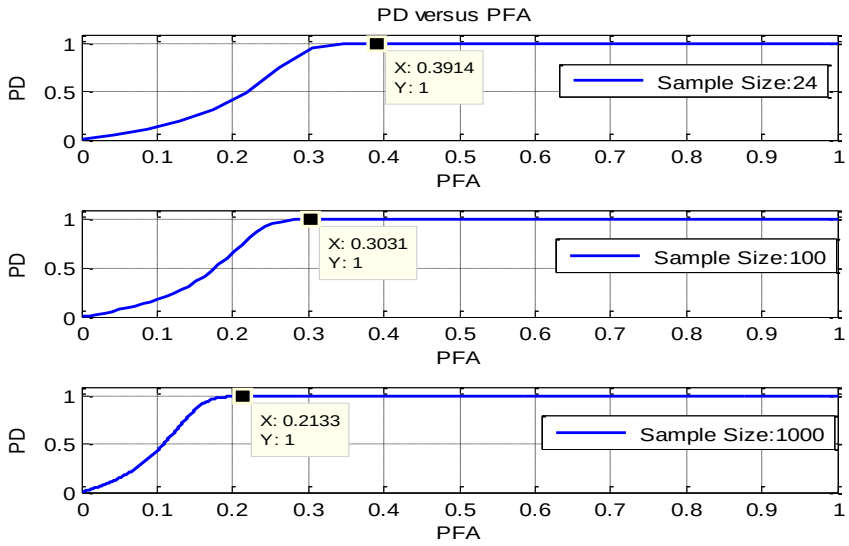

Figure 3-11: PD versus PFA Using Different Sample Sizes

3.4 PROBABILITY OF DETECTION AND MISSED DETECTION

The PD is the likelihood that the LDS will correctly detect an actual leak. The probability of missed detection (PMD) is the probability that the system will not declare an actual leak. The signal here is a combination of true signal power and noise power that respectively correspond to measured temperature change and the measurement error of the temperature change. Figure 3.12 shows the probability density for power signal plus noise. Detection

occurs in the event the measured signal power exceeds or is equal to the predetermined threshold.

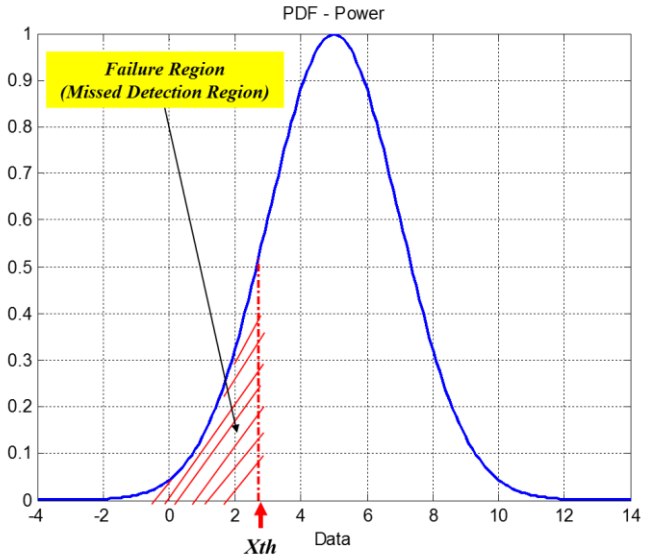

Figure 3-12: Amplitude Distribution of the Power Signal

Probability of missed detection *(PMD)* is expressed as:

$$PMD = 1 - PD \tag{3.20}$$

Let us define the lowest detectable power change as X_{th} and power change as X; then the PD can be expressed as:

$$PD = \frac{1}{\sqrt{\frac{2\pi\sigma^2}{n}}} \int_{Xth}^{\infty} e^{\frac{-(X-\mu)^2}{2\sigma^2/n}} dX \tag{3.21}$$

X_{th} is the threshold power level change and the μ is the mean value taken for every group of measurements, X is the amplitude that represents the measured power level of the incoming signal, and σ^2 is the noise power. Integrating the above equation, Equation 3.22 yields:

$$PD = \frac{1}{2}\left[1 - \ erf\left(\frac{Xth - \mu}{\sqrt{\frac{2\sigma^2}{n}}}\right)\right] \tag{3.22}$$

Four possible cases result from modeling the detection and false detection:

PD	:	*Leak exists and LDS indicates that a leak exists*	***- (hit)***
PMD	:	*Leak exists and LDS does not report the leak*	***- (miss)***
PFA	:	*Leak does not exist and LDS indicates it exists*	***- (false alarm)***
POCR	:	*Leak does not exist and LDS indicates it does not exist*	***- (correct rejection)***

Figures 3.13 and 3.14, respectively, show the PD versus the power level and temperature changes at a given threshold. As the figures illustrate, the PD is directly proportional to the power level and temperature changes: the greater the power or temperature changes the higher the PD. According to Equation 3.23, there are three parameters that need to be determined: the noise variance and the mean of the data samples, which are obtained from the characteristics of the received signal, and the threshold, which is determined as a function of PFA using Equation 3.16.

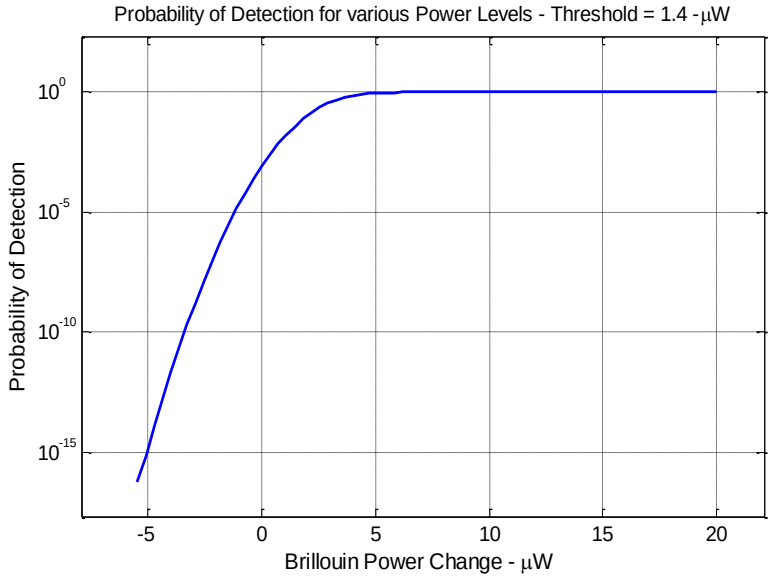

Figure 3-13: PD versus Signal Power Level Change

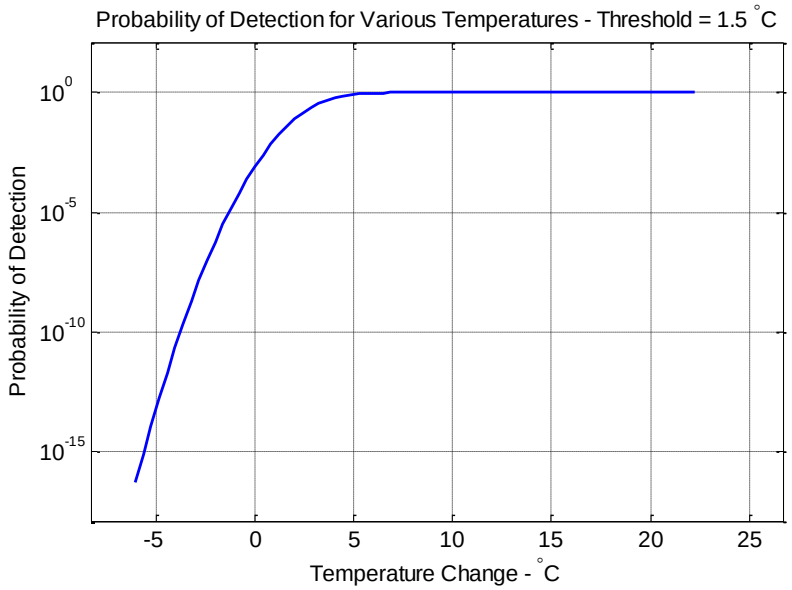

Figure 3-14: PD versus Signal Temperature Change

PD can be expressed in terms of PFA by substituting Equation 3.17 into Equation 3.22 to yield:

$$PD = \frac{1}{2}\left[erfc\left(erfc^{-1}(2PFA) - \frac{\mu\sqrt{n}}{\sqrt{2\sigma^2}}\right)\right] \tag{3.23}$$

Where *erfc* is the complementary error function and $erfc^{-1}$ is the inverse of the complementary error function. Referring to Equation 3.9, which is shown below as Equation 3.25, the power is μ^2 and noise power is σ^2/n.

$$SNR = \frac{\mu^2}{\sigma^2/n} \tag{3.24}$$

$$\sqrt{SNR} = \frac{\sqrt{n}\mu}{\sigma} \tag{3.25}$$

Equation 3.23 can be expressed in terms of SNR as:

$$PD = \frac{1}{2}\left[erfc\left(erfc^{-1}(2PFA) - \sqrt{\frac{SNR}{2}}\right)\right] \tag{3.26}$$

The PD can be expressed in terms of the threshold by substituting Equation 3.19 into Equation 3.22:

$$PD = \frac{1}{2}\left[1 - erf\left[\sqrt{\frac{n}{2\sigma^2}}\left(\frac{\Delta V_B}{\sqrt{2}\,SNR^{0.25}\alpha_T} - \mu\right)\right]\right] \tag{3.27}$$

Figure 3.15 illustrates that the PD increases with the increase of the temperature change. This means that there is higher probability of detection for higher temperature change. Another observation that can be noted is the increase of the SNR leads to a better PD and PFA tradeoff. Furthermore, the probability of detection is improved when the number of sample size (alternatively called scans) for one measurement gets larger. This is illustrated very clearly in Figure 3.17.

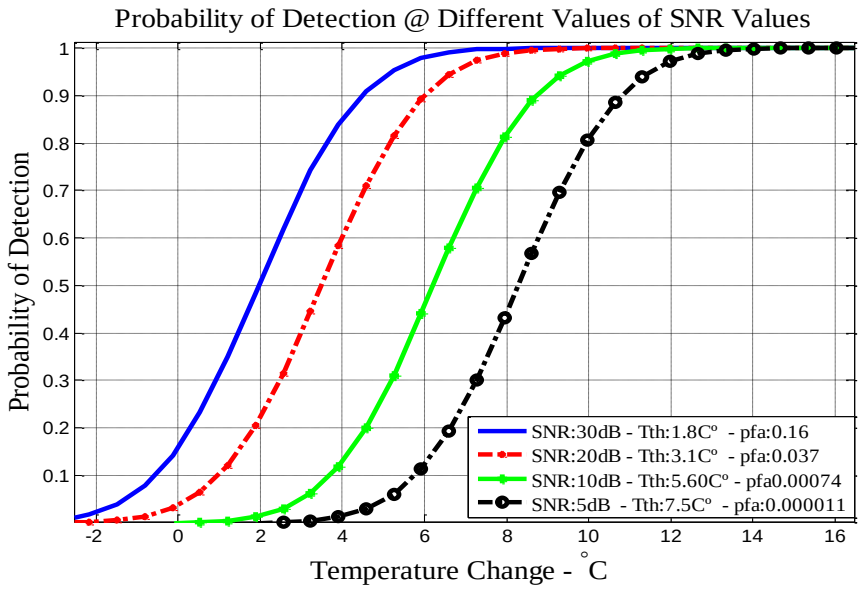

Figure 3-15: PD at Different Values of SNR

Figure 3.16 shows the relationship between PD and PFA—for every PD value there is a corresponding PFA value. The figure also illustrates that as the PFA increases, PD simultaneously increases.

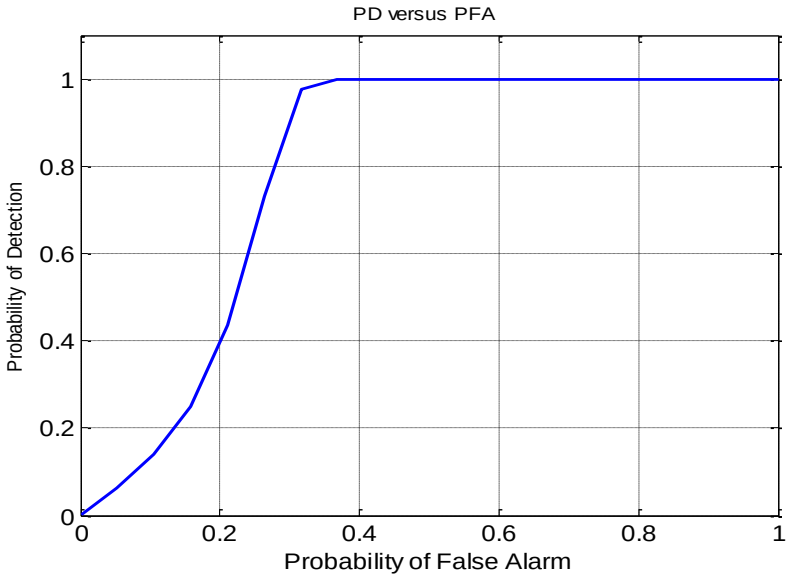

Figure 3-16: PD versus PFA

Moreover, the larger the sample sizes or number of scans, the better the SNR and PD values. Figure 3.17 illustrates that as the sample size increases the PD increases when the detected T is higher than the threshold.

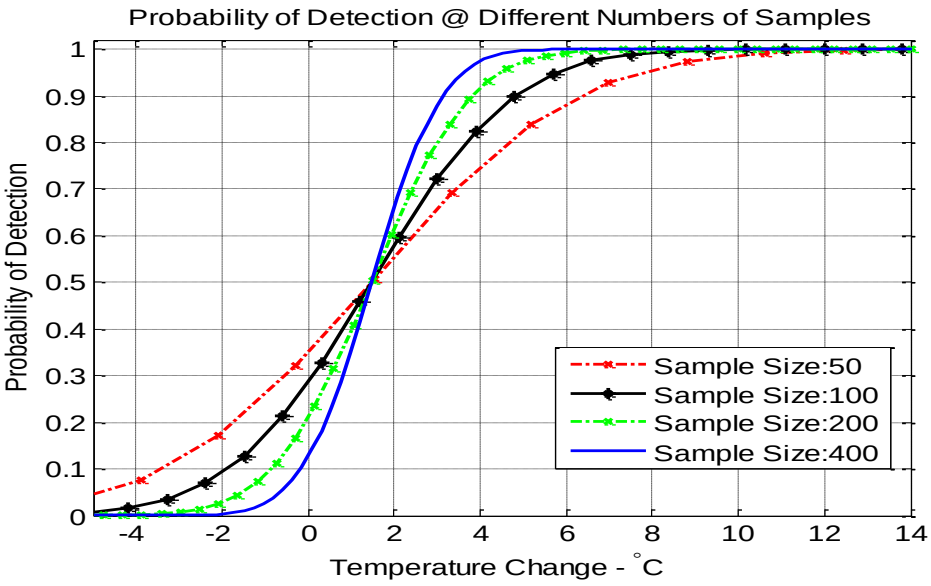

Figure 3-17: PD for Different Sample Sizes

3.5 TOTAL PROBABILITY OF MISSED DETECTION AND FALSE ALARM

The system is considered a series system because the failure of one LDS segment will lead to a complete failure of the system. Assuming the pipeline has n number of independent pump stations every 50 kilometers, where the station is equipped with an optical repeater to boost and regenerate the signal to achieve complete sensing coverage, then the total PMD (PMD_T) for the entire LDS can be expressed as:

$$PMD_T = 1 - \prod_{i=1}^{n}(1 - PMD)^n, \quad i = 1, 2, \ldots., n \tag{3.28}$$

Similarly, the total probability of false alarm (PFA_T) for the entire LDS can be expressed as:

$$PFA_T = 1 - \prod_{i=1}^{n}(1 - PFA)^n, \quad i = 1, 2, \ldots, n \tag{3.29}$$

3.6 SUMMARY

The PFA and the PD have been formulated and analyzed for a fiber optic-based LDS. The missed detection and false detection are both critical to the system performance, and the consequences of their occurrence cost time and money. The consequences of missed detection result in a greater financial burden than the consequences of false detection. Therefore, the first and foremost step in the design process is to determine the magnitude of the tolerable or acceptable risk in the event a missed detection takes place.

CHAPTER 4
PROBABILISTIC PERFORMANCE ASSESSMENT OF FIBER OPTIC LEAK DETECTION SYSTEMS

This part of the research develops a probabilistic performance assessment scheme based on limit state approach for the entire fiber optic LDS. The probabilistic assessment outcome includes the probability of failure for the entire LDS along the pipeline. The probability of failure encompasses detection failure and false detection. Detection failure is the combination of missed detection and delayed detection. Additionally, this chapter assesses the response time for the entire LDS along the pipeline. Probabilistic methods and Monte Carlo simulation have been used to accomplish the research that has been undertaken under this chapter. Matlab was used as a programming tool to run the assessment and simulation.

Overlap may exist between this chapter and chapter 3, but they address two different topics. Chapter 3 tries to present a formulation of the PD and the PFA and this chapter tries to determine these two parameters using the limit state approach. Essentially, this chapter demonstrates how the limit state approach can be used to calculate the probability of failure (probability of missed detection) for fiber-optic-based LDS. This is a departure from traditional approaches, where the limit state approach is strictly used in structural reliability. In the electronic domain, the same concept can be used to determine the reliability or the probability of failure. In the analysis, the operating voltage, or the achievable/operating sensitivity is considered to be the load, and the specified voltage or

sensitivity is considered to be the capacity. The load gets affected by the noise, inherent uncertainty of the electronic device, and some other external factors that affect performance. In the same manner, as elaborated in chapter 5, for the pipelines the limit state approach is used to calculate the probability of failure (the load there is the operating pipeline pressure and the capacity is the specified or design pressure). Likewise, for the corrosion the load is the measured corresponding depth at time *T* and the capacity is the specified critical corrosion depth.

4.1 LEAK DETECTION SYSTEMS

LDS play a major role in enhancing reliability and operability of oil and gas pipelines. They have the functional capabilities to detect, locate, and quantify leaks before they can cause drastic effects to environment and operation. LDS performance is typically affected by three types of failures that have severe consequences: delayed detection, missed detection, and false detection of a leak. These failures pose a financial burden on operating companies. For example, missed detection leads to oil spills and exposes operating companies to financial risk and destroyed image, while false detection results in unnecessary deployment of personnel and equipment. To ensure operation continuity and a safe environment, LDS should be assessed regularly. To fulfill this need, this research has developed a probabilistic performance assessment scheme based on limit state approach for fiber optic LDS. The inherent uncertainties associated with leak detection and reporting capabilities are modeled to determine the LDS detection failure probability that

combines two failure events, missed detection and delayed detection. Moreover, the probability of false detection is derived in terms of the lowest detectable change, the threshold. These three parameters, the probability of detection, probability of delayed detection and probability of false alarm establish the basis for an overall assessment scheme that can be used at any time to provide an up-to-date assessment of the LDS. The results will serve as the basis for deciding whether to upgrade, repair, or replace system components or the system as a whole. The proposed assessment scheme has been applied to a case study to demonstrate its usefulness and feasibility.

4.2 WHY LEAK DETECTION SYSTEMS NEED TO BE ASSESSED

The main task of any monitoring process in the oil and gas industry is to ensure that safety and integrity of the plant are intact at all times. Continuous monitoring provides timely information about the status of the monitored components and detects the existence of anomalies before they can cause catastrophic failures; such anomalies include cracks or corrosion that may eventually lead to pipeline rupture or leak. Fiber optic distributed sensing is one of the most promising technologies that can provide ongoing monitoring, with the ability to perform continuous sensing along the entire length of the monitored structure. The fiber optic acts as a sensor, providing sensing and advance warning capabilities in real time and on a continuous basis. LDS based on this technique work by comparing the temperature variations against a previously recorded baseline temperature. Any deviations from the baseline will indicate an abnormality has occurred. In this study,

the temperature change as the main determining factor for the presence of a leak will be studied using probabilistic methods.

Asset integrity guidelines mandate that the assets should perform their required functions in a safe, efficient, and effective manner (HSE, 2009). Therefore, there is a need to have a reliable and effective system to provide the assurances that the monitored pipeline is safe and functioning as per operating conditions. Hence, the behavior of the monitoring system should be assessed frequently and the assessment should take into consideration the probabilistic nature of the system.

Traditional assessment methods are deterministic and do not consider the probabilistic or random nature of the environment and its impact on the system. Due to the randomness, uncertainties exist and present a great challenge to the assessment. To deal with this challenge and be able to provide a measurable value of the performance, a probability based assessment approach should be adopted.

In light of the above, this research will apply a probabilistic assessment of key performance parameters for a fiber optic-based LDS. Factors that degrade the performance of a typical LDS include missed detection, delayed detection, and false detection. These failures will be grouped into detection failure, which is expressed in terms of missed detection and delayed detection, and false detection (or false alarm). The rationale behind these two

groups is that the failure consequences are different. Missed detection affects the ability of the LDS to detect a true leak while delayed detection influences the response time. And false detection affects system performance in terms of sensitivity.

4.3 DISTRIBUTED SENSING AND FIBER-OPTIC-BASED LDS

Distributed sensing technology can provide ongoing sensing capabilities along the monitored structure. As a result, systems based on this technology can provide early warnings of any abnormalities that may occur. One of the systems based on this technology is the fiber-optic-based LDS.

Fiber-optic-based LDS works by comparing the previously recorded baseline temperature with the measured temperature. If the transported product is oil, a higher than previously recorded temperature causes a signal to scatter back to the source, indicating the presence of a leak (Nikles, 2009). If the transported product is gas and the pipeline is leaking, the released gas will cool down the area surrounding the leaking spot, which will reduce the temperature than the previously recorded temperature, thereby causing the signal to scatter back to the source and indicate the presence of a leak.

4.3.1 FIBER OPTIC SENSING

One of the distributed sensing techniques is the Brillouin Optical Time Domain Analysis (BOTDA) (Soto et al., 2011), which is the focus of this section. It is widely used by the industry for condition monitoring and reporting.

BOTDA configuration, as shown in Figure 4.1, works by transmitting two different signals in opposite directions. The difference in the frequency of the two signals is used to measure strain and temperature changes along the sensing fiber optic cable. When the fiber is attached to an object, any changes in the object's temperature or the occurrence of any strain will affect the sensing fiber.

Figure 4-1: Simplified Illustration of BOTDA System

A linear relationship exists between the frequency shift, the temperature and strain changes that may occur along the sensing fiber. This relationship can be expressed as indicted in Equation 4.1 (Smith et al., 1999b; Bao et al., 2001; Brown, 2006).

$$v_B - v_o = \alpha_\varepsilon \Delta\varepsilon + \alpha_T \Delta T_{temp} \quad (4.1)$$

Where v_B is the Brillouin frequency shift, v_o is the reference Brillouin frequency at no strain and at the ambient temperature expressed in MHz, α_T is the temperature coefficient expressed in MHz/ºC, α_ε is the strain coefficient expressed in MHz/ μ ε , ΔT_{temp} is the temperature change, and $\Delta\varepsilon$ is the strain change.

The frequency shift is dependent on both temperature and strain, and thus it is difficult to determine which change has occurred along the fiber optic cable. The temperature change should be determined in order to conclude if a leak has occurred or not. To solve this issue, the fiber optic cable should be strain free; in other words, the fiber should be laid near the pipe, as indicated in Figure 4.2.

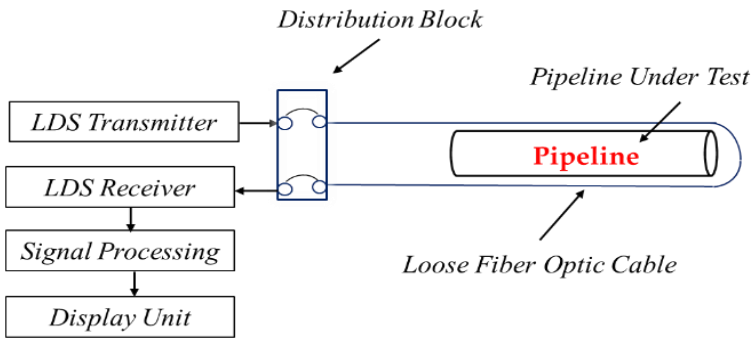

Figure 4-2: Configuration for Temperature Change Detection

The system sends a signal along the sensing fiber. If a leak takes place the returning signal will be shifted in frequency, which will indicate the presence of a leak and its location. From Figure 4.2, and Equation 4.1, the new relationship between frequency shift and temperature change becomes:

$$v_B - v_o = \alpha_T \Delta T_{temp} \tag{4.2}$$

The minimum detectable temperature change (ΔT_{temp}) in Equation 4.2 depends on spectrum bandwidth, signal-to-noise ratio (SNR), as well as the temperature coefficient (Horiguchi et al., 1992). This relationship is expressed in Equation 4.3. Let us define the minimum detectable temperature change (ΔT_{temp}) as δT, then the minimum detectable temperature change becomes (Horiguchi et al., 1992):

$$\delta T = \frac{\Delta v_B}{\sqrt{2}\,\alpha_T (SNR)^{0.25}} \tag{4.3}$$

Where δT is the minimum detectable temperature, Δv_B is the Brillouin spectral width, SNR is the signal-to-noise ratio, and α_T is the temperature coefficient change (expressed in MHz/ºC).

4.4 MODELING FAILURE

The main assumption of the performance assessment is that the parameters that influence the performance of the system vary and does not stay the same during operation. The capacity, or as it is sometimes called the resistance, is a design parameter that dictates the system's ability to deliver. It represents the maximum capability of the system to sustain the maximum operational load imposed on it. The variability of the level of capacity is mainly attributed to the inherent uncertainties associated with the operating characteristics and sometimes due to external factors that impact system performance. Thus, the capacity is assumed to be probabilistic. Using the same argument, the load of the system is also assumed to be randomly fluctuating.

These fluctuations result from varying operating conditions, operational demand, or environmental loads. Within this context, the performance function is defined as the difference between the capacity and the load. Since both are probabilistic, the performance is assumed to be probabilistic as well. Referring to Figure 4.3, the probability of failure can be computed as (Nowak & Collins, 2000):

$$P(\ Failure) = P(C < L) \tag{4.4}$$

Where L is the load and C is the capacity or resistance of the system. Equation 4.4 expresses the fact that the probability of failure is a conditional probability and encompasses all possible combinations of $L = x$ and $C < L$; x is a specified limit value that the load should not exceed (Nowak & Collins, 2000). Considering this fact, Equation 4.4 yields (Nowak & Collins, 2000):

$$P_f = \Sigma P(C < L|L = x)P(L = x) \tag{4.5}$$

Figure 4.3 illustrates the PDF of both the load and resistance. The probability of failure can be estimated by taking into consideration the PDFs of the load and resistance. Referring to Figure 4.3, the summation in Equation 4.5 can be evaluated as an integral to yield:

$$P_f = \int_0^{\infty} F_C(x)\, f_L(x) dl \tag{4.6}$$

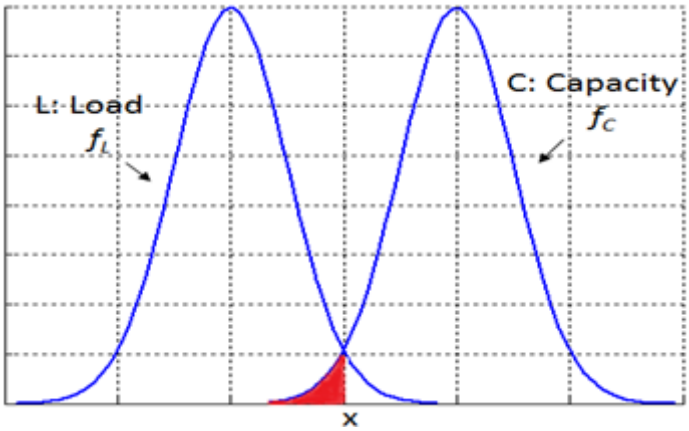

Figure 4-3: Probability Density Functions of Load and Resistance

Equation 4.6 defines the probability of failure; the parameter $F_C(x)$ is the Cumulative Distribution Function (CDF) of the capacity (C) evaluated at *x*; and $f_L(x)$ is the Probability Density Function (PDF) of load (L) evaluated at *x.* The load that needs to be evaluated for all possible values of *L* is random, which is represented by the PDF, $f_L(x)$. An alternative approach for evaluating the integral is to use limit state functions (LSF), as indicated in Equations 4.7–4.14 (Haldar & Mahadevan, 2000; Nowak & Collins, 2000) using limit state function (LSF) and Monte Carlo simulation techniques.

An LSF represents the shift from desirable or safe operation to undesirable or unsafe operation (failure). In essence, it defines the difference between the capacity and the load of the system. If the difference between the capacity and load is positive, the system is in a safe operating state. If it is zero, the system is at the limit state; if negative, the system is at a failure state.

Two methods are presented in this thesis: sample statistics and counting method. Equation 4.7 expresses the LSF as the difference between the capacity (*C*) and the load (*L*), which is formulated as:

$$Z = C - L \tag{4.7}$$

Where Z is the performance function, C is the capacity of the system, and L is the load imposed on the system. The probability of failure (P_f) is defined in Equation 4.8. It defines the event when the specified capacity goes below the load of the system; at such an event, the LSF is violated.

$$P_f = P(Z < 0) \tag{4.8}$$

Equation 4.8 can be rewritten as:

$$P_f = P(C < L) \tag{4.9}$$

This is the probability of failure that represents the event when the capacity becomes less than the load. Using Equations 4.7 and 4.8, the probability of failure can be expressed as:

$$P_f = \Phi\left(\frac{0 - (\mu_C - \mu_L}{\sqrt{\sigma_C^2 + \sigma_L^2}}\right) \tag{4.10}$$

Where μ_C is the mean of the capacity of the system, and μ_L is the mean of the load imposed on the system, σ_C^2 and σ_L^2 are the variances of the capacity and the load respectively. Solving Equation 4.10 to yield:

$$P_f = 1 - \Phi\left(\frac{(\mu_C - \mu_L}{\sqrt{\sigma_C^2 + \sigma_L^2}}\right) \quad (4.11)$$

The reliability index is taken as the difference between the means of the capacity and the load divided by their standard deviations and is designated as *β:*

$$\beta = \frac{\mu_z}{\sigma_Z} \quad (4.12)$$

The reliability index is computed for every failure mode, where the probability of failure is expressed as:

$$P_f = \phi(-\beta) = 1 - \phi(\beta) \quad (4.13)$$

Alternatively, the probability of failure is calculated when the LSF is less than zero using Monte Carlo simulation. Let us define N_f to be the number of simulation trials when the LSF is less than zero and N is the total number of simulation trials. Then the probability of failure can be expressed as:

$$P_f = N_f/N \quad (4.14)$$

4.5 DETECTION FAILURE AND LIMIT STATE FUNCTIONS

Detection failure comprises two key components: missed detection and delayed detection. Missed detection occurs when a leak takes place and the system fails to detect it. The lowest detectable temperature change is the determining factor for leak detection. Application of the concept discussed above in section 4.3 to model the failure for an LDS will result in two limit state functions (LSFs), one for missed detection and the other for delayed detection.

4.5.1 Missed Detection

When the system senses that the amplitude of the signal coming back to the source is equal to or exceeds the threshold (that is, the lowest detectable change), an alarm is declared to indicate the presence of a leak. A missed detection occurs when the system fails to estimate this change correctly. The LSF for the missed detection is defined in terms of parameters that are probabilistic that include, power, noise power, temperature coefficient and the operational temperature change threshold. The first three parameters belong to the specified threshold. All these parameters represent the sources of uncertainties in the missed detection LSF. The LSF for detection is formulated as:

$$Z_1 = \alpha_{Specified} - \alpha_{Operating} \tag{4.15}$$

Where $\alpha_{specified}$ is the minimum detectable change in temperature, and $\alpha_{operating}$ is the operational temperature change threshold at a given point in time. In other words, $\alpha_{operating}$ is the attainable threshold by the system. The specified minimum detectable change represents the capacity, i.e., the minimum temperature change that can be detected by the system. The specified minimum detectable change is a design parameter that the system should be able to detect.

The operating minimum detectable temperature change represents the load. In this case, the system has been adjusted to provide detectability for the lowest temperature change, $\alpha_{operating}$. This is the demand or the load imposed on the system, which varies due to inherent uncertainties associated with the system. Variability in the noise levels is a major factor that affects the quality of the signal.

As indicated in Equation 4.3, the minimum detectable temperature (δT) is basically the specified minimum detectable temperature change. Substituting Equation 4.3 into Equation 4.15 yields:

$$Z_1 = \frac{\Delta v_B}{\sqrt{2}\,\alpha_T (SNR)^{0.25}} - \quad \alpha_{Operating} \tag{4.16}$$

The SNR is the signal-to-noise ratio. Noise is the standard deviation from the mean power of the incoming signal (Ravet, 2011), while the temperature accuracy is specified as twice the standard deviation, as per the specifications for fiber optic distributed strain and temperature sensors (OZ Optics, 2013).

4.5.2 Delayed Detection

The response time consists of three elements: pulse transmission time, signal-processing time, and the response time of the fiber optic cable to the temperature change (Liu et al., 2003). The pulse transmission time is the time it takes to make one measurement of the temperature. The total pulse transmission time is dependent on the number of measurements made; in other words, it is the measurement time. The response time can be expressed as:

$$R.T. = t_{TPT} + t_{SP} + t_{FRT} \tag{4.17}$$

R.T. is the response time, $t_{TPT}$is the total pulse transmission time, t_{SP} is the signal processing time, and t_{FRT} is the fiber optic cable response time. The measurement time (t_M), which is the total pulse transmission time, is given by Mahar (2008):

$$\textit{Measurement Time} = \textit{(No. of Measurements)} \text{ x } (t_{PTi}) \tag{4.18}$$

t_{PTi} is the pulse transmission time for a single measurement; it is expressed as a function of the fiber optic refractive index, distance, and speed of light in vacuum, which can be expressed as:

$$t_{PTi} = \frac{2n\Delta z}{c} \tag{4.19}$$

Where n is the refractive index of the fiber core, Δz is the fiber optic cable length in kilometers, and c is the speed of light (km/s) in vacuum.

For a 100-km fiber, fiber optic refractive index is 1.5, speed of light in vacuum is 3e8 m/s, and pulse transmission time ($t_{PTi} = 2n\Delta z/c$) is 1 millisecond. For a system programmed to make 1,000 measurements at a time, the measurement time or the total pulse transmission time will be (1e-3 s x 1,000 measurements = 1 second).

Signal processing time (t_{SP}) can take a few milliseconds and is dependent on the system design and specifications, and how fast the algorithm processes the signal. The fiber optic response time to temperature change is in the nanoseconds range and can be ignored.

Considering the above example, assuming a signal processing time for every scan or measurement to be 10 milliseconds, then the response time (*R.T.* = pulse transmission time + data processing time + fiber's response time) will be 11 seconds.

The delayed detection causes missed detection for a period of time during which the system fails to detect the change. This occurs when the reading is displayed to be below the specified threshold. The limit state function for the response time can be formulated as shown below:

$$Z_2 = t_{Specified} - t_{Operating} \tag{4.20}$$

Where $t_{specified}$ is the maximum specified response time (assumed to be a constant value), and $t_{operating}$ is the operating response time at a given time. Only one element of the response time is assumed to be random, the data processing time. The time it takes to process the data is affected by the type of algorithm used and by internal electronics. $t_{operating}$ is the demand imposed on the system; this demand varies due to inherent uncertainties associated with the electronic components of the system and the thermal noise that affects performance. All these factors influence the performance of the system and create a varied response time. Substituting Equation 4.17 into Equation 4.20 yields:

$$Z_2 = (t_{TPT} + t_{SP} + t_{FRT}) - \quad t_{Operating} \tag{4.21}$$

Therefore, missed detection and delayed detection are two elements that cause detection failure.

4.6 PROBABILITY OF FAILURE

The delayed detection and missed detection events cannot occur simultaneously. This is due to the fact that during the delayed detection event, the detection will be delayed for a while before the system detects the leak, while for the missed detection event, the detection is missed altogether. Thus, the two events are mutually exclusive. Let us denote the missed detection event as MD, the delayed detection event as DD, and false detection (false alarm) as FA. Then the probability of failure becomes:

$$PD_f = P(MD \cup DD) \ = P(MD) + P(DD) \tag{4.22}$$

Assuming the sensing range is 50 km, then at every interval of 50 km there will be an optical amplifier to boost and regenerate the signal. If the pipeline has *n* independent stations, then the total probability of detection failure is computed as a series system (Ebeling, 1997):

$$Pf_{LDS} = 1 - (1 - PD_{f1})(1 - PD_{f2}) \dots (1 - PD_{fn}) \quad (4.23)$$

Where Pf_{LDS} is the LDS total probability of detection failure and $PD_{f1} \dots \dots PD_{fn}$ are the LDS probability of detection failure for each segment of the pipeline. The false alarm is formulated in the same manner as:

$$PFA = 1 - (1 - PFA_1)(1 - PFA_{2n}) \dots (1 - PFA_n) \quad (4.24)$$

The flow chart in Figure 4.4 shows that the probability of failure is calculated using two Monte Carlo simulation methods: the sample statistics method and the counting method.

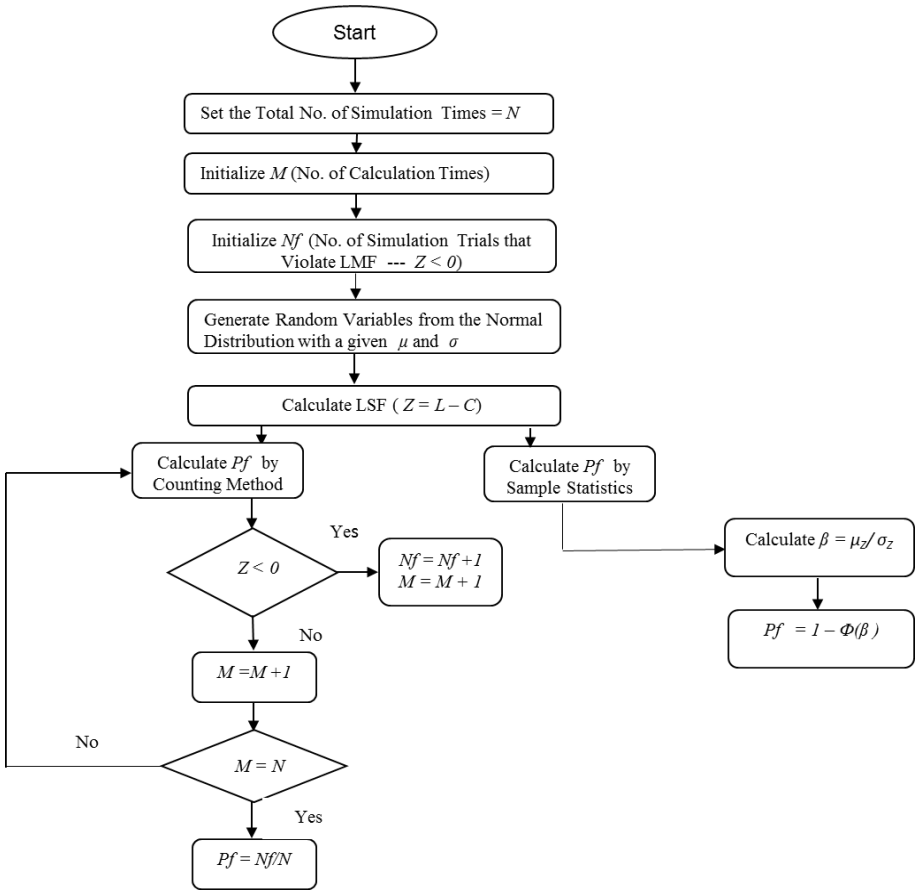

Figure 4-4: Flow Chart for the Probability of Failure Simulation

4.7 CASE STUDY

A fiber optic LDS was installed along a 1,000-km pipeline that has regeneration units installed at every 50 km. It has been specified to have a probability of false alarm of 0.0007. The LDS Threshold parameters including power, noise power, temperature coefficient, and bandwidth (Smith, 1999a) are provided in Table 4.1. Moreover, the table provides the parameters for the DATA processing time; these parameters were assumed based on (OZ

Optics, 2013). The probability distribution for each parameter as indicated in the Table were assumed. All the given data represent typical specifications used by the industry for such systems. Figure 4.5 depicts the layout of the pipeline system and the LDS. The fiber optic LDS has the cable laid on the top and bottom of the pipeline to increase the coverage and sensitivity of detection.

Table 4-1: Capacity and Load Variables

Variables	Units	Mean	S.D	Distribution
1.0 Capacity				
1.1 Threshold Temperature				
Bandwidth: $\Delta V_{B,}$	MHz	35		Deterministic
Power: P	μW	1	0.013	Normal Distribution
Noise: N	mW	0	0.013	Normal Distribution
Temperature Coefficient: α_T	MHz/C˚	1.1	0.014	Normal Distribution
1.2 Data Processing Time				
Data Processing Time: t_P	ms	10	0.1	Normal Distribution
2.0 Load				
Lowest Detectable Temperature	C˚	2.4	0.04	Normal Distribution
Signal/Data Processing Time	ms	10.2	0	Deterministic

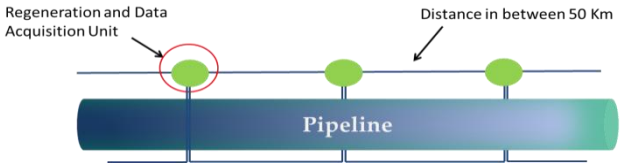

Figure 4-5: Schematic of the Pipeline and the LDS Under Study

The following assumptions were considered in the case study:

- The signal bandwidth is maintained at a fixed value of 35 MHz and is assumed to be deterministic.

- The signal power of the incoming signal is kept at 1 μW; this power corresponds to the lowest detectable temperature and is assumed to follow normal distribution.

- The variance of the power is the noise power, which is 0.013^2 μW.

- The noise signal is assumed to follow normal distribution with a mean of 0 and standard deviation of 0.013. The noise power fluctuates up and down, the summation of the amplitudes is zero, and therefore the mean is equal to zero.

- From the given power and the noise power we can determine that the SNR = P/N for the lowest detectable temperature; in this example SNR = 38 dB.

- The temperature coefficient is assumed to follow normal distribution with a mean of 1.1 MHz/ºC and variance of 0.014. There is a 1.1 MHz change for every 1 ºC.
- Signal processing time is the time required to process the data contained in the signal by the system. It follows a normal distribution with a mean value of 10 ms for the entire length of each pipeline segment of 50 km.

4.8 RESULTS AND DISCUSSION

The failure probabilities and reliability indices shown in Table 4.2 were calculated and simulated according to the flow chart shown in Figure 4.4. Table 4.2 shows the calculated probability of missed detection and delayed detection using sample statistics (using reliability index β) and counting method (*Nf/N*).

Table 4-2: Simulation Results

		PMD	
Simulation Cycles	***β***	***Pf =1 – Φ(β)***	***Nf/N***
7.00E+03	3.217	0.013	0.023
1.00E+05	3.240	0.012	0.011
1.00E+07	3.239	0.012	0.009
PDD			
Simulation Cycles	***β***	***Pf =1 – Φ(β)***	***Nf/N***
7.00E+03	3.017	0.025	0.034
1.00E+05	3.005	0.026	0.030
1.00E+07	3	0.027	0.027
PDf			
Simulation Cycles	***Pf***	***Nf/N***	
7.00E+03	0.038	0.056	
1.00E+05	0.038	0.041	
1.00E+07	0.038	0.036	

The estimate of the probability of failure approaches true value as N approaches infinity. The results indicate that the estimated probabilities of missed detection, delayed detection, and detection failure by the counting method converge to 0.009, 0.027, and 0.036, respectively.

Figures 4.6, 4.7, and 4.8 illustrate the probability of failures associated with delayed detection, missed detection, and detection failure, respectively. The probabilities are shown for various lengths of the pipeline with varying number of simulation cycles. The figures indicate that as the length of the pipeline increases, the probability of failure increases.

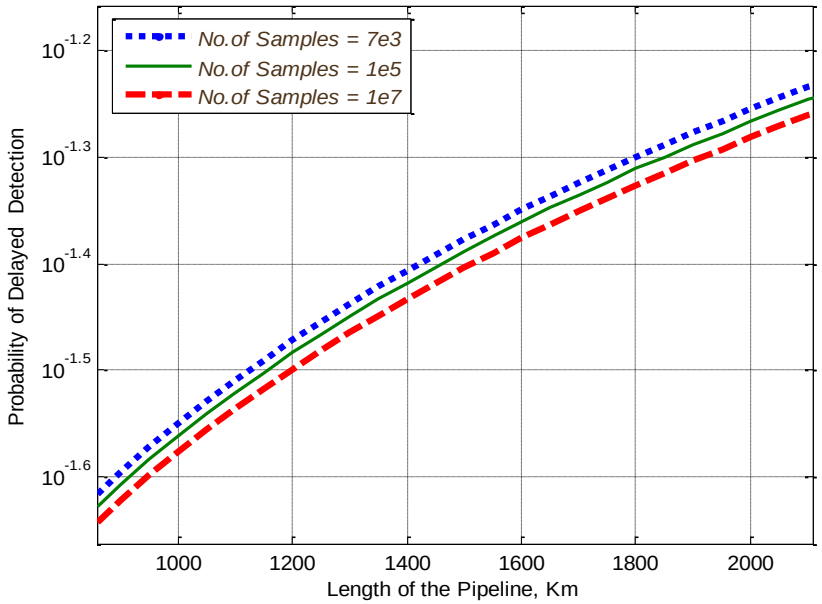

Figure 4-6: Probability of Delayed Detection

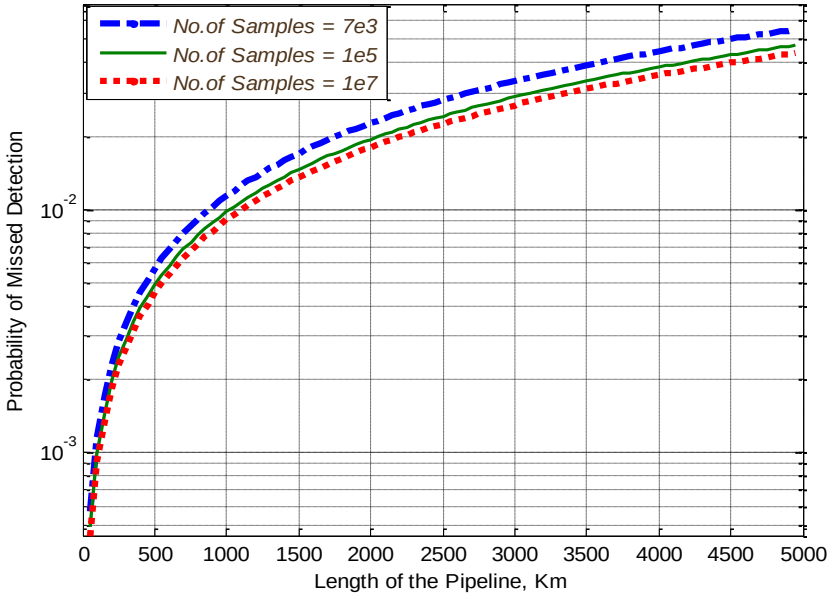

Figure 4-7: Probability of Missed Detection

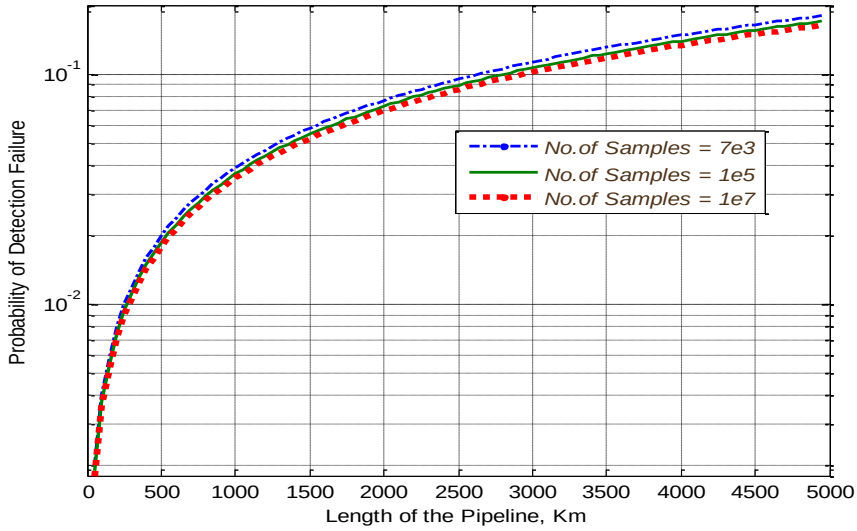

Figure 4-8: Probability of Detection Failure

Figure 4.9 depicts the probability of detection failure for the 1,000-km pipeline for three different simulation cycles: 7e3, 1e5, and 1e7.

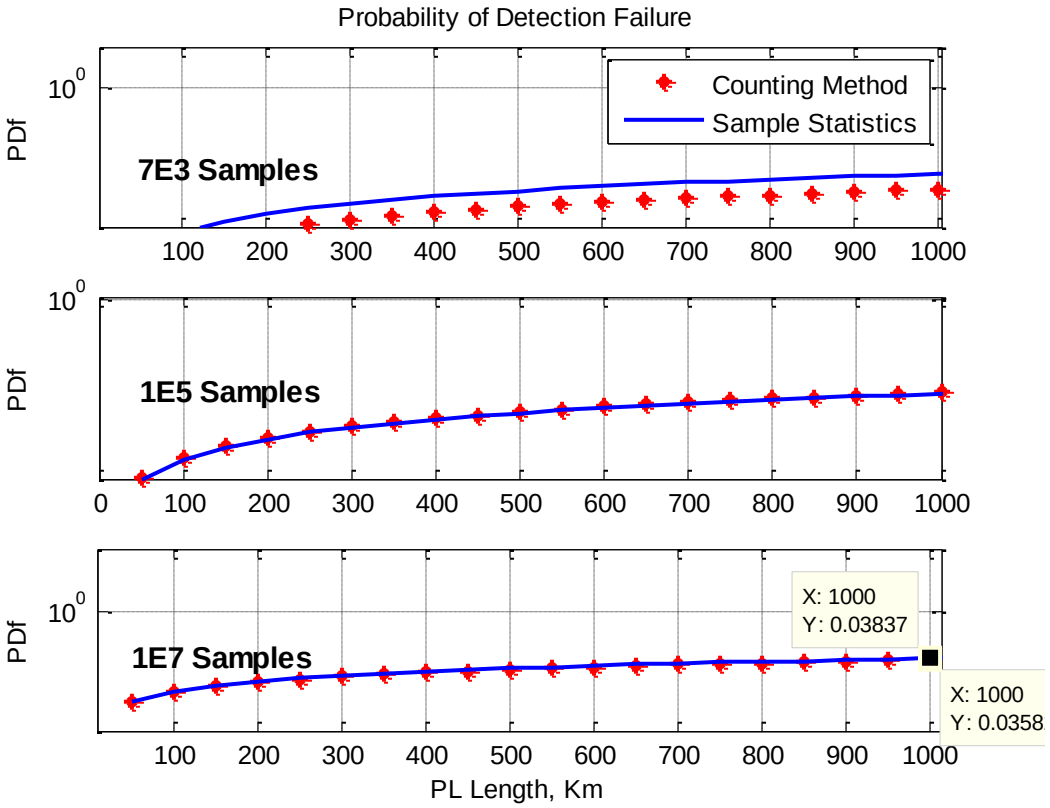

Figure 4-9: Probability of Detection Failure versus Distance

The figure reveals that the counting method and sampling method are in very close agreement. Figure 4.10 shows that the probability of false detection increases with the increase in the length of the pipeline. Usually the probability of false detection is a given parameter as part of the specifications; the PFA is given as 0.0007 in the case study.

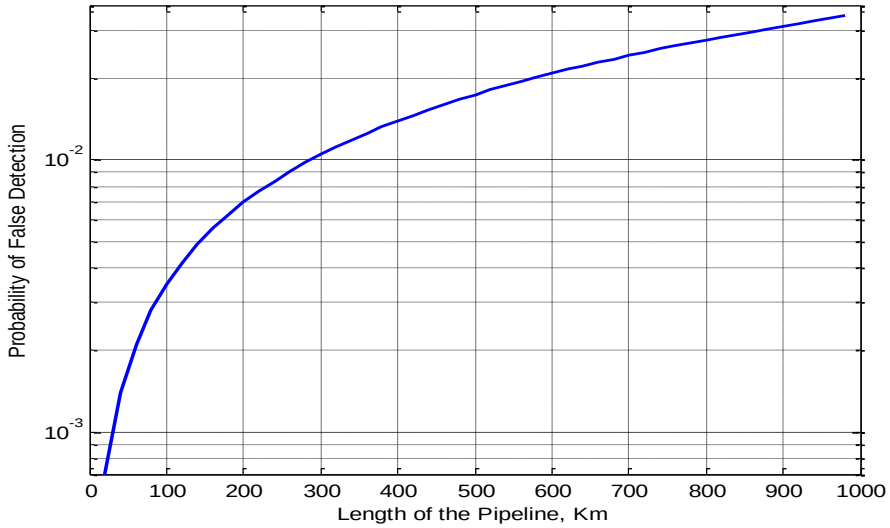

Figure 4-10: Probability of False Detection versus Distance

The effect of the coefficient of variation (CoV) on the probability of missed detection and delayed detection is obvious, as shown in Figures 4.11 and 4.12, respectively. These figures show that the calculated probability of missed detection and delayed detection are in close agreement for both the counting and sample statistics methods. It is evident from these figures that as the CoV is varied the probability of missed detection or delayed detection both increase with the increase in the length of the pipeline.

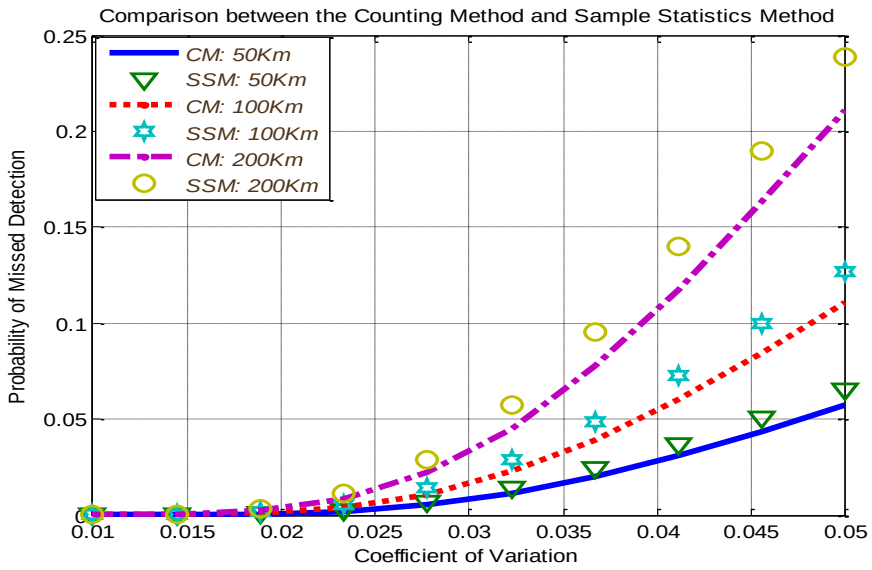

Figure 4-11: Sensitivity of Probability of Missed Detection Due to Changes of CoV for the Temperature Coefficient

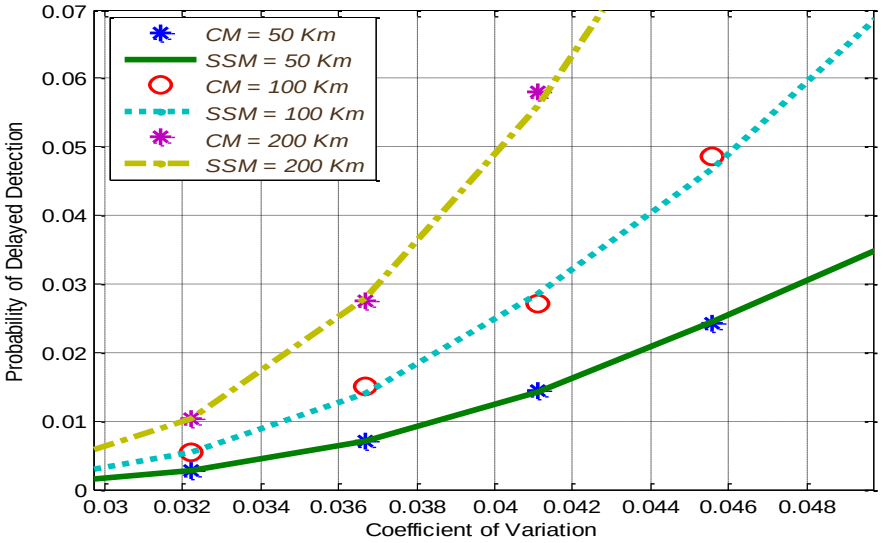

Figure 4-12: Sensitivity of Probability of Delayed Detection Due to Changes of CoV for the Data Processing Time

4.9 SUMMARY

A probabilistic methodology based on limit state approach for assessing the performance of fiber optic LDS has been developed. The detection failure and false detection establish the basis of an overall assessment scheme. The limit state equations were formulated on the assumption that the capacity and load are probabilistic as they are affected by the varying operational demand and the environmental conditions. From the study, it was found that the sample statistics technique and the counting method for calculating the probability of failure almost produce the same results.

CHAPTER 5
APPLICATION OF PROBABILISTIC METHODS FOR ASSESSING THE INTEGRITY OF OFFSHORE PIPELINES

This chapter presents and applies a developed probabilistic methodology for assessing the integrity of a pipeline and determining its probability of failure. The probability of failure is compared against a target probability of failure to determine the remaining life of the assessed pipeline. A limit state approach in conjunction with Monte Carlo simulations and failure pressure models available in codes and standards have been used to accomplish this task. Matlab software was used as a programming tool to run the simulation and analysis.

5.1 WHY CONDUCT PROBABILISTIC ASSESSMENT OF AGING PIPELINES

When offshore pipelines approach the end of their design life, their condition could threaten oil flow continuity as well as become a potential safety or environmental hazard. Hence, there is a need to assess the remaining life of pipelines to ensure that they can cope with current and future operational demand and integrity challenges.

This chapter presents a methodology for assessing the condition of aging pipelines and determining the remaining life that can support extended operation without compromising safety and reliability. Applying this methodology would facilitate a well-informed decision that enables decision makers to determine the best strategy for maintaining the integrity of aging pipelines.

5.2 INTEGRITY ASSESSMENT OF AGING PIPELINES

One of the main objectives for carrying out an assessment on an aging pipeline is to ensure that it is safe to operate and does not pose any threat to the environment, operations, or safety. Other objectives might be to increase the pipeline life beyond its design life in order to accommodate unforeseen oil and gas reserves, support increased oil and gas production, or incorporate new assets that are tied into the existing pipeline system. Some circumstances may require operators to maintain the pipeline's design life even though there may be unexpected premature aging caused by increased corrosion growth or any other anomalies.

A strong case exists that mandates the assessment of the remaining life of an aging pipeline in order to determine its ability to cope with current and future integrity challenges. This is where probabilistic methods are useful in assessing pipeline fitness for service and predicting remaining life based on the current condition.

The initial step in the assessment process is to determine the failure modes. The next step is to define the limit states. The failure modes represent degradation mechanisms, i.e., corrosion, cracks, or other flaws, while the limit state represents the failure events, i.e., the leak or rupture of the pipe.

The probability of failure is estimated by probabilistic modeling in terms of the failure modes where uncertainty is included in the estimation. The Monte Carlo simulation method is used to assess and analyze the probabilistic characteristics of the random variables and then determine the probability of failure, either by sample statistics or by counting methods (Haldar & Mahadevan, 2000).

Uncertainty in the collected inspection data, pipeline geometry, pipeline material properties, and operating characteristics present a great challenge to the analysis. A probability-based assessment approach was adopted as it is best suited to deal with uncertainty, where a quantifiable value of the probability of failure can be estimated (Lindley, 1982).

The assessment study should take into account, but not be limited to, pipeline original design parameters, operations history, previous inspection data, extent of metal loss, corrosion rates, fatigue damage, coating breakdown, and cathodic protection degradation (ISO/TS 12747, 2011).

This chapter presents a methodology that adopts probabilistic methods for assessing the current and future ability of pipelines to support operational demand without jeopardizing safety and reliability. Based on the outcome of the assessment, the pipeline fitness for

service as well as the remaining life is determined. The methodology is tested by a case study to demonstrate its applicability.

Section 5.3 provides an overview of pipeline remaining life assessment; section 5.4 briefly discusses the pressure failure models, as recommended by various internationally recognized codes and standards; section 5.5 discusses the methodology undertaken to assess the pipeline remaining life; section 5.6 presents a case study; and section 5.7 provides the results and discussion. Finally, summary and concluding remarks are presented in section 5.8.

5.3 OVERVIEW OF REMAINING LIFE ASSESSMENT

Remaining life is estimated as the time it takes the pipeline system to exceed the target failure probability. For an oil and gas pipeline to continue operating safely and reliably, a repair or replacement strategy should be in place that becomes readily available for implementation before the occurrence of failure.

Sometimes de-rating the operating pressure might be the most viable option to extend the life of an aging pipeline. A corrosion flaw is the main contributor that accelerates the deterioration of pipelines. It reduces the pipeline strength over time, leading to premature failure and subsequently potential environmental damage and production losses. Every

corrosion flaw point along the pipeline can potentially lead to either a failure, resulting from the flaw penetrating the pipeline wall, or a burst when the internal operating pressure exceeds the maximum allowable pressure. Corrosion is the second leading cause of pipeline failure in Europe, the first cause being third-party interference (EGIG, 2011). Fifty percent of "loss of containment" events in Europe have been attributed to corrosion and other degradation mechanisms (HSE, 2010). Between 1996 and 2013, there were about 3,616 offshore loss of containment incidents, as indicated by the U.K. HSE (2014).

According to U.S. Department of Transportation – Pipeline & Hazardous Materials Safety Administration (PHMSA) there were about 10,620 pipeline-related incidents from 1994 to 2013. Nearly 18.2% of these incidents were attributed to corrosion, causing 23 fatalities, 77 injuries, and property damage costing $750,433,953. Out of these corrosion incidents, there were about 170 property damage offshore-related incidents costing nearly $49,335,245 (PHMSA, 2014).

Deteriorating pipelines may fail and the consequences of their failures may have an impact on health, safety, and the environment. Assessment techniques such as structural reliability–based analysis is applied to determine the extent to which the asset life could be increased beyond the design life for a high-pressure natural gas pipeline having both onshore and offshore sections (Francis, Gardiner, & McCallum, 2002).

The available codes and standards can be used for assessing pipeline integrity and determining remaining life. However, the codes and standards follow a deterministic approach for calculating the different parameters that are part of the assessment. Furthermore, the methods presented in these codes and standards calculate the pressure failure only. Moreover, these methods are for general cases and are not site specific, as every pipeline is unique in terms of its geographic location, operating conditions, and operational demand. Considering these limitations, this chapter introduces a generic probabilistic method to reduce the uncertainties involved in the remaining life assessment by comparing several codes and standards.

5.4 CODES AND STANDARDS

Some of the codes and standards that could be used for assessing the remaining life of the pipeline include DNV (DNV-RP-F101, 2010); American Society of Mechanical Engineers, (ASME B31G, 2012); British Standards (BS-7910, 2005); and American Petroleum Institute (API-579-1, 2007). The recommended failure pressure models incorporated in some of these standards are discussed in section 6.4.

This assessment focuses on corrosion flaws. There are three different categories of flaws: single flaw, interaction flaw, and complex-shaped flaw. A single flaw is one that does not interact with nearby flaws and it has its own failure pressure. An interacting flaw interacts

with other flaws in the same area, either axially or circumferentially, and the complex-shaped flaw is a collection of groups of interacting flaws (DNV-RP-F101, 2010).

The scope of this study focuses on the assessment of a single corrosion flaw or defect subject to internal pressure. Measured flaws that exceed 80% of the pipe wall thickness are not considered. Figure 5.1 illustrates a single flaw with its dimension in reference to the pipe wall thickness.

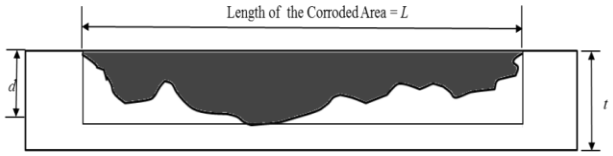

Figure 5-1: Illustration of Flaw and Its Dimensions

5.5 METHODOLOGY FOR FAILURE MODELING BASED ON LIMIT STATE FUNCTIONS

The initial steps in the analysis of the remaining life assessment include determining the failure modes of the pipeline and establishing the limit states. The limit state represents the failure events (the leak or rupture of the pipe) while the failure modes represent degradation mechanisms (corrosion, fatigue cracking, etc.). The probability of failure is estimated by probabilistic modeling in terms of the failure modes where uncertainty is included in the estimation. The methodology presented in this study focuses on localized single corrosion

flaws. Matlab codes have been generated to implement the methodology and perform the simulation. The methodology is broken down into seven steps, as presented in the following subsections.

5.5.1 Collect Data Pertaining to the Pipeline

The data should include, but not be limited to, inspection, operation, and design data. Failure and inspection reports, repair reports, and assessment studies conducted previously should be included as part of the data to be studied prior to conducting the assessment.

5.5.2 Determine the Failure Modes and Failure Events

Two failure events could take place at any flaw point in the pipeline. The first one takes place when the pipeline pressure is below the failure pressure but the flaw has penetrated the pipeline wall, causing a small leak. In the second event, the operating pressure exceeds the burst pressure at the flaw point (i.e., exceeds the remaining strength of the flaw) causing a burst, which results in a large leak.

It is assumed that the two events cannot occur simultaneously at any given point in time. This is because a leak resulting from corrosion will occur only when the flaw penetrates the wall, while the other failure event occurs when the operating pressure exceeds the specified maximum allowable pressure at a through-wall flaw point that is not yet entirely penetrating the wall.

It is assumed that a pipeline leak that results from corrosion penetrating the pipeline wall occurs if the maximum depth of the flaw equals the wall thickness and the operating pressure is at a level below the failure pressure (i.e., burst pressure).

Furthermore, it is assumed that a pipeline leak that results from burst pressure occurs when the pipeline suffers plastic collapse at the corrosion flaw point. This is the event when the operating pressure goes higher than the failure pressure (i.e., burst pressure) at the flaw location and its depth is below the critical depth. These two limit state functions are considered in the analysis.

5.5.3 Formulate the Limit State Functions

An LSF represents the shift from safe operation to unsafe operation or failure. The evolution of an insignificant corrosion flaw on a pipeline over time to a through-wall corrosion flaw is a good example that describes the transition from safe to unsafe operation. Essentially, it expresses the difference between the capacity and the load of the system. If the difference between the capacity and load is positive, the pipeline is in a safe operating state. If it is zero, the pipeline is at the limit state; if negative, the pipeline is at a failure state. The extent of the axial and radial flaw, pipeline geometry, pipeline operating pressure, and pipeline material properties are the main random variables of the LSF. The LSF is used to predict the probability of failure and it is expressed as (Haldar & Mahadevan, 2000):

$$Z = R - L \tag{5.1}$$

Where R is the resistance (capacity) of the system and L is the load imposed on the system. Then the probability of failure is computed as: *Probability of Failure* = $P\ (Z < 0)$.

5.5.3.1 Limit State Functions (LSF)

5.5.3.1.1 Leak Due to Corrosion

Based on the discussion in section 5.4.2, there are two LSFs; the first one expresses the difference between the critical corrosion depth (d_c) and the measured corrosion depth $d(T)$ at a given time T (refer to Equation 5.7). The second one expresses the variation between the burst pressure (P_f) and the operating pressure (P_O) (refer to Equation 5.10). The first LSF describes the failure caused by the flaw penetrating the entire pipe wall thickness, causing a small leak. It must be noted that the pipeline does not undergo plastic collapse at the flaw point causing a burst. The only flaw involved here is the penetration of pipe wall by the corrosion.

As per DNV-RP-F101, flaw depths that are greater than 85% of the pipe wall thickness are excluded from evaluation. Therefore, a value of 85% or less of the wall thickness should be considered as the capacity (resistance) of the pipe, i.e., the critical corrosion depth (d_c). In this study, corrosion depths greater than 80% of the wall thickness will be excluded. Pipelines with corrosion depths exceeding 80% of the wall thickness are at a greater risk if

they continue transporting hydrocarbons (Ahmmed, 1998; Kiefner & Vieth, 1990). Thus, the critical flaw depth can be set at 80% of the wall thickness (Caleyo, Gonzalez, & Hallen, 2002), as indicted below.

$$d_c = 0.8t \tag{5.2}$$

Alternatively, it can be derived in terms of the failure pressure or flow stress and hoop stress (Muhammed & Speck, 2002). The corrosion growth is assumed to be constant over time. In this study, the measured corrosion depth d and length L at a given point in time T are formulated as (Ahmmed, 1998):

$$d\,(T) = d_o + d_{rate}\,(T - T_o) \tag{5.3}$$

$$L\,(T) = L_o + L_{rate}\,(T - T_o) \tag{5.4}$$

Where d_o is the initial measured flaw depth, L_o is the initial measured flaw length, T_o is the time when the previous inspection was conducted, and d_{rate} and L_{rate} are the corrosion depth and length rates, respectively. Assuming that the corrosion rates, d_{rate} and L_{rate}, are constant throughout the evaluation interval, the corrosion rates can be expressed as:

$$d_{rate} = \Delta d/\Delta T \tag{5.5}$$

$$L_{rate} = \Delta L/\Delta T \tag{5.6}$$

Δd and ΔL are the difference in mm between the current and the previous flaw depth and length measurements, respectively, and ΔT is the time difference between the current and the previous measurement. This will lead us to the first LSF for the flaw depth:

$$Z_1 = d_c - d\,(T) \tag{5.7}$$

This LSF evaluates the difference between the critical corrosion depth and the measured corrosion depth at time T. The initial corrosion is defined as d_{o1}; the measured corrosion growth for the next interval is the multiplication of the estimated corrosion annual growth rate by the interval added to the estimated corrosion growth of the previous interval (refer to Equation 5.9). Therefore, for every time interval T_i there is an LSF that can be expressed as:

$$Z_1\,(T_i) = dc - d\,(T_i), \qquad i = 1, 2 \ldots n \tag{5.8}$$

Further, the corrosion growth for each interval can be expressed as:

$$\left.\begin{aligned} d(T_1) &= d_{01} \\ d(T_2) &= d_{01} + d_{rate}(\Delta T_2) \\ &\vdots \\ d(T_n) &= d(T_{n-1}) + d_{rate}(\Delta T_n) \end{aligned}\right\} \quad (5.9)$$

d_{01} is the initial flaw depth for interval 1 or year 1, and $d(T_1)$, $d(T_2)$, …, $d(T_n)$ are the estimated cumulative corrosion depths at the end of each interval or year 1, 2,…, N, respectively.

ΔT_2, ΔT_3, and ΔT_n are the differences between two time intervals where the corrosion flaw measurement has been made, which can be expressed in the same order as ($T_2 - T_1$),

($T_3 - T_2$), ($T_n - T_{n-1}$). d_{rate} is the corrosion annual growth rate (mm/year) or the growth rate per time interval (mm/time interval).

5.5.3.1.2 Leak Due to Burst

The second LSF (i.e., Z_2) defines the pressure change, which is the difference between the burst pressure P_f (failure pressure) and the operating pressure P_O:

$$Z_2 = P_f \quad - \quad P_O \tag{5.10}$$

Pf is the pressure that causes the pipe wall to undergo plastic collapse at the flaw point subsequent to a through-wall flaw. In essence, this failure occurs at a location that has a partial through-wall corrosion flaw, which is typically less than 80% of the wall thickness.

The LSF here is defined as a function of parameters that are probabilistic. These parameters include yield strength (*YS*), ultimate tensile strength (*UTS*), pipe diameter (*D*), pipe wall thickness (*t*), flaw depth *d* ($T - T_o$), and flaw length *L* ($T - T_o$). ($T - T_o$) is the time difference between the current and previous inspection times. Pressure failure is computed using the formulas presented in codes and standards: ASME B31G modified method; ASME B31G effective area method DNV-RP-F101 Part B; and BS-7910.

Modified Method – ASME B31G

Using ASME B31G modified method, the second LSF (Z_2) can be expressed as:

$$Z_2 = \frac{2t}{D}(SMYS + 69\ MPa)\left[\frac{1 - 0.85\left(\frac{d(T)}{t}\right)}{1 - 0.85\left(\frac{d(T)}{t}\right)\left(\frac{1}{M}\right)}\right] \quad - \quad P_O \tag{5.11}$$

Where t is the specified wall thickness, D is the specified outside diameter of the pipe, d (T) is the measured depth of the metal loss at time T, $SMYS$ is the specified minimum yield strength, and M is referred to as a correction factor, as indicated in Equations 5.13 and 5.14.

Effective Area Method – ASME B31G

When using ASME B31G effective area method the second LSF (Z_2) becomes:

$$Z_2 = \frac{2t}{D}(SMYS + 69\ MPa)\left[\frac{1-\left({}^{A(T)}/_{Ao}\right)}{1-\left({}^{A(T)}/_{Ao}\right)/_{M}}\right] - P_O \tag{5.12}$$

A is the area of the metal loss (Ld), and A_O is the local original area (Lt).

$$\left.\begin{array}{l} M = \left(1 + 0.6275\frac{L^2}{Dt} - 0.003375\frac{L^4}{D^2t^2}\right)^{0.5} \\ for\ \frac{L^2}{Dt} \leq 50 \end{array}\right\} \tag{5.13}$$

$$M = 0.032\frac{L^2}{Dt} + 3.3 \qquad for\ L^2/Dt > 50 \tag{5.14}$$

L is the length of the metal loss.

DNV-RP-F101 (Part B)/BS-7910

Similarly, when using DNV-RP-F101 (Part B), the second LSF (Z_2) can be expressed as:

$$Z_2 = \frac{(2t)(UTS)}{(D-t)}\left[\frac{(1- d(T)/t)}{\left(1-\frac{d(T)}{tM}\right)}\right] - P_O \tag{5.15}$$

$$M = \left(1 + 0.31\ \frac{L^2}{Dt}\right)^{0.5} \tag{5.16}$$

UTS is the ultimate tensile strength. Likewise, for every interval, there is an LSF that can be expressed as:

$$Z_2\ (T_i) \quad = P_f\ (T_i) \quad - \quad P_O, \quad i = 1, 2....n \tag{5.17}$$

Essentially, the model presented by BS-7910 mirrors the DNV-RP-F101 Part B model. As an example, the LSF based on the DNV-RP-F101 Part B becomes:

$$Z_2\ (T_i) = \frac{(2t)(UTS)}{(D-t)}\left[\frac{(1- d(Ti)/t)}{\left(1-\frac{d(Ti)}{tM}\right)}\right] - P_{O,} \quad i = 1, 2....n \tag{5.18}$$

$$M_i = \left(1 + 0.31\ \frac{L_i^2}{Dt}\right)^{0.5}, \qquad i = 1, 2....n \tag{5.19}$$

L is the corrosion length at interval i:

$$\left.\begin{aligned} L(T_1) &= L_{01} \\ L(T_2) &= L_{01} + L_{rate}(LT_2) \\ &\vdots \\ L(T_n) &= L_{0(n-1)} + L_{rate}(LT_n) \end{aligned}\right\} \tag{5.20}$$

L (T_1) is the estimated initial length of the corrosion flaw at the end of the first interval (LT_1); $L(T_n)$ is the estimated cumulative corrosion length at the end of the last interval (LT_n); and L_{rate} is the corrosion rate (mm/year) or (mm/time interval).

Figure 5.2 shows the framework for calculating the limit state functions. The first LSF evaluates the difference between the critical corrosion flaw depth and the measured corrosion depth at a given point in time. The second LSF calculates the pressure change at a given point in time. The failure pressure model of three standards, DNV-RP-F101, BS7910, and the modified and effective area methods by ASME B31G are considered in the assessment.

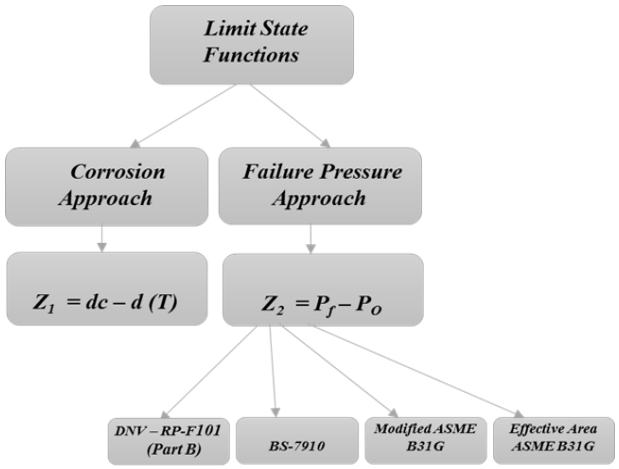

Figure 5-2: Framework for Limit State Function Evaluation

5.5.4 Perform Uncertainty Analysis

The random variables that belong to each LSF are analyzed where a probability density function is determined for each variable based on the available pipeline configuration and industry standard data. Once the probability distribution function (PDF) is determined for each variable, the distribution parameters are calculated and then the probability of failure is determined for the limit state functions. Matlab software is used to run the Monte Carlo simulation to calculate the probability of failure and thus the remnant life.

5.5.5 Determine the Probability of Failure

The probability of failure is expressed as:

$$Probability\ of\ Failure = P\ (Z < 0) \tag{5.21}$$

The reliability index, β, (Haldar & Mahadevan, 2000) is given by:

$$\beta = \frac{\mu_Z}{\sigma_Z} = \left[\frac{\mu_R - \mu_L}{\sqrt{\sigma_R^2 + \sigma_L^2}}\right] \tag{5.22}$$

The reliability index is computed for every failure mode whose probability of failure can be expressed as:

$$Probability\ of\ Failure = 1 - \Phi(\beta) \tag{5.23}$$

As an alternative method, when using the Monte Carlo simulation technique, the probability of failure is computed when the LSF becomes less than zero.

$$Probability\ of\ Failure = N_f/N \tag{5.24}$$

N_f is the number of simulation cycles when LSF is violated (i.e., when it becomes less than zero) and N is the total number of simulation cycles. The corrosion probability of failure for a flaw i at a given time T_i can be expressed as:

$$Pof_{Corri} = P\ (Z_{1i}\ (Ti) \quad < 0),\ i = 1,2,\dots,n, \tag{5.25}$$

This failure could occur at any time when ($d(T) \leq d_c$) and the operating pressure becomes less than the burst pressure ($P_O < P_f$). The burst probability of failure at a flaw *i* at a given time T_i can be expressed as:

$$Pof_{Bursti} = P\ (Z_{2i}\ (T_i) \quad < 0),\ \ i = 1,2,\dots,n \tag{5.26}$$

This failure could occur at any time when the flaw depth becomes less than the critical wall thickness ($d(T) < d_c$) and the operating pressure becomes less than or equal to the burst pressure ($P_O \leq P_f$). The probability of failure for each single flaw at each interval combines the probability of failure for the corrosion, as addressed in the first LSF, and the probability of failure due to a burst, as addressed in the second LSF. Therefore, the total probability of failure (Pof_T) at each time interval for each flaw *i* becomes:

$$Pof_{Ti} = \ Pof_{Corri} \cup Pof_{Bursti}\ , \qquad i = 1,2,\dots\dots,n \tag{5.27}$$

The overall probability of failure for the entire pipeline for all flaws at a given time becomes:

$$Pof_{T\,(PL)} = 1 - (1 - Pof_{T1}) \ldots\ldots\ldots \left(1 - Pof_{T(n)}\right) \quad (5.28)$$

Where *1, 2… n* represent the flaw number.

5.5.6 Determine the Target Reliability/Target Probability of Failure

The target reliability is determined based on the recommendation of standards and codes, engineering judgment, and acceptable risk criteria. Upon establishing the target reliability, the target probability of failure can be determined; this is the maximum allowable failure probability. For subsea pipelines, DNV-RP-F101 safety class: normal recommends 10^{-4} towards target probability of failure. In this study, 10^{-4} will be used as the target annual probability of failure per flaw (km) of the pipeline segment corresponding to a reliability of 0.9999. If the calculated probability of failure during operation exceeds the target probability of failure, then the pipeline is not safe to operate.

5.5.7 Determine the Remaining Life

The remaining life is the time when the pipeline probability of failure surpasses the specified target failure probability. In this study, failure probability is estimated through LSF using time-dependent deterioration mechanisms, as well as the burst pressure. The simulation was performed to determine the time that the failure probability exceeds the target failure probability.

The approach here is to determine the remaining life for each defective area of the pipeline and to give an idea of the overall probability of failure for the pipeline. Figure 5.A.1 shown in Annex A depicts a flow chart that summarizes the steps outlined in the methodology section.

5.6 CASE STUDY

5.6.1 Description

A pipeline having an initial corrosion depth and length of 4.6 mm and 200 mm, respectively, was considered for the case study. Other relevant information pertaining to the pipeline is presented in Table 5.1. Figure 5.3 illustrates the relevant details of the pipeline. The goal is to determine the remaining life of the pipeline before it experiences a failure.

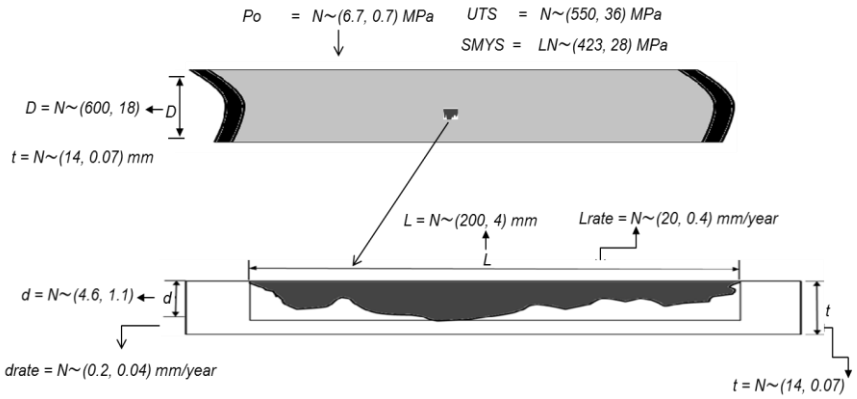

Figure 5-3: Pipeline and Corrosion Flaw Details

Table 5-1: Pipeline Parameters Used in the Case Study

Variable		**Unit**	**Mean**	**CoV**	**Distribution**
Internal Pressure	*Po*	*MPa*	6.7	0.14	Normal Distribution
Pipe Diameter	*D*	*mm*	600	0.03	Normal Distribution
Pipe Wall Thickness	*t*	*mm*	14	0.05	Normal Distribution
Pipe Yield Strength	σ_y	*MPa*	423	0.07	Log Normal Distribution
Pipe Ultimate Tensile Strength	σ_U	*MPa*	550	0.065	Normal Distribution
Initial Corrosion Depth	*do*	*mm*	4.6	0.24	Normal Distribution
Initial Corrosion Length	*Lo*	*mm*	200	0.02	Normal Distribution
Corrosion Depth Rate	d_{rate}	*mm/yr*	0.2	0.2	Normal Distribution
Corrosion Length Rate	L_{rate}	*mm/yr*	20	0.2	Normal Distribution

The corrosion depth and length rates were assumed to be 0.2 mm/year and 20 mm/year, and assumed to follow normal distribution. The inspection was conducted at the end of 2013; the inspection will be conducted every 5 years going forward. It is assumed that the estimated initial corrosion length and depth as well as the corrosion growth rates are obtained from in-line inspection. Matlab software was used to run Monte Carlo simulations $2x10^5$ times.

5.7 RESULTS AND DISCUSSION

5.7.1 Remaining Life Assessment Based on Corrosion Limit State Approach

Figure 5.4 illustrates the histogram for the flaw depth at year 1 and the predicted flaw depth for years 5, 10, 15, 20, and 25. The figure indicates that the mean value for the flaw depths for years 1, 5, 10, 15, 20, and 25 are 4.5, 5.5, 6.5, 7.5, 8.5, and 9.5 mm, respectively.

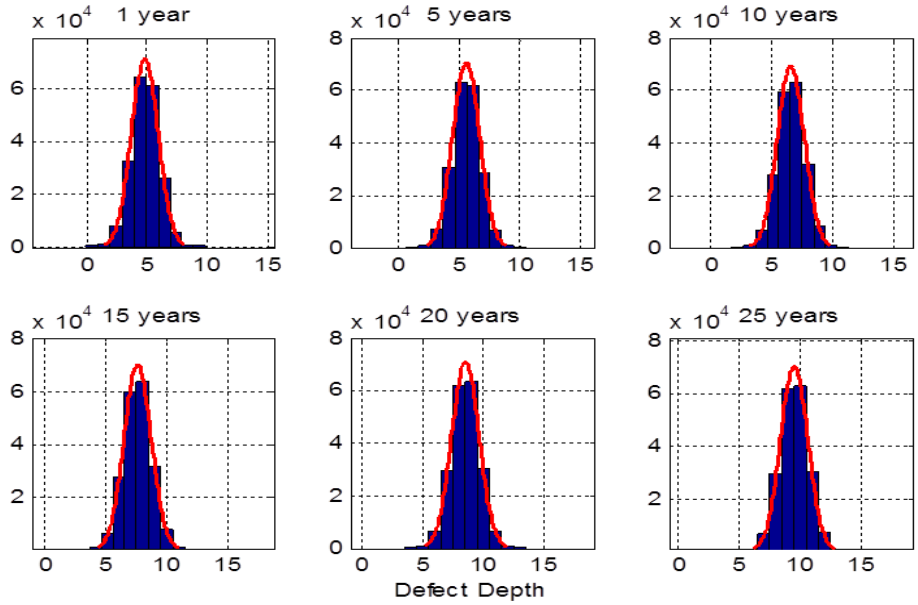

Figure 5-4: Histogram of the Simulated Flaw Depth

Figure 5.5 shows the estimated probability of failure with 10% error intervals. It is evident that the pipeline life can be safely extended from 11 to 13 years, 12 years being the most feasible remnant life.

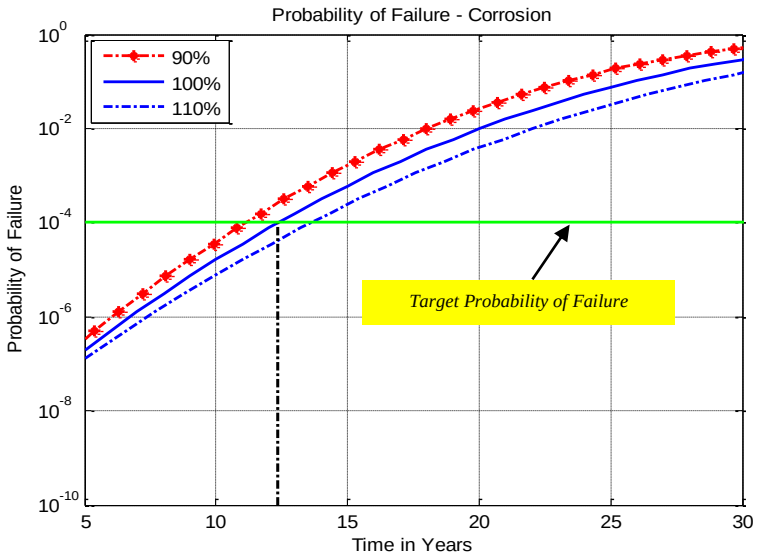

Figure 5-5: Probability of Failure Due to Corrosion

5.7.2 Remnant Life Based on Burst Limit State Approach

5.7.2.1 DNV-RP-F101 (Part B)/BS-7910

Figure 5.6 illustrates the probability of failure due to burst pressure based on DNV-RP-F10. The figure indicates the remaining life within an estimated error band of ± 10%, which is 12.5 years.

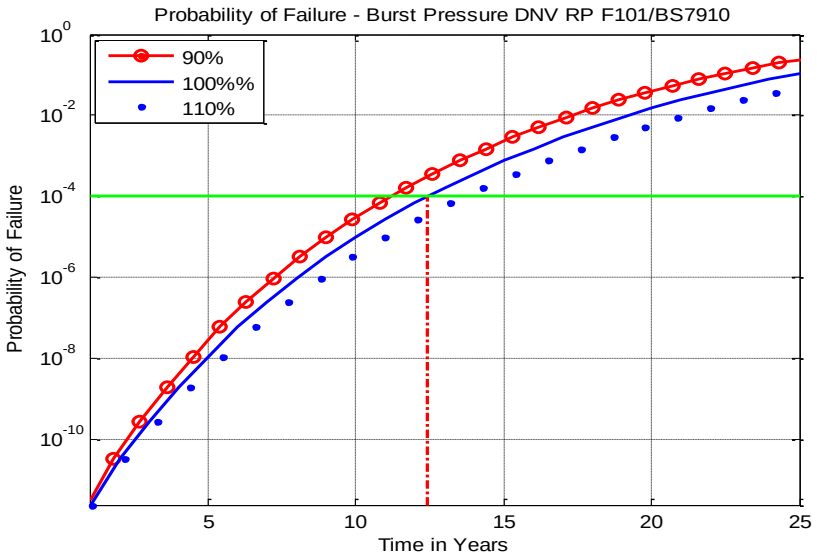

Figure 5-6: Probability of Failure Due to Burst Pressure (DNV/BS)

5.7.2.2 Modified ASME B31G

Figure 5.7 illustrates the probability of failure due to burst pressure based on the modified ASME B31G methodology.

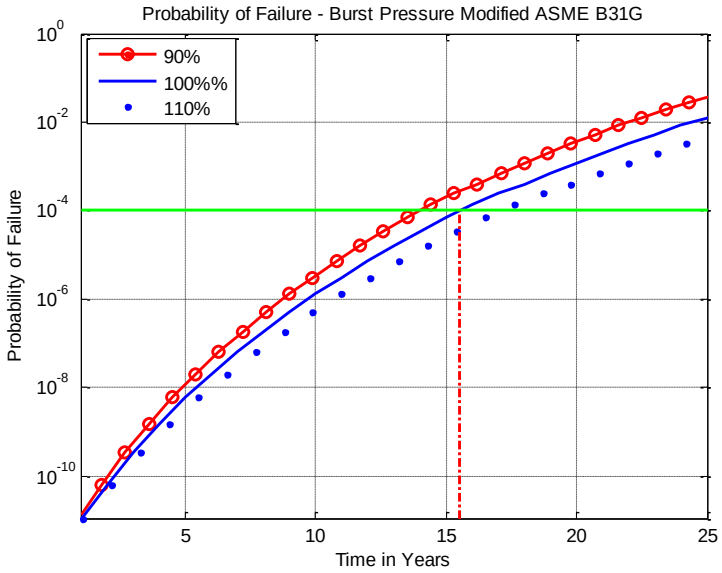

Figure 5-7: Probability of Failure Due to Burst Pressure (ASME)

The figure reveals that the pipeline can operate safely up to 16 years before it might suffer a burst failure.

5.7.2.3 Effective Area Method – ASME B31G

Figure 5.8 shows the probability of failure due to burst pressure based on the effective area method of ASME B31G.

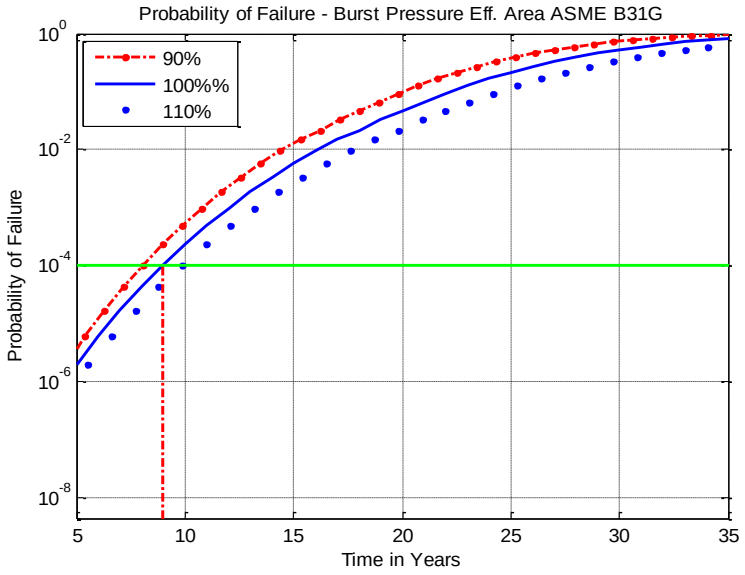

Figure 5-8: Probability of Failure Due to Burst Pressure – ASME Effective Area Method

The figure reveals that the pipeline can operate up to 9 years before it may suffer a burst failure. This indicates that the DNV model is more conservative than the ASME modified model.

5.7.2.4 Combined Probability of Failure Based on All Methods

Figure 5.9 illustrates the probability of failures for the two failure events. The figure shows the probability of failure using the three methods: DNV-RP-F101, and modified and effective area methods by ASME-B31G.

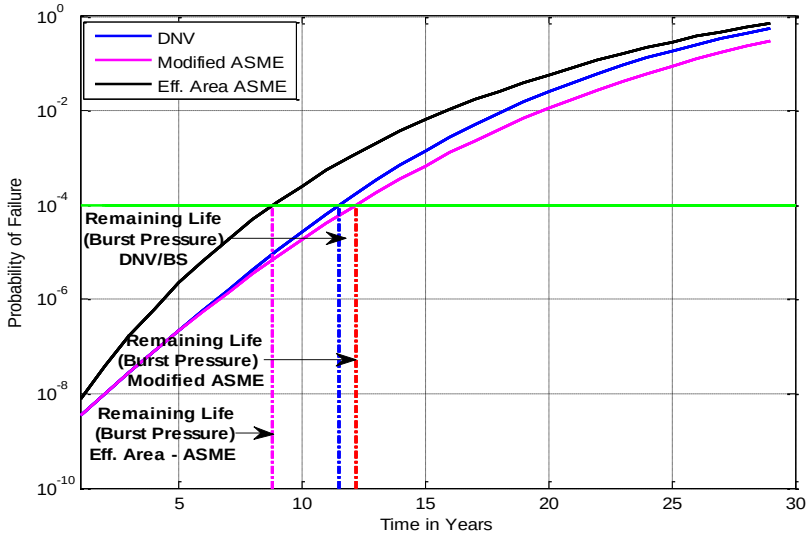

Figure 5-9: Probability of Failure for the Two Failure Events

Figure 5.10 shows the probability of failures for the two failure events and the remaining life in a linear scale.

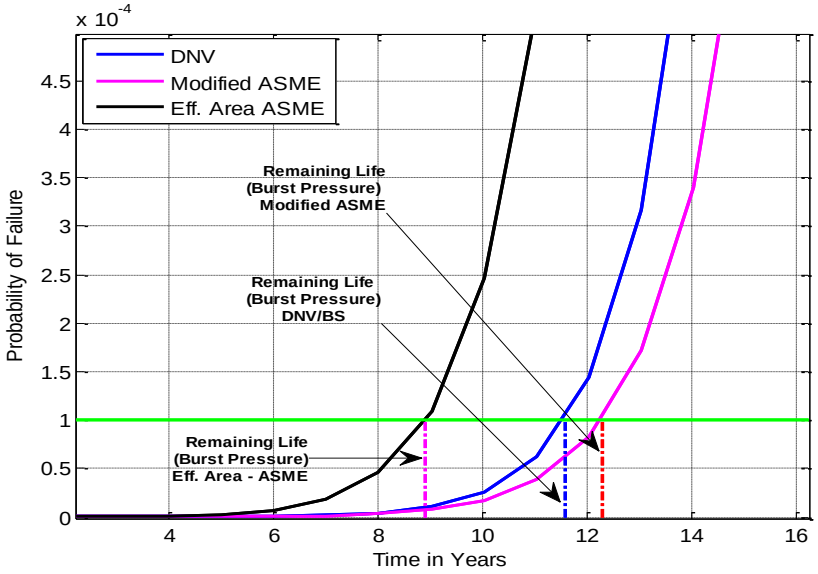

Figure 5-10: Probability of Failure for the Two Failure Events – Linear Scale

The estimated remaining life is presented in Table 5.2. The table clearly shows that the ASME effective area method provides the most conservative estimate.

Table 5-2: Summary of Results

COMBINED PROBABILITY OF FAILURE	REMAINING LIFE (YEARS)
DNV-RP-F101 (Part B)/BS-7910	11.5
Modified ASME B31G	12
Effective Area Method – ASME B31G	9

It is evident from the analysis, that using probabilistic method provided results that are more accurate. This method allows a researcher to explore and predict the behavior of the system more easily. Using deterministic approach may not provide accurate results because it considers only one point estimate of the parameters under study.

5.8 SUMMARY

A probabilistic methodology based on limit state approach for determining the probability of failure and the remaining life of pipelines has been developed. The methodology adopted the models presented in codes and standards. The results revealed that ASME B31G effective area method is the most conservative method. The differences in these models are attributed mainly to the different approaches for calculating the area of defect shapes, and whether tensile or yield strength is used.

ANNEX 5.A

Figure 5.A.1 – Flow Chart Outlining the Steps for the Methodology

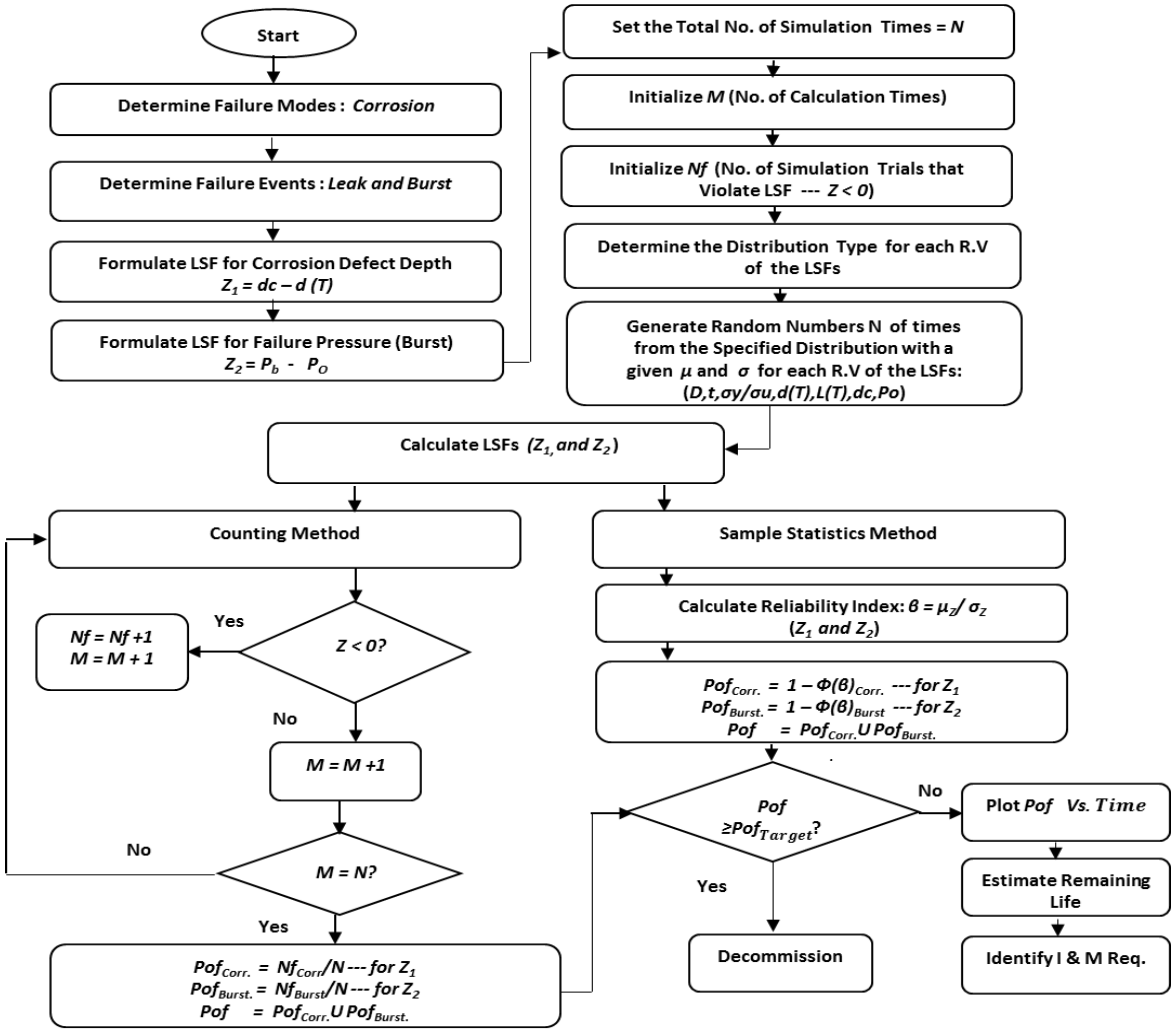

Abbreviations

I &M: *Inspection & Maintenance*, **LSF:** *Limit State Function*, **MCS:** *Monte Carlo simulation*, **P_b:** *Burst Pressure*, **P_o:** *Operating Pressure*, **Pof :** *Probability of Failure*, **Pof_{Target}:** *Target Probability of Failure*, **R.V:** *Random Variable*, **Req.:** *Requirements*, **T:** *Time*

CHAPTER 6
RISK ASSESSMENT OF OFFSHORE CRUDE OIL PIPELINE BURST FAILURE

Condition monitoring systems play a major role in ensuring the continuity of operation and maintaining the reliability and safety of oil and gas infrastructure. One specific system is the Leak Detection System (LDS). The failure of this system to detect hydrocarbon releases from an offshore pipeline can have devastating effects on the operation and environment. Moreover, the failure consequences may bring about excessive financial losses and could threaten the survivability of the operating company in the market. The financial losses result from the cost incurred for repairing the damage caused by the released hydrocarbon product into the sea/ocean. Further losses are incurred as a result of the lost and deferred production due to the shutdown of the facility for repair. It is crucial that operating companies continually conduct risk-based assessments of their pipeline network and leak detection systems to ensure their integrity and operability are intact and that they do not pose any threat to the continuity of oil flow. Two fundamental components establish the risk-based assessment: the probability and consequences of failure for both the pipeline and the LDS. The joint probability of failure, which encompasses the pipeline failure and the detection failure is used to determine the overall probability of failure. The consequences of failure include economic as well as environmental consequences expressed in terms of monetary value. This chapter provides a risk-based assessment methodology to assess the reliability of offshore pipelines and leak detection systems in

order to help determine the level of risk associated with their failure. The assessment outcome is compared against a target or acceptable risk level that can help decision makers to decide the most feasible action for averting risk. This chapter provides a methodology to assess the consequences of the simultaneous failure of the offshore pipelines (rupture) and its leak detection.

6.1 BACKGROUND INFORMATION

Failure of a hydrocarbon processing facility is a major concern for operating companies, which requires careful and considerate attention by all levels of the management hierarchy. Two critical components of the processing facilities that require ongoing attention are the oil and gas pipeline and its LDS. They require more attention as their failure is so critical, threatening the environment, safety, and production. To obtain an all-inclusive and accurate assessment of these components, a risk-based assessment approach should be adopted.

It is estimated that about 29% of pipeline failures are related to pipeline deterioration, 27% are related to operation error, and 27% are related to third-party interference. Other causes include mechanical failure and geo-hazards, with 11% and 6%, respectively (Andersen & Misund, 1983). In Europe, 50% of loss of containment events were caused by corrosion (HSE, 2010), which is the second leading cause of pipeline failure (EGIG, 2011).

As per the U.K. Health and Safety Executive (2014), in the past 10 years there were 1,694 incidents involving offshore hydrocarbon releases. According to the U.S. Department of Transportation, in the past 10 years there were about 306 incidents related to offshore pipeline systems resulting in US$514,225,096 in property damage (PHMSA, 2014). Approximately 71 of these incidents were related to the damage caused by hazardous liquid releases, costing about US$157,296,006, and 15,194 barrels of hazardous liquid spilled in the sea.

To prevent such incidents from occurring and to minimize their destructive impact on environment and safety, the integrity of the pipelines and the functionality of the systems should be assessed on a regular basis. If the outcome of the assessment reveals that either one or both systems is likely to pose a safety or operational threat, immediate corrective action should be taken to prevent the occurrence of undesirable consequences.

This chapter presents an integrated risk-based assessment approach for oil and gas process components, specifically pipelines and LDS. This approach can be used to predict and quantify the future financial impact in the event a pipeline or condition monitoring system (i.e., LDS) fails. The assessment will provide the expected level of risk expressed in monetary value. Knowing the level of risk beforehand will enable operating companies to allocate the required financial resources, and to cover the unexpected future financial losses that may result from the failure of a process component.

To demonstrate the applicability and viability of the assessment approach, it will be applied to a case study. The chapter starts by providing an overview and background of risk-based assessment in section 6.2. Section 6.3 discusses the first step in the assessment process, which is to formulate the probability of failure for the pipeline and the LDS. Section 6.4 discusses the next step in the assessment process, which is to determine the consequences of failure (including economic and environmental consequences). Section 6.5 discusses the next step, which is to determine the level of risk. Section 6.6 applies the risk-based approach to a case study followed by a discussion of the results. Finally, section 6.7 provides summary and concluding remarks.

6.2 OVERVIEW OF RISK-BASED ASSESSMENT

Earlier efforts by researchers in the area of risk-based assessment are cited in the references (Dey, 2001; Khan et al., 2004; Khan et al., 2006; Singh & Markeset, 2010; Thodi et al., 2009; and Thodi et al., 2013). Risk-based assessment incorporates the likelihood and consequences of failure and is used to determine the expected level of risk. The estimation of the probability of failure, which can be calculated by statistical methods or expert judgments, is a major step in the assessment process. As per (ISO/TS 12747, 2011), failure is defined as "an event in which a component or system does not perform according to its operational requirements." For instance, a subsea pipeline may fail to operate safely due to rupture or leakage caused by excessive corrosion or cracking. Obviously, the leaked

product will damage the surrounding environment and the problem becomes worse if the LDS fails to detect this failure in time.

It can be understood from the above definition that failure of a system or a component of a system causes malfunction or degraded performance. It renders the system or a component of the system either partially or totally incapable of satisfying operational requirements. Moreover, the consequences of failure may threaten lives and the environment, and may bring about financial losses and liabilities that could ultimately affect the survivability of the operating company in the market.

It is therefore of great importance that operating companies know in advance the expected level of risk when a pipeline fails. Knowing the level of risk beforehand enables planners and financial officers to allocate the resources and funding required to effectively deal with such accidents and to be better prepared when accidents do happen. Figure 6.1 illustrates the failure and risk components in relation to the oil and gas pipeline and LDS.

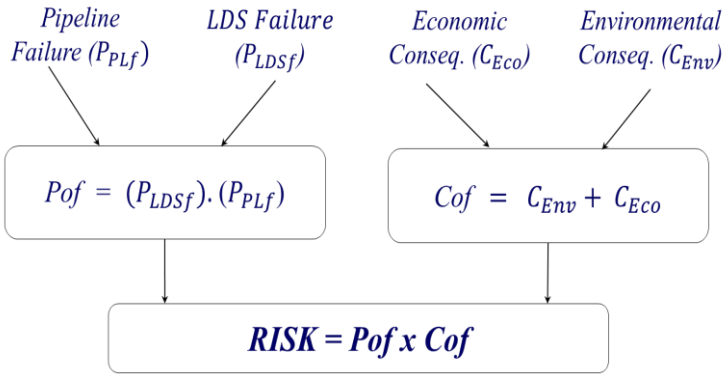

Figure 6-1: Failure and Consequences

The figure indicates that in order to know the risk, the probability of failure (*Pof*) and consequences of failure (*Cof*) should be known beforehand. The LDS failure and the pipeline failure events are independent, and as such the probability of their occurrence at the same time is the product of both probabilities. The consequences of failure incorporate environmental as well as economic consequences.

Some codes and standards provide models for assessing corroded pipelines, but these codes and standards are based on a deterministic approach and exclude condition monitoring systems such as LDS from the assessment. In order to provide a reliable and comprehensive assessment of the integrity of the pipeline and its LDS, one should consider a probabilistic approach by providing a joint probabilistic assessment. Adopting this approach will provide a realistic assessment that better describes the actual condition of the system being evaluated. Additionally, it will enable evaluators to determine correctly if the systems are operating in a safe and reliable manner.

6.3 PROBABILITY OF FAILURE

The probability of failure can be modeled using LSF that defines the change from safe operation to unsafe operation. The failure state is determined when the LSF is violated; in other words, when the LSF becomes less than zero. Equation 6.1 expresses the LSF that defines the difference between the capacity and the load as:

$$Z = C - L \tag{6.1}$$

Where Z is the performance function, C is the capacity of the system, and L is the load imposed on the system. The probability of failure, which is indicated in Equation 6.2, defines the event when the specified capacity goes below the load of the system; at such event, the LSF is violated (Haldar & Mahadevan, 2000).

$$P_f = P\,(Z < 0) \tag{6.2}$$

6.3.1 Pipeline and LDS Failures

Every corrosion defect along the pipeline can lead to one of two failure events: a gradual leak due to the penetration of corrosion into the entire pipeline wall thickness or a sudden leak due to rupture. Sudden leaks take place when the internal operating pressure exceeds the maximum allowable pressure at the defect point. Similarly, the LDS may have two

different failure events: the missed detection and delayed detection. This is illustrated clearly in Figure 6.2.

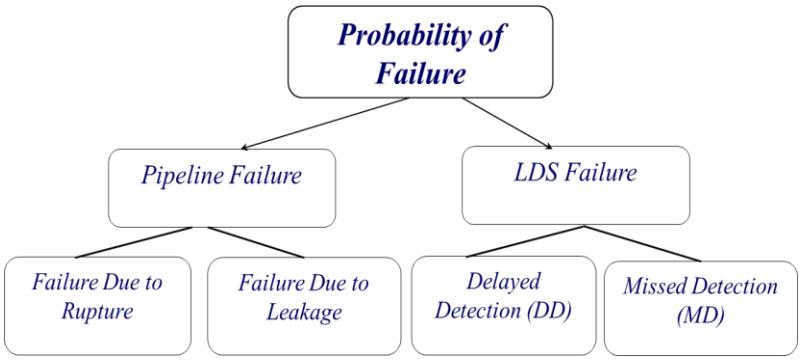

Figure 6-2: Pipeline and LDS Failures

6.3.1.1 Pipeline Failures

The causes of pipeline failure are broadly divided into two categories: time-dependent and time-independent (or random failures). Time-dependent failure encompasses corrosion or cracking. On the other hand, time-independent failure includes third-party interference, geo-hazards, or operation errors. The focus of this section is on the time-dependent failure, which is the corrosion.

Every corroded point along the pipeline may fail due to the weakness of that point to resist the operating pressure (i.e., load). Initially, corrosion partially penetrates the pipeline wall until it eventually penetrates the entire thickness of the pipeline wall, causing a gradual leak. During the partial penetration, the pipeline poses a threat to the environment since the

pipeline could rupture at any time, causing a sudden leak due to the weakness of the corroded spot. Figure 6.3 illustrates the dimensions of a typical defect. The maximum depth is taken as the depth of the defect, *d*.

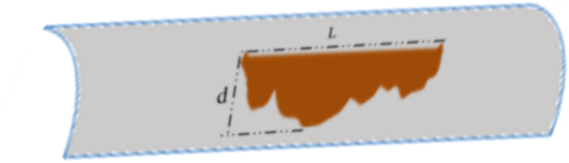

Figure 6-3: Illustration of Flaw and Its Dimensions

Each pipeline's failure event might be associated with another failure event related to the LDS. When the LDS fails to detect a leak or rupture, then the failure consequences will have greater risk impact on the environment and production.

The probability of pipeline failure can be expressed using the LSF, as indicated in Equation 6.3.

$$Z(T) = \quad d_C - d(T) \tag{6.3}$$

Z is the LSF that defines the difference between the critical corrosion depth d_C and the corrosion depth $d(T)$ measured at time T.

The depth of the corrosion plays a major role in the occurrence of the pipeline failure. Therefore, the focus should be on the depth of the corrosion that could cause failure events. As illustrated in Figure 6.3, the depth that is considered for the assessment is the maximum depth; thus it is crucial that this depth should be derived in terms of the pipeline operating characteristics and pipeline material properties.

The ASME effective area model, as indicated in Equation 6.4 (ASME-B31G, 2012), expresses the pressure failure or the burst pressure for the corroded pipeline in terms of yield strength and defect area.

$$\left.\begin{aligned} P_{fi}(T) &= \frac{2t}{D}\left(\sigma_y + 69\ MPa\right)\left[\frac{1-\left({}^{A_i(T)}/_{Ao}\right)}{1-\left({}^{A(T)}/_{Ao}\right)/_{M}}\right] \\ M &= \left(1 + 0.6275\frac{L^2}{Dt} - 0.003375\frac{L^4}{D^2t^2}\right)^{0.5} \quad for\ \frac{L^2}{Dt} \leq 50 \\ M &= 0.032\frac{L^2}{Dt} + 3.3, \quad for\ L2/Dt > 50 \\ A_i(T) &= d_i(T) * L_i(T) \\ A_o &= t * L_i(T) \end{aligned}\right\} \qquad (6.4)$$

$P_{fi}(T)$: Pressure Failure for Defect i at Time T – MPa
t : Pipe Wall Thickness, mm

σ_y : Specified Minimum Yield Strength – It is a design-specified parameter
$A_i(T)$: Measured Defect Area at Time *T* – mm
$A_O(T)$: Original Area Before Defect Has Occurred – mm
$d_i(T)$: Measured Defect Depth at Time *T* – mm
$L_i(T)$: Measured Defect Length at Time *T* – mm
$M_i(T)$: Folias Factor

The corrosion growth is assumed to be constant over time, and the depth and length of the defect over the years are calculated using Equations 6.5, 6.5.1, and 6.5.2 (Aljaroudi et al., 2014a).

$$\left.\begin{aligned} d_i(T_0) &= d_{i0} \\ d_i(T_1) &= d_{i0} + C_{rate}x(\Delta T_1) \\ \Delta T_1 &= T_1 - T_0 \\ d_i(T_n) &= d(T_{n-1}) + C_{rate}x(\Delta T_n) \\ \Delta T_n &= T_n - T_{n-1} \end{aligned}\right\} \quad (6.5)$$

d_{i0} : Initial Defect Depth – mm
$d_i(T_1)$: Estimated Cumulative Depth of Corrosion Defect *i* at the End of Interval 1, mm
$d_i(T_n)$: Estimated Cumulative Depth of Corrosion Defect *i* at the End of Interval *n*, mm
ΔT_1 : Time Interval 1
ΔT_n : Last Time Interval
C_{rate} : Corrosion Annual Growth Rate (mm/year)

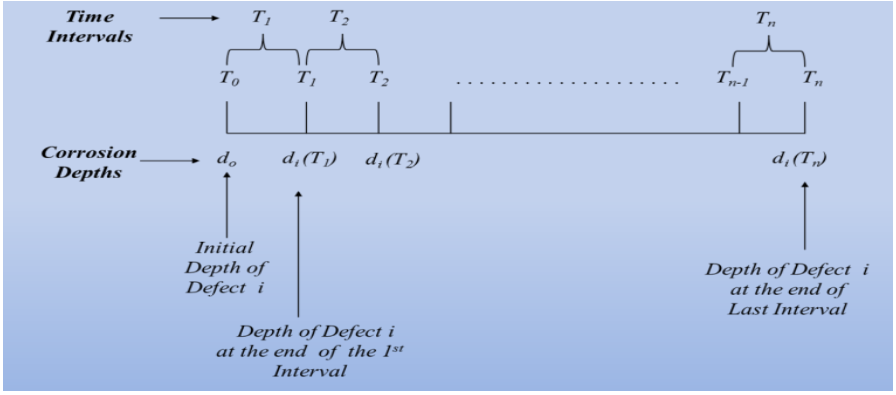

Figure 6-4: Illustration of How to Determine the Time Interval ΔT

Figure 6.4 illustrates how to compute the duration of each interval. T_o is the time when the intial coorosion dpeth is measured. T_1 is the end of the first time inetrval; at this time, another measuremnt of the depth is made. The first time interval will be (T_1 - T_o) and will be deisgnated as $\Delta T1$ refereeing to time interval 1. It is assumed that the corrosion length grows as a percentage of the depth, as indicated in Equation 6.5.1 (ABS, 2006):

$$L_i(T_1) = L_{i0}\left(1 + \frac{C_{rate}\Delta T_1}{d_{i0}}\right) \quad (6.5.1)$$

$L_i(T_1)$ is the length of defect *i* at the end of year 1, $L_o$is the initial or current length, and d_{io} is the initial depth. Then the length over time can be calculated as indicated in Equation 6.5.2.

$$L_i(T_n) \quad = L(T_{n-1}) \left(1 + \frac{C_{rate}\Delta T_n}{d(T_{n-1})}\right) \tag{6.5.2}$$

$L_i(T_n)$ is the length of defect *i* at the end of year *n*, $L(T_{n-1})$ and $d(T_{n-1})$ are respectively the length and depth of defect *i* at the end of year *n-1*.

To determine the corrosion depth that could cause a rupture failure event, Equation 6.4 is used to yield:

$$d_C \; = \quad \left[\frac{1-\frac{PD}{2t(\sigma_y+69)}}{1-\frac{PD}{2t(\sigma_y+69)M}}\right] \tag{6.6}$$

This is the same approach adopted by Muhammed and Speck (2002) for the ASME B31G modified method, but this chapter uses the ASME B31G effective area method (ASME-B31G, 2012). Substituting Equation 6.6 into Equation 6.3 yields:

$$Z_i(T) = \quad \left[\frac{1-\frac{PD}{2t(\sigma_y+69)}}{1-\frac{PD}{2t(\sigma_y+69)M}}\right] \quad - \; d_i(T) \tag{6.7}$$

Then the probability of failure will be:

$$P\big(Z_i(T)\big) \leq 0, \qquad i = 1, 2, \ldots \ldots n \tag{6.8}$$

This is the probability of the pipeline failure that may result from a burst or rupture at the defective spot *i* at time *T*.

6.3.1.2 Leak Detection System Failures

The LDS major failure components include missed detection and false detection. However, another failure element is the delayed detection, which is assumed to be negligible. The focus of this chapter will be only on missed detection. Missed detection adversely affects the ability of LDS to detect a true leak, while false detection influences the LDS detection sensitivity. Missed detection is only known during or after the occurrence of the pipeline failure, leak, or rupture, and at that event no alarm is declared to indicate the presence of a leak. In contrast, false detection is known only when an alarm is declared indicating the presence of a leak when in fact there is no leak present.

The missed detection event occurs when the threshold value, which is the lowest detectable leak rate for volume-balance LDS, pressure change for negative-pressure LDS, or temperature change for fiber-optic-based LDS becomes greater than the specified threshold. This takes place due to fluctuations in the performance of the internal electronics of the system, inherent uncertainties of the system, or thermal noise.

The LDS fails when a missed detection of a true leak takes place; to determine the probability of missed detection (PMD), the probability of false alarm (PFA), the threshold and the probability of detection (PD) should be determined first.

6.3.1.2.1 Probability of False Alarm

PFA is the probability that the system declares the presence of a leak when in fact there is none present. The PFA for a fiber-optic-based LDS can be expressed in terms of the threshold, which is the lowest detectable temperature change (Aljaroudi et al., 2014b):

$$PFA = \frac{1}{2}\left[1 - \ erf\left(\frac{Xth}{\sqrt{2\sigma^2}}\right)\right] \tag{6.9}$$

PFA is the probability of false alarm, X_{th} is the threshold power, and σ^2 is the variance of the noise power. Similarly, the threshold can be derived in terms of the PFA as (Aljaroudi et al., 2014b):

$$Xth \ = \sqrt{2\sigma^2}erf^{-1}(1 - 2PFA) \tag{6.10}$$

It is assumed that either the specified threshold or the PFA is a given parameter as part of the LDS specification. The above discussion is about a general case that applies to all LDS

types. Let us assume that a fiber-optic, BOTDA-based LDS is used. Thus, the minimum detectable temperature change can be formulated as indicated in Equation 6.11 (Horiguchi et al., 1992):

$$\delta T = \frac{\Delta v_B}{\sqrt{2}\,\alpha_T (SNR)^{0.25}} \tag{6.11}$$

δT	:	Minimum Detectable Temperature Change – ºC
Δv_B	:	Brillouin Spectral Width – MHz
SNR	:	Signal-to-Noise Ratio
α_T	:	Temperature Coefficient Change – MHz/ºC

δT is the specified minimum temperature change that can be detected by a fiber-optic LDS based on BOTDA technique. A linear relationship exists between the power of the output signal and the temperature change, as indicated in Equation 6.12 (Smith et al., 1999):

$$P_B = P_O + \frac{dP}{dT}\,\Delta T + \frac{dP}{d\varepsilon}\Delta\varepsilon \tag{6.12}$$

P_B is the measured power of the signal in µW, P_O is the power measured at the reference or the ambient temperature in µW, $\frac{dP}{dT}$ is the power temperature coefficient (µW/ºC), and

$\frac{dP}{d\varepsilon}$ is the power strain coefficient (mW/με). Assuming zero strain when the fiber is laid near the pipeline, Equation 6.12 reduces to:

$$P_B = P_O + \frac{dP}{dT}\,\Delta T \tag{6.12.1}$$

6.3.1.2.2 Probability of Detection (PD)

This is the probability that the system declares an actual leak; probability of missed detection (PMD) is the probability that the system does not declare the presence of a leak when in fact the leak is present. The PD can be expressed as (Aljaroudi et al., 2014b):

$$PD = \frac{1}{2}\left[1 - \ erf\left(\frac{Xth - \mu}{\sqrt{2\sigma^2}}\right)\right] \tag{6.13}$$

X_{th} is the threshold power level change, μ is the mean value taken for every group of measurements, X is the amplitude that represents the measured power level of the incoming signal, and σ^2 is the noise power. The PD can be expressed in terms of the PFA (Aljaroudi et al., 2014b) as:

$$PD = \frac{1}{2}\left[erfc\left(erfc^{-1}(2PFA) - \sqrt{\frac{SNR}{2}}\right)\right] \tag{6.14}$$

The PMD can be calculated using the following equation:

$$PMD = 1 - \frac{1}{2}\left[erfc\left(erfc^{-1}(2PFA) - \sqrt{\frac{SNR}{2}}\right)\right] \quad (6.15)$$

This is the probability of missed detection or the probability of LDS failure (Pof_{LDS}).

$$Pof_{LDS} = PMD_{LDS} \quad (6.16)$$

6.3.2 THE JOINT PROBABILITY OF FAILURE FOR THE PIPELINE AND LDS

At any moment in time, two undesirable events may take place. A leak or burst failure may occur, due to the weakness of the defective point to resist the internal pressure load imposed on it; and the LDS may be unable to detect the leakage at the defective point. The failure probability for both events occurring at the same time (time *T*) for defect *i* is:

$$Pof_i(T) = [Pof_{LDSi}][Pof_{PLi}], \quad i = 1, 2, \ldots n \quad (6.17)$$

$Pof_i(T)$ is the LDS and pipeline joint probability of failure at time *T* at defective spot *i*; Pof_{LDSi} is the probability of LDS failure and can be calculated using Equation 6.15; and Pof_{PLi} is the pipeline probability of failure (for pipeline segment *i*) and can be calculated

using Equation 6.8. Each segment of the pipeline has its own failure and risk depending on the surrounding environment, the characteristic of the pipeline, and its operating condition (Bai & Mustapha, 2010). One approach is to consider each pipeline segment falling between two joints, and the probability of failure will be the probability of failure per joint (Hallen, Caleyo, & González, 2003). Each defect has its own probability of failure and risk that contributes to the overall probability of failure and risk of the entire pipeline. In this case, the probability of failure for the entire pipeline can be computed as a series system.

The total probability of failure (Pof_T) for every segment *i* along the entire pipeline and the LDS at time interval *T* becomes:

$$Pof_T(T) = 1 - \left(1 - Pof_1(T)\right) \dots \left(1 - Pof_n(T)\right) \quad (6.18)$$

$Pof_T(T)$ is the total probability of failure at time *T*, $Pof_1(T)$ is the probability of failure for segment i, and $Pof_n(T)$ is the probability of failure for segment *n* at time *T*.

6.4 CONSEQUENCES OF FAILURE

Risk combines the probability of failure and its consequences. The consequences consist of economic as well as environmental consequences expressed in terms of monetary value. Risk can be expressed as:

$$Risk = Pof \; x \; Cof \quad (6.19)$$

Where *Pof* is the probability of failure and *Cof* is the consequences of failure. If there is more than one failure event (let us say *n* events) and each event has its own probability of failure and consequences of failure, then risk is the summation of individual risks (Faber, 2007).

$$Risk = \sum_i^N Pof_i . Cof_i \tag{6.20}$$

Figure 6.5 illustrates that economic consequences include lost production, deferred production, and repair costs, and the environmental portion consists of socioeconomic, oil spill cleanup, and environmental damage costs (Kontovas, Psaraftis, & Ventikos, 2010). The total cost that might be incurred as a result of failure consequences can be calculated as:

$$C_T = C_{Eco} + C_{Env} \tag{6.21}$$

Where C_T is the total cost associated with the consequences of failure, C_{Eco} is the total cost associated with the economic consequences, and C_{Env} is the total cost associated with the environmental consequences.

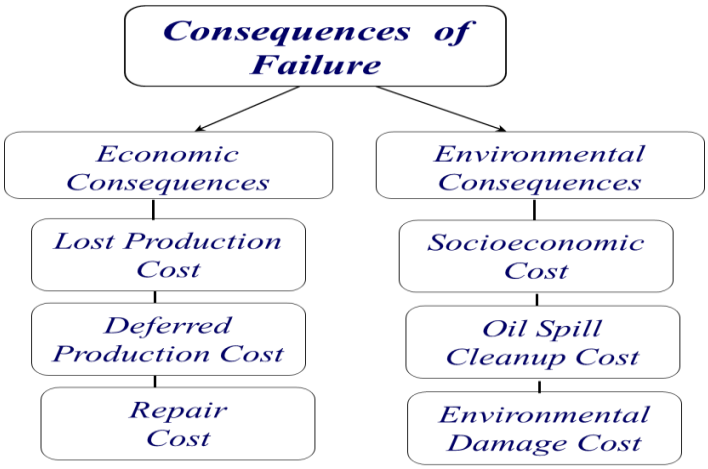

Figure 6-5: Consequences of Failure

6.4.1 ENVIRONMENTAL CONSEQUENCES

Environmental consequences can be divided into three general categories: socioeconomic consequences, oil spill cleanup, and environmental damage repair (Kontovas et al., 2010). A model for calculating the total spill cleanup cost was developed that calculates the compensation provided by the International Oil Pollution Compensation Fund (IOPCF) for damage resulting from spills (Kontovas et al., 2010). The total spill cost is expressed as (Kontovas et al., 2010):

$$C_{Env} = Total\ cost\ of\ a\ spill = 51432{Q_T}^{0.728} \quad (6.22)$$

Where Q_T is the size of a spill in tonnes and C_{Env} is the total cost associated with the environmental consequences. This covers the financial losses associated with the

environmental consequences, including socioeconomic consequences, oil spill cleanup, and environmental damage repair.

This model, developed based on oil spill data from tankers, estimates the compensation cost, which is the amount of money paid by IOPCF to the owners of the tankers to cover the costs associated with the environmental consequences. The model incorporates the costs associated with the three major environmental consequences mentioned above. The socioeconomic loss comprises income losses and property damage; the income losses include the lost income of the fishery and tourism industries (Liu & Wirtz, 2006; Kontovas & Psaraftis, 2008), while the cost of property damage includes the cost of restoring the property to its original condition.

Every tanker owner is obligated to pay insurance to cover liability, and in the event that the tanker causes oil to spill in the ocean or the sea, the owner is compensated by IOPCF. The compensation is then used to cover the damage claims by the fishery and tourism entities, and to repair the environmental damage. Although this model was developed based on data from oil spills caused by tankers to estimate compensation costs, it can be used for oil spills caused by pipelines as well. This is because oil spills in the ocean or sea have the same cost regardless of the source of the spill.

6.4.2 ECONOMIC CONSEQUENCES

The first step in the analysis of the economic consequences is to determine the mass leak rate. It is derived in terms of the area of the leak opening, and the pressure and density of the leaked products.

6.4.2.1 Mass Leak Rate

The leak rate can be expressed as (DNV-RP-G101, 2010):

$$Q = A1C_d\sqrt{2\rho(P_o - P_s)} \tag{6.23}$$

Where Q is the leak rate – kg/s; $A1$ is the leak opening cross section area – m^2; C_d is the discharge coefficient – 0.61 is used for oil (DNV-RP-G101, 2010); ρ is the liquid density – (kg/m^3); P_o is the operating pressure of the pipeline segment – (N/m^2); P_s is the external pressure surrounding the leaking spot – (N/m^2); and 1Kg/s = 0.52 barrels/60 seconds.

6.4.2.2 Lost Production

The lost production value can be calculated using the following equation:

$$C_{LP} = (Q_{LP}) \text{ x } (C_{oil}) \text{ x } (T_{LP}) \tag{6.24}$$

C_{LP} is the cost of lost production, Q_{LP} is the quantity of lost production in barrels/hour, C_{oil} is the oil price ($/barrel), and T_{LP} is the time duration of the lost production in hours.

6.4.2.3 Deferred Production

As per DNV-RP-G101, the deferred production losses in dollar value can be calculated by multiplying the amount of production (barrels/hour) by the oil price per barrel ($/barrel), and the duration of the deferred production (hours) at a reduced production rate. This chapter assumes that no reduced production rate will be applied, based on the assumption that the pipeline and the associated equipment are installed in series and no backup or redundancy is used. Therefore, the deferred production losses can be calculated in dollar value using the following equation:

$$C_{DP} = Q_{DP}\ x\ C_{oil}\ C\ x\ T_{DP} \tag{6.25}$$

C_{DP} is the cost of deferred production, Q_{DP} is the quantity of deferred production in barrels/hour, C_{oil} is the oil price ($/barrel), and T_{DP} is the time duration of the deferred production from the start of the shutdown until the completion of the repair.

6.4.2.4 Repair

The cost of repair involves the cost of repairing the affected pipeline and may also involve adjacent equipment, if it had been damaged. Comparing the cost of repair with that of the deferred production, repair costs become small (DNV-RP-G101, 2010). The cost of repair

will mainly consist of two elements: unplanned inspection (UI) and unplanned maintenance (UM) costs.

$$C_{Repair} = C_{UM} + C_{UI} \tag{6.26}$$

Economic consequences can be calculated as:

$$C_{Eco} = C_{LP} + C_{DP} + C_{Repair} \tag{6.27}$$

6.4.3 TOTAL FAILURE COST

The total failure cost encompasses all cost components—the environmental, economic, and repair costs. Obviously, the increase of corrosion growth over the years will lead to an increase of the expected leak rate and the failure cost. The failure cost at year T is estimated by finding the future value of the currently estimated total cost at predetermined annual interest and inflation rates. The future value (FV) for an amount with inflation rate I and interest rate i can be expressed as (Ayyub, 2014):

$$FV(T) = PV\left(\frac{1+i}{1+I}\right)^{T} \tag{6.28}$$

The total failure cost (C_T) at year T can be expressed as:

$$C_T(T) = [C_{Eco}(T) + C_{Env}(T)]\left(\frac{1+i}{1+I}\right)^T \quad (6.29)$$

6.5 CALCULATION OF RISK

Referring to Equation 6.19 and making use of Equation 6.29, risk (expressed in dollar value at year T for a pipeline segment i) can be calculated by multiplying the probability of failure and the consequences of failure, which mainly becomes the expected cost:

$$Risk_i(T) = Pof_i(T)x\ C_{T_i}(T) \quad (6.30)$$

If both the LDS and the pipeline fail, it takes quite some time to isolate the leaking pipeline segment and thus the failing pipeline will cause an oil spill. The total risk at year T for the entire pipeline can be expressed as:

$$Risk_T(T) = \sum_i^N Risk_i(T) \quad (6.31)$$

6.6 CASE STUDY

The case study involved a 500-km subsea pipeline laid at a depth of 10 meters underwater; one of its segments at the upstream side is suffering from an isolated metal loss defect.

Table 6-1: Pipeline and Defect Parameters

Variable	Unit		Mean	CoV	Distribution
Internal Pressure	*Po*	*MPa*	*7.7*	*0.07*	*Normal Distribution*
Pipe Diameter	*D*	*mm*	*400*	*0.003*	*Normal Distribution*
Pipe Wall Thickness	*t*	*mm*	*10*	*0.005*	*Normal Distribution*
Pipe Yield Strength	σ_y	*MPa*	*420*	*0.07*	*Normal Distribution*
Pipe Tensile Strength	σ_U	*MPa*	*520*	*0.065*	*Normal Distribution*
Initial Defect Depth	*do*	*mm*	*3*	*0.24*	*Normal Distribution*
Initial Defect Length	*Lo*	*mm*	*800*	*0.2*	*Normal Distribution*
Corrosion Depth Rate	d_{rate}	*mm/yr*	*0.2*	*0.02*	*Normal Distribution*
Corrosion Length Rate	L_{rate}	*mm/yr*	*20*	*0.2*	*Normal Distribution*

The densities of oil and ocean water are 850 kg/m^3 and 1,050 kg/m^3, respectively. Table 6.1 provides the details of the defect geometry and the information pertaining to the pipeline operating characteristics and mechanical properties. The pipeline is equipped with a fiber-optic-based LDS that has a probability of false alarm of 0.023, power-temperature coefficient of 0.9 µW/ºC, and SNR of 11 dB. The cost of unplanned inspections for the pipeline is estimated at $15,000, and the cost of unplanned maintenance is $100,000.

If both the LDS and the pipeline fail, the response time to isolate the leaking pipeline segment is estimated at 96 hours and 120 hours to repair the leaking pipeline segment. It is necessary to determine the expected failure cost in year 2 and every two years afterwards up to the year when the probability of failure reaches the target probability of failure, which has been set at 10^{-4} for two cases. In the first case, the pipeline is not protected by an LDS and in the second case the pipeline is protected by an LDS with the assumption that the

corroded pipeline segment is left without being repaired. The cost is estimated at an annual interest rate of 3% and inflation rate of 7%. The corrosion flaw details, the pipeline and the LDS relevant details are illustrated in Figure 6.6.

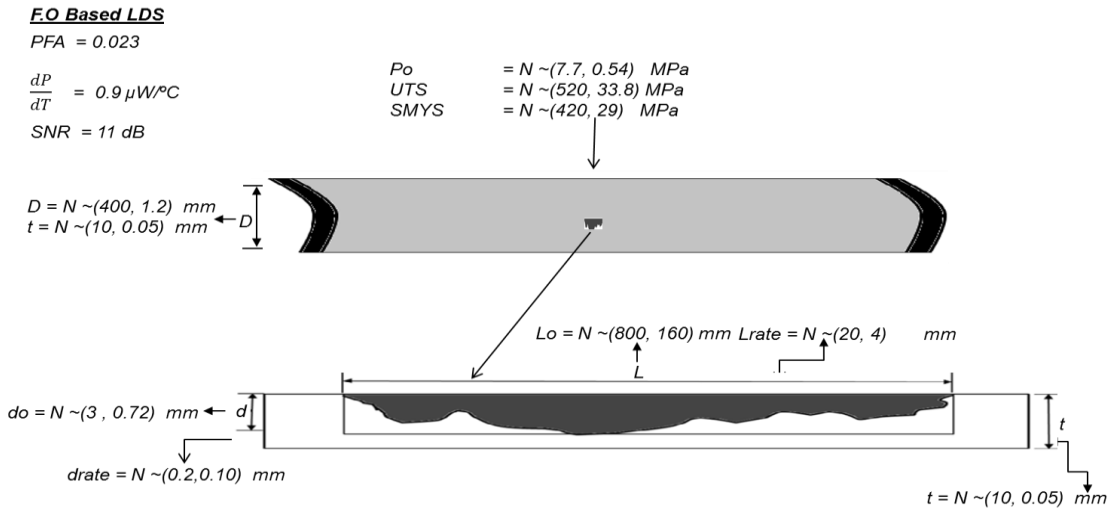

Figure 6-6: Pipeline and Corrosion Flaw Details

6.6.1 Results and Discussion

Table 6.2 shows the estimated PD, PMD, PFA, and temperature change threshold for the LDS.

Table 6-2: LDS Parameters

LDS Parameters	Value
PD	0.94
PMD	0.06
PFA	0.023
Threshold	2.6°C

Figure 6.7 illustrates the pipeline probability of failure with ±10% error interval. It is replotted in Figure 6.8 at the center point of the 10% error interval. The Figure indicates that it will exceed the target probability of failure after the sixth year.

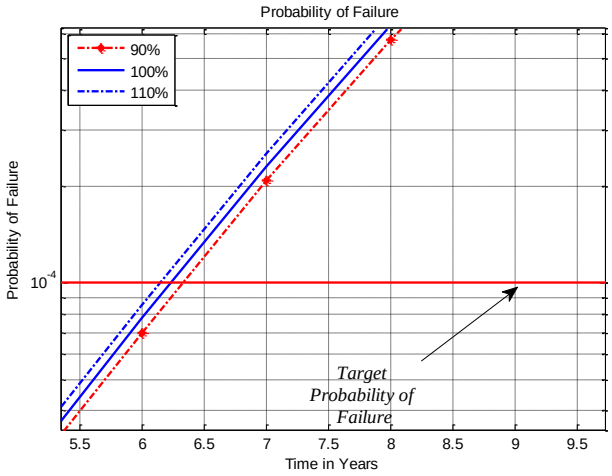

Figure 6-7: Pipeline Probability of Failure with 10% Error Interval

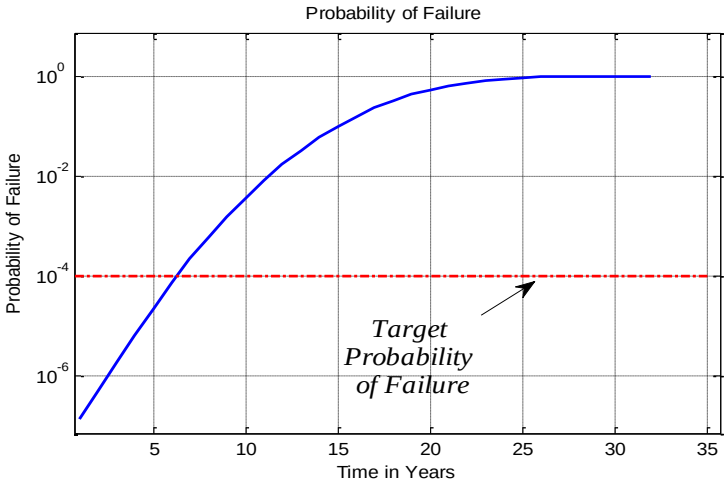

Figure 6-8: Pipeline Probability of Failure

The probability of failure for the LDS and the pipeline for the corroded segment is shown in Figures 6.9. It is obvious from the figure that the probability of failure for both the LDS and the pipeline is lower than that of the pipeline alone. Moreover, the joint probability of failure for both the LDS and the pipeline exceeds the target probability of failure after the ninth year. DNV-RP-F-101 recommends a value of 10^{-4} as the maximum allowable annual probability of failure for offshore pipelines. The probability of failure for the pipeline alone corresponds to a pipeline without LDS, basically a pipeline without protection. As the figure indicates, the pipeline with LDS takes longer to reach the target probability of failure. Undoubtedly, the LDS will minimize environmental and safety impacts of a pipeline failure. This shows that there is a very slim chance that both the LDS and the pipeline will fail at the same time for which a leak is miss detected. Knowing the probability of failure for both the LDS and the pipeline will help in determining the expected level of risk in the event a failure occurs.

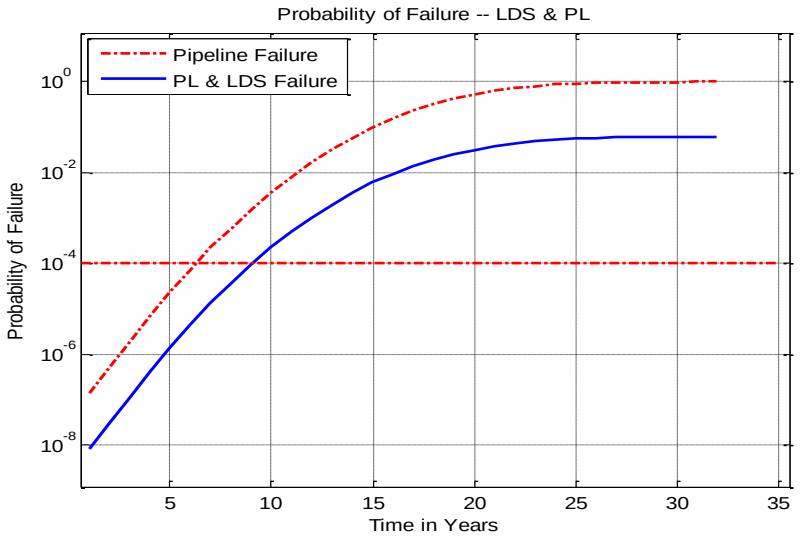

Figure 6-9: Comparison of the Probability of Failures for the Pipeline without LDS and the Pipeline with LDS

The distribution of the expected defect depth and length are shown in Figures 6.10 and 6.11, respectively.

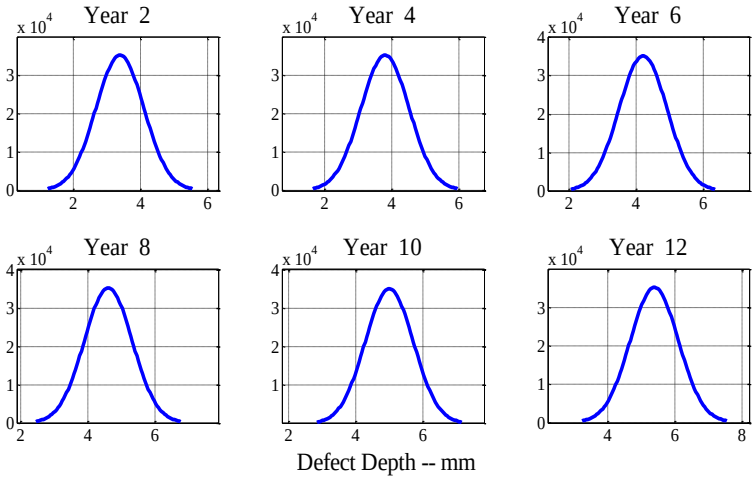

Figure 6-10: Distribution of the Expected Defect Depth Growth

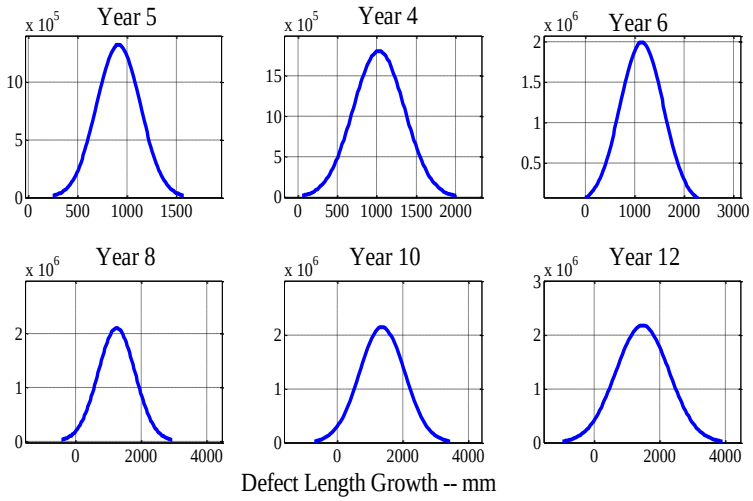

Figure 6-11: Distribution of the Expected Defect Length Growth

Figure 6.12 illustrates the expected leak flow rate in the event the pipeline fails. The leak rate is in kg/s and the time interval is in years.

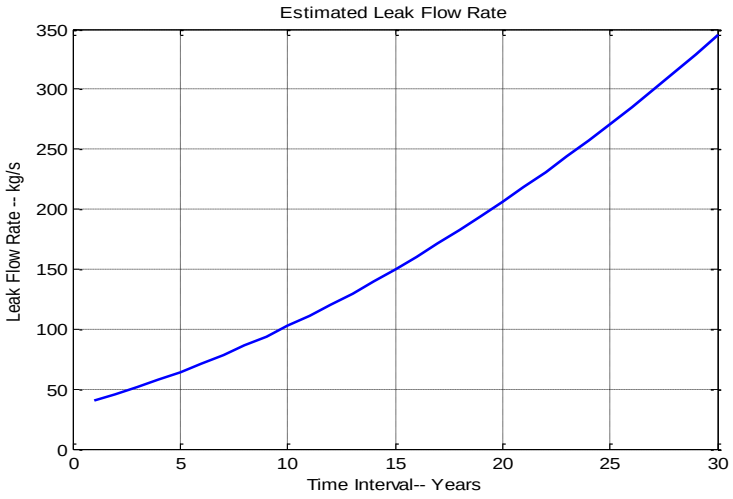

Figure 6-12: Expected Leak Flow Rate over Time

Figure 6.13 illustrates the expected level of risk in dollar value and Figure 6.14 shows the results in bar format. The expected failure cost at year 10 exceeds US$62,000.

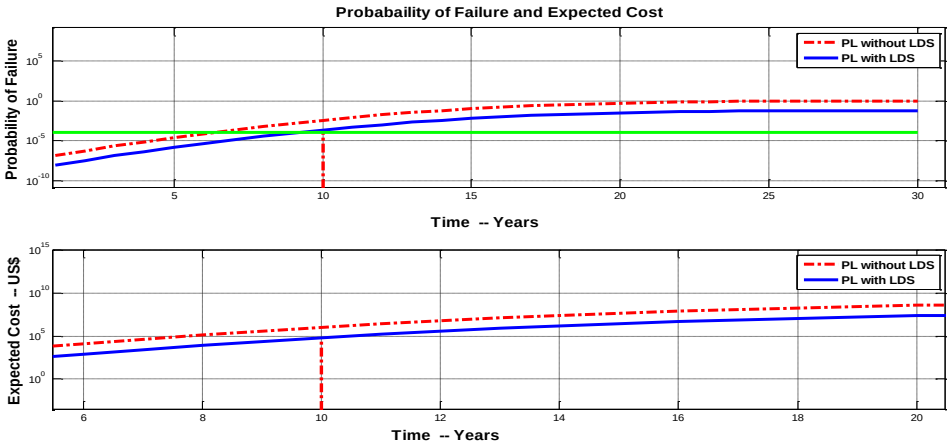

Figure 6-13: Estimated Total Financial Losses Due to Failure Consequences

This number is based on the assumption that the corroded segment of the pipeline is left without being repaired and that no inspection or preventive maintenance is conducted for the entire pipeline and the LDS. A summary of the expected failure cost is illustrated in Table 6.3.

Table 6-3: Expected Failure Cost

	With LDS			*Without LDS*
Year	***Pof***	***Expected Cost (US$)***	***Pof***	***Expected Cost (US$)***
2	2.99077E-08	3.08	4.93E-07	50.85
4	4.09072E-07	55.38	6.75E-06	913.70
6	4.44894E-06	775.95	7.34E-05	12,801.19
8	3.66254E-05	8,094.79	0.000604229	133,544.02
10	0.000225274	62,257.70	0.003716468	1,027,098.39

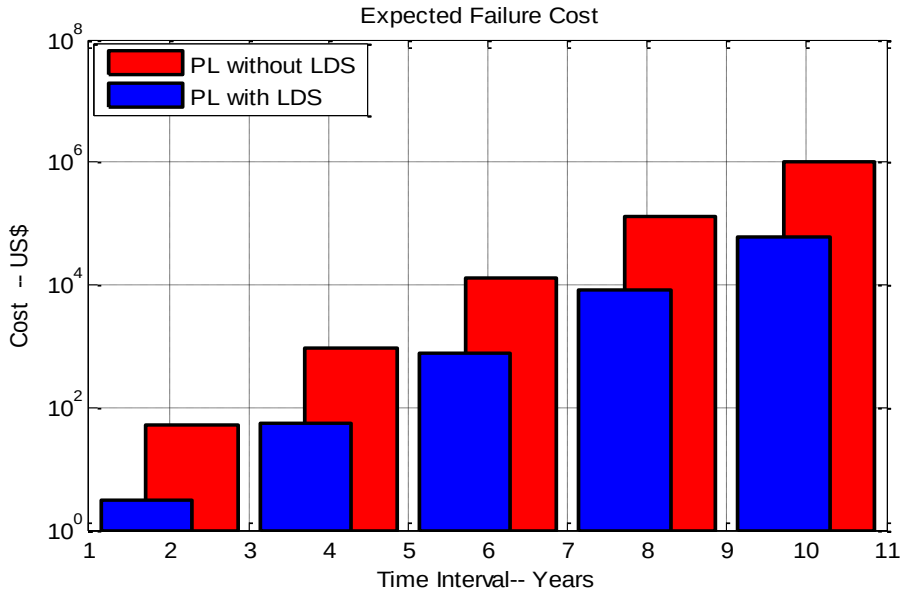

Figure 6-14: Estimated Total Financial Losses Due to Failure Consequences

It is evident from the study that probabilistic methods provided accurate results because they allow the incorporation of the parameters' inherent uncertainties in the analysis.

6.7 SUMMARY

An integrated probabilistic methodology for assessing the integrity of a corroded pipeline and its leak detection system has been presented. The limit state function approach was used to calculate the pipeline probability of failure. The limit state function was formulated to define the difference between critical corrosion depth and the estimated corrosion depth at time *T* for the pipeline.

The LDS probability of failure was derived in terms of probability of false alarm. Every defect spot along the pipeline fails due to the weakness of the spot to resist the load imposed on it, i.e., operating pressure. Regardless of the failure event, a leakage or a rupture, the failure occurs as a result of the inability of the defect spot to resist the operating pressure. The pressure model recommended by ASME B31G [14] effective area method was used in this study and the model was rearranged to calculate the defect depth that could cause one of the two failure events (the leakage or rupture).

The consequences of failure consist of economic and environmental damages that have been estimated in monetary value. The economic consequences comprise the repair cost, and lost and deferred production costs. The environmental consequences include socioeconomic consequences, oil spill clean-up, and environmental damage repair. It is of great interest to oil and gas operators to know in advance the expected level of risk in the event the system fails so that they can be better prepared to deal with such failure incidents.

CHAPTER 7
RISK ASSESSMENT OF OFFSHORE CRUDE OIL PIPELINE FAILURES: LEAKAGE AND BURST

Failure of Leak Detection System (LDS) to detect pipeline leakages or ruptures may result in drastic consequences that could lead to excessive financial losses. To minimize the occurrence of such failure, the functionality of the LDS and the integrity of the pipeline should be assessed on a priority basis. This chapter presents an integrated risk-based assessment scheme to predict the failure and the failure consequences of offshore crude oil pipelines. To estimate risk, two important quantities have to be determined, the joint probability of failure of the pipeline and its LDS and the consequences of failure. Consequences incorporate the financial losses associated with environmental damage, oil spill cleanup and lost production. The assessment provides an estimate of the risk in monetary value and determines whether the estimated risk exceeds a predefined target risk. Moreover, the critical year for the asset can be determined. In essence, the outcome of the assessment facilitates an informed decision-making about the future of the asset.

7.1 BACKGROUND INFORMATION

Pipeline rupture or leakage that has been miss-detected by LDS exposes public, or the environment to safety and health hazards. Moreover, it decreases oil and gas production and in the worst cases scenario causes a partial or complete shutdown of the production facility. According to the UK Health and Safety Executive (HSE UK, 2011) there were

about 1,978 incidents involving offshore hydrocarbon releases between 2001 and 2011 in the UK continental shelf. As per the US Pipeline & Hazardous Materials Safety Administration (PHMSA, 2014), there were about 306 offshore pipeline incidents in the U.S in the past 10 years. Out of these incidents, 71 involved hydrocarbon releases. Any failure involving the release of hydrocarbons may end up in a catastrophic incidents resulting in fatalities, damage to the environment and may threaten the corporate economy. The worst impact of all is the exposure of the public to danger in areas where the pipelines are close to shorelines or residential areas.

In light of the above, assessing the pipeline and its LDS to ensure that they do not present any safety or operational risks is highly recommended. Such assessment should take into consideration the pipelines degradation mechanisms and their growth rate. Moreover, the assessment should be comprehensive and should consider the likelihood and consequences of failure of the pipeline and the LDS. To address these issues, a risk-based assessment method is recommended to determine the level of risk expressed in dollar value. Having such information will enable operators to determine when and where to take the appropriate action to mitigate risk.

Several authors have contributed to the subject of risk-based assessment for maintenance planning, optimum replacement of the degraded components or risk assessment and its impact on safety and the environment. Risk-based assessment methods have been used to

determine the optimal replacement of offshore process components, based on the likelihood and consequence of failure caused by time-dependent degradation mechanisms (Thodi, et al., 2013). Bayesian theory along with risk-based assessments have been applied to update the probabilistic pipelines deterioration (Khan, et al., 2006; Straub & Faber, 2005; Tang, 1973) and to determine the optimal inspection plans (Straub & Faber, 2005). Moreover, risk based methodology has been used in conjunction with other techniques such as fuzzy logic to address subjectivity and uncertainty. Risk-based assessment methodology based on fuzzy logic has been used to perform risk-based assessment for pipelines, (Singh & Markeset, 2009). Likewise, risk-based methodology has been used in conjunction with Analytical Hierarchy Process (AHP) to select a maintenance strategy, (Bevilacqua & Braglia 2000; Zhaoyang, et al., 2011). Multi attributes decision making techniques have been used to improve risk assessment methodology to analyze risk and to provide a maintenance model for oil and gas process components, (Khan et al., 2004).

The cost associated with the offshore or subsea facilities is much higher than that of the onshore facility (Rangel-Ramı-rez, & Sorensena, 2012). For the offshore cases, the unplanned inspection, repair or replacement work requires mobilization of equipment and personnel transported by boats or by a helicopter, and in some cases may require the deployment of Remotely Operated Vehicles (ROVs). In addition, the extensive coordination effort and logistics are very difficult to undertake.

As per the reviewed literature, the subsea pipeline was not specifically addressed in the risk based integrity assessment as a distinct component; all what had been indicated is a general case scenario for either a whole plant or other assets associated with the processing facility. The risk-based assessment should take into account the degradation mechanisms, their growth rate and should determine the likelihood and consequences of failure.

The objective of this chapter is to provide a risk-based methodology for assessing offshore crude oil pipeline leakage and burst failures. The calculated risk is the expected financial losses that an operating company may incur as a result of the joint failure of the pipeline and the LDS. Essentially, the assessment helps decision makers to determine when and which component of the asset that requires an immediate remedial action.

Section 7.2 provides an overview and background information; section 7.3 summaries pipeline risk assessment; section 4 outlines the methodology to assess the pipeline risk; section 5.0 presents a case study; section 6.0 presents the results and provides a discussion about the results and finally section 7.0 provides a summary and concluding remarks.

7.2 OVERVIEW

The key elements of risk assessment are the estimation of the probability of failure and assessment of its consequences. Pipeline degradation takes place as a result of corrosion,

cracks or any other anomalies that grow over time. If the anomalies are overlooked or ignored and left without being repaired or the affected assets are not replaced, they may grow randomly over time. Hence, the pipeline probability of failure, which can be calculated by limit state approach, can be estimated by stochastic modeling of the degradation mechanisms. For the corrosion, the limit state function defines the difference between the measured and the critical corrosion flaw depth, and for the collapse pressure, it defines the difference between the operating and failure pressures. The LDS probability of failure is the probability of missed detection that can be expressed in terms of the signal to noise ratio and the probability of false alarm (Aljaroudi et al., 2014b). The consequence of failure is estimated as the cost of failure, which comprises the cost of pipeline replacement, environmental damage repair, and financial losses associated with lost production.

7.3 PIPELINE RISK ASSESSMENT

The assessments starts by determining the damage mechanisms and the rate of their growth over time and the likely failure events (leakage or burst). The limit state approach is used to estimate the probability of failure where the probabilistic methods is used in the estimation. The variables that influence the limit state function are random and possess an inherent uncertainties that can only be modeled by probabilistic methods. The probability distribution of each variable is determined from the collected data or from historical

records. Once the distribution is determined, the distribution parameters can be easily calculated. The consequences of failure are estimated in terms of environmental damage repair costs and financial losses due to lost and deferred production. Critical year for the asset is the year that the asset's probability of failure or the expected future risk exceeds a pre-established limit.

7.4 METHODOLOGY FOR ASSESSING PIPELINE RISK

7.4.1 Collect the Information Pertaining to the Pipeline

Information should include but not limited to, pipeline mechanical properties, pipeline operating characteristics and the extent of the corrosion flaws.

7.4.2 Determine the Failure Events

Each corrosion flaw point along the pipeline is subject to two failure events, either a leakage or burst. The leakage failure event occurs when the corrosion penetrates the entire thickness of the pipeline wall. While the burst failure event occurs when the operating pressure exceeds the failure pressure at a partially penetrated flaw spot along the pipeline. The failure consequences will be more sever if the LDS fails to detect the occurrence of leakage or burst causing oil spill and extensive production loss. Therefore, the focus of this chapter will be on the simultaneous failure of both the pipeline (leakage and burst) and the LDS.

7.4.3 Evaluate Corrosion Growth

The expected corrosion growth over time can be calculated using Equation 7.1 (ABS, 2006):

$$d = d_o + V_{cr} T \tag{7.1}$$

$$L = L_O \left(1 + \frac{V_{cr} T}{d_o}\right) \tag{7.2}$$

where d_o is the initial corrosion depth, V_{cr} is the corrosion depth growth rate, T is the time interval and L_O is the initial corrosion length, d and L are the estimated corrosion depth and length respectively at time T.

7.4.4 Define the Limit State Functions (LSF)

Limit state approach can be used to determine the probability of failure for the pipeline. Based on the discussion at the beginning of section 7.4.2, two limit state functions can be defined. The first one expresses the difference between the critical corrosion and the measured corrosion at time T. the second limit state function expresses the difference between the critical pressure which is the burst or failure pressure and the operating pressure.

Equation 7.3 expresses the difference between the capacity (C) and the load (L) of the system being evaluated (Haldar and Mahadevan, 2000; Nowak and Collins, 2000).

$$Z = C - L \tag{7.3}$$

Every flaw point along the pipeline has two possible failure events that can occur any point in time. The first failure event occurs as a result of the penetration of the corrosion flaw through the entire wall thickness of the pipeline leading to a small leak. The second failure event occurs when the operating pressure exceeds the maximum allowed pressure or the burst pressure at the corrosion flaw point causing a burst and then large leak (Aljaroudi et al., 2014a).

a. Perform Uncertainty Analysis

Operating pressure, ultimate stress, yield stress, pipeline diameter, pipeline wall thickness, radial and axial extent of the corrosion flaw establish the basic random variables of the limit state function. These variables have inherent uncertainties that make the computation

of the limit state function a difficult task to undertake. To deal with this problem, a probabilistic assessment is used to better describe uncertainty in the limit state function variables. The first step in the probabilistic assessment is to determine the probability distribution for each variable from the available pipeline data. Then the distribution

parameters can be calculated from which the probability of failure can be estimated using Monte Carlo simulation.

b. Formulate Leakage LSF

The capacity of the system for the first failure event will be the maximum allowed corrosion depth, *dc* that should not exceed 85% of the wall thickness (DNV-RP-F101, 2010). The load will be the measured corrosion depth *d(T)* at time *T* (Aljaroudi et al., 2014a). Equation 7.3 can be rewritten as indicated in Equation 7.4.

$$Z_1 = dc - d(T) \tag{7.4}$$

c. Formulate Burst LSF

The failure pressure can be calculated as recommended by the DNV part B allowable stress approach model for single defect (DNV-RP-F101, 2010) and (BS-7910, 2005):

$$P_f = \frac{2t\sigma_U}{(D-t)}\left[\frac{(1- d(T)/t)}{\left(1-\frac{d(T)}{tM}\right)}\right] \tag{7.5}$$

$$M = \left(1 + 0.31\,\frac{L^2}{Dt}\right)^{0.5} \tag{7.6}$$

substituting Equation 7.5 into Equation 7.3 yields:

$$Z_2 = \frac{2t\sigma_U}{(D-t)}\left[\frac{(1- d(T)/t)}{\left(1-\frac{d(T)}{tM}\right)}\right] \quad - \quad P_O \tag{7.7}$$

P_f is the failure pressure, *D* is the specified outer diameter of the pipe in *mm*, *t* is the wall thickness in *mm*, *d (T)* is the measured corrosion depth of the metal loss in *mm* at time *T*, σ_U is the ultimate tensile strength in *MPa* and P_O is the operating pressure in *MPa*.

7.4.5 Determine the Pipeline Probability of Failure

The probability of failure can be expressed as:

$$Pof = P\ (Z\ <\ 0) \tag{7.8}$$

Two methods can be used to determine the probability of failure when using the limit state approach in conjunction with Monte Carlo simulation. These are the counting method and the sample statistics method. Under the first method, the sum of the number of simulation trials that volatile the LSF (N_f) is computed, i.e. when the LSF becomes less than zero and this sum is divided by the number of simulation trials *(N)* to obtain the probability of failure.

$$Pof = \frac{N_f}{N} \tag{7.9}$$

Under the second method, the reliability index (β) is computed as indicated in Equation 7.10:

$$\beta = \frac{\mu_Z}{\sigma_Z} \tag{7.10}$$

μ_Z is the mean of the LSF and σ_Z is the standard deviation of the LSF. μ_Z is taken as the summation of the LSF divided by the number of simulation trials.

$$Pof = 1 - \phi(\beta) \tag{7.11}$$

The probability of failure due to corrosion can be expressed as (Aljaroudi et al., 2014a):

$$Pof_{leak} = P\ (Z_{1i}\ (Ti) < 0),\ d(T) \leq d_c \text{ and } P_O < P_f, i = 1,2, \dots, n \tag{7.12}$$

Pof_{leak} is the probability of leakage failure for a corrosion flaw i at time T_i. The capacity of the system for the second failure event will be the failure or burst pressure and the load

will be the operating pressure. The probability of burst failure can be expressed as shown in Equation 7.13, (Aljaroudi et al., 2014a).

$$Pof_{Burst} = P\ (Z_{2i}\ (Ti) \quad < 0),\ \ d(T) < d_c \ \text{and}\ P_O \leq P_f\ ,\quad i = 1,2, \dots, n \tag{7.13}$$

7.4.6 Determine the LDS Probability of Failure

Probability of LDS failure will be the probability of missed detection. It is assumed that the LDS is a fiber optic based system using a Brillouin Optical Time Domain Analysis (BOTDA) technique for sensing. The probability of false alarm and missed detection can be expressed as shown in Equations 7.14 and 7.15 respectively (Aljaroudi et al., 2014b).

$$PFA = \frac{1}{2}\left[1 - \ erf\left(\frac{Xth}{\sqrt{2\sigma^2}}\right)\right] \tag{7.14}$$

As stated above that the probability of LDS failure is the probability of the LDS missed detection, hence, $Pof_{LDS} = PMD$.

$$PMD = \ 1 - \frac{1}{2}\left[erfc\ \left(erfc^{-1}(2PFA) - \sqrt{\frac{SNR}{2}}\right)\ \right] \tag{7.15}$$

7.4.7 Determine Joint Probability of failure

The joint probability of failure for the pipeline (Pof_{PL}) and the LDS (Pof_{LDS}) can be expressed as:

$$Pof = Pof_{LDS}\, x\, Pof_{PL} \tag{7.16}$$

7.4.8 Determine the Failure Consequences

a. Quantity of Leaked Products

Quantity of leaked products can be calculated using Equation 7.17 (DNV-RP-G101, 2010):

$$Q_h = (3600)\, x\, \frac{\pi D^2}{4} C_a \sqrt{2\rho(P_o - P_s)} \tag{7.17}$$

D is the estimated diameter of the leak opening that was caused by the corrosion or burst pressure, C_a is the discharge coefficient – 0.61 (DNV - RP - G101,2010), P_o is the operating pressure of the pipeline segment - *(MPa),* ρ is the liquid density – *(Kg/m^3),* P_s is the external pressure surrounding the leaking spot - *(MPa),* Q_h is the leak rate – Kg/h.

b. Consequences

Primarily, the consequences of failure (*Cof*) are the financial losses attributable to lost production cost (*LPC*), inspection cost (*IC*), segment replacement cost (*RC*) and environmental consequences cost (*EC*).

$$Cof = LPC + IC + RC + EC \quad (7.18)$$

As per (DNV- managing risk, 2015), the estimated pipeline replacement cost in the U.S is about $643800 per/km. The inspection cost involves the cost of sending Autonomous Underwater Vehicle (AUV) with a ship to perform scanning of the pipe to determine and confirm the location of the pipeline leaking spot. The estimated cost for using AUV is approximately $26,000/day, (Wernli, 2000). This cost is based on year 2000, 1% percent is added per year as a cost trend (annual projected increase in the cost) to estimate the present cost. The cost of lost production consists of the cost of the lost quantity of oil spilled in the ocean and the cost of the delayed production due to the shutdown of the pipeline for repair; it can be expressed as indicated in Equation 7.19.

$$LPC = Q_h \, x \, C \, x \, (T_{lp} + T_{dp}) \quad (7.19)$$

Where Q_h is the leak rate (*Barrels per hour*), *C* is the price of oil – ($/Barrel), T_{lp} is the period of time where the production was lost due to spill (*hours*), T_{dp} is period of time where the production was lost due to the shutdown of the pipeline for repair.

The costs associated with environmental consequences include the compensation paid to the fishery and tourism companies, environmental damage repair cost and oil spill cleanup cost. The fishery and tourism companies are compensated for that lost income during the presence and cleanup of oil spill (Kontovas et al., 2008; Liu and Wirtz, 2006). The cost associated with environmental consequences can be expressed as indicated in Equation 7.20 (Kontovas et al., 2010).

$$EC = \ 51432[0.001\ (Q_h\ x\ T_{lp})]^{0.728} \tag{7.20}$$

The term $(0.001\ (Q_h\ x\ T_{lp}))$ is the quantity of oil spilled into the ocean or the sea in tonnes.

7.4.9 Determine Target Risk and the Expected Risk

7.4.9.1 Establish Target Risk and Critical Risk Year

The critical risk year is defined as the year that a pipeline segment exceeds the target risk. This is different than the critical failure year which is the year that the probability of failure exceeds the target probability of failure.

The critical year (Y_C) will be the minimum of the critical failure years and critical risk years as indicated in Equation 21. The critical failure years include the critical failure year

due to leakage ($Y_{L-failure}$) and the critical failure year due to burst ($Y_{B-failure}$). The critical risk years include critical risk year due to leakage (Y_{L-risk}) and critical risk year due to burst (Y_{B-risk}).

$$Y_C = Min\,[\,Y_{L-failure},\ Y_{B-failure,}\ Y_{L-risk},\ Y_{B-risk}\ ] \quad (7.21)$$

In practice, the target risk is specified in accordance with the guidelines of the operating company that dictate the acceptable level of risk that the company can tolerate. In this chapter, it is assumed that the product of the maximum allowable probability of failure of offshore pipeline and the estimated value of the asset is used to provide the target risk. As per DNV-RP-F-101, 10^{-4} is the maximum allowed probability of failure for offshore pipelines.

$$Risk_{Target} = Pof_{Target}\ x\ Value\ of\ the\ Asset \quad (7.22)$$

7.4.9.2 Determine Cost of Failure

The cost of failure consists of all cost elements associated with environmental damage, production losses due to oil spill and due to shutdown of the facility for repair and facility repair. It should be noted that all future cost elements are driven by the interest and inflation rates. The environmental consequences cost (*EC*) is driven by the expected quantity of oil

spill only; the lost production cost is driven by the quantity of the oil spill and the quantity of the lost production due to shut down. This chapter considers that the damaged pipeline is replaced and a flat rate is used to calculate the cost of inspection. Moreover, the interest and inflation rates are used to calculate future cost. The real interest rate or sometimes is called inflation-free interest rate can be calculated as (Ayyub, 2010):

$$i^* = \left(\frac{1+i}{1+I}\right) - 1 \tag{7.23}$$

i^* is the real interest rate, i is the market interest rate or nominal interest rate, and I is the inflation rate. Using Equation 7.23 the FV can be estimated as:

$$FV(T) = PV\ (1 + i^*)^T \tag{7.24}$$

FV is the future value, PV is the present value and T is the number of years. Alternatively, the equation can be expressed as:

$$FV(T) = PV\ \left(\frac{1+i}{1+I}\right)^T \tag{7.25}$$

Using Equation 7.25, the failure cost ($Cost_{failure}$) at year T can be expressed as:

$$Cost_{failure}(T) = [Cof]\left(\frac{1+i}{1+I}\right)^{T} \quad (7.26)$$

7.4.9.3 Calculate Risk

Risk is the expected financial losses which is the product of joint probability of failure (Pof) and the estimated cost of failure as indicated in Equation 7.27.

$$Risk(T) = Pof(T)\ x\ Cost_{failure}(T) \quad (7.27)$$

7.5 CASE STUDY

Three pipeline segments, each has a length of 200 meters and each has been suffering corrosion. They have a mean diameter of 700 mm and wall thickness of 14 mm. The measured initial corrosion depth and length as well as the corrosion growth have been assumed to follow normal distribution. The pipeline is equipped with a fiber optic LDS that has been specified to achieve a signal to noise ratio of *15 dB* and PFA of *0.00025*. The value of the operating facility is estimated to be 100 Million dollars. It is assumed that it will take four business days to realize or know with high certainty that a leakage or a burst has occurred. Furthermore, it is assumed that will take seven working days to restore the damaged pipelines. The maximum risk that the operating company can accept is 10,000 Dollars. The other details are summarized in Table 7.1. It is required to determine the

critical years for the three pipeline segments based on the predicted annual probability of failure and expected financial losses.

Table 7-1: Pipeline Information

			PL1		***PL2***		***PL3***		
Variable		***Unit***	***Mean***	***CoV***	***Mean***	***CoV***	***Mean***	***CoV***	***Distribution***
Operating Pressure	*Po*	*MPa*	*7*	*0.1*	*7*	*0.1*	*7*	*0.1*	*Normal Distribution*
Ultimate Tensile Strength	σ_U	*MPa*	*550*	*0.07*	*550*	*0.07*	*550*	*0.07*	*Normal Distribution*
Corrosion Depth Rate	V_{cr}	*mm/yr*	*0.3*	*0.033*	*0.4*	*0.0075*	*0.6*	*0.067*	*Normal Distribution*
Pipe Diameter	*D*	*mm*	*700*	*0.029*	*700*	*0.029*	*700*	*0.029*	*Normal Distribution*
Pipe Wall Thickness	*t*	*mm*	*14*	*0.005*	*14*	*0.005*	*14*	*0.005*	*Normal Distribution*
Initial Corrosion Depth	*do*	*mm*	*4*	*0.25*	*5*	*0.16*	*5.5*	*0.16*	*Normal Distribution*
Initial Corrosion Length	*Lo*	*mm*	*500*	*0.02*	*400*	*0.01*	*600*	*0.009*	*Normal Distribution*

The corrosion flaw details, the pipeline and the LDS relevant details are illustrated in Figure 7.1.

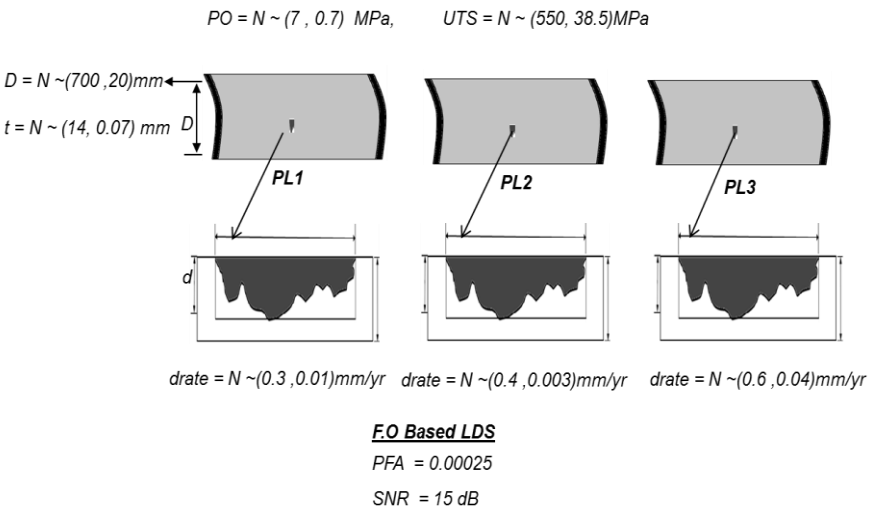

Figure 7-1: Pipeline Segments and Corrosion Flaw Details

7.6 RESULTS AND DISCUSSION

Matlab codes have been developed to run Monte Carlo simulation to generate simulated values of the random variables, and these values are used to compute the limit state function. In this study, 2x105 simulation cycles were used to run the simulation. The initial step in the analysis was to estimate the expected cumulative corrosion growth as indicated in Figures 7.2 and 7.3. These figures illustrate the expected corrosion depth and length over time respectively.

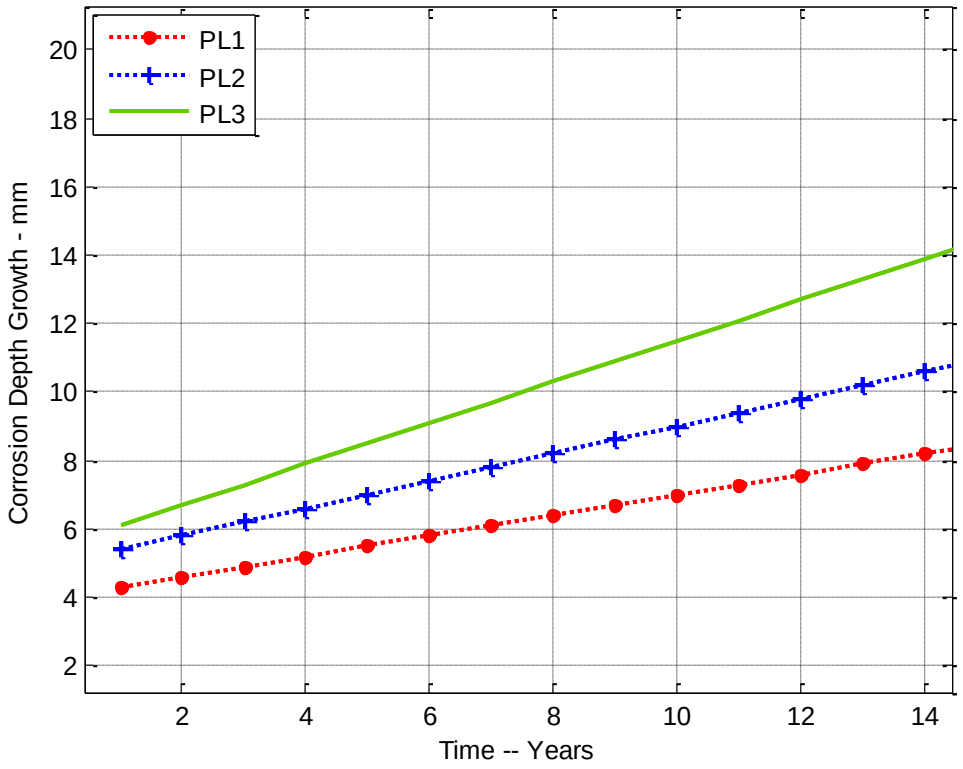

Figure 7-2: Cumulative Corrosion Depth Versus Time

Figure 7.2 indicates that the third segment is the worst among the three segments. As per DNV-RP-F101, a pipeline that has a corrosion depth exceeding 85% of the wall thickness is considered unsafe for operation. Hence, this will be considered as the critical corrosion depth. The Figure indicates that the third segment exceeds the critical corrosion (85% of the wall thickness) at the 12th year, the second segment at the 17th year and the first segment at the 27th year. Similarly, Figure 7.3 shows that the corrosion length growth for the third segment is the worst segment among the three segments. The figure reveals that the second

segment has the lowest cumulative corrosion length because it has the lowest initial defect length among the three pipeline segments.

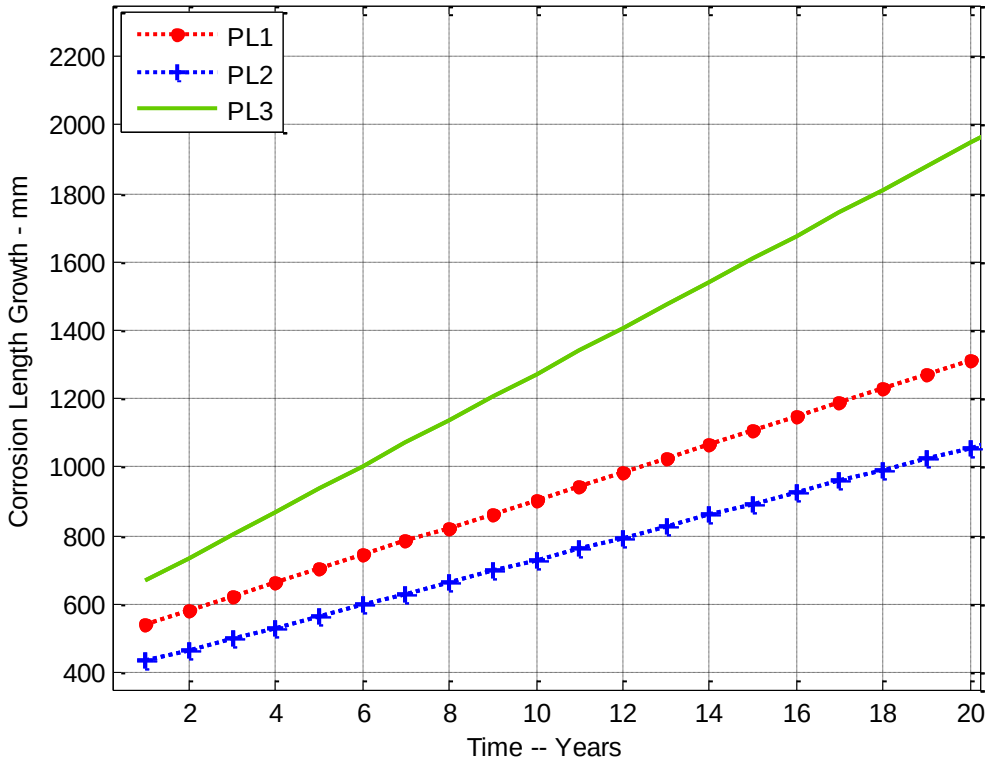

Figure 7-3: Cumulative Corrosion Length Versus Time

The next step in the analysis was to compute the limit state functions from which the probability of failures is computed for the two failure events, failure due to leakage and failure due to burst. The joint failure events are considered, failure of the pipeline and the LDS. The LDS threshold can be calculated using Equation 7.14 to yield 3.5σ, assuming standard deviation of the measurements to be *0.7 °C,* then the threshold will be *2.5 °C;* using Equation 7.15, the PMD is estimated to be 0.016.

The probability of failure plots for the three pipelines are illustrated in figures 7.4 and 7.5 respectively. Figure 7.4 illustrates the probability of leakage failure over time. As the Figure illustrates that, the probability of failure is increasing due to the increase of corrosion over time. Moreover, the Figure reveals that the third pipeline segment has the worst probability of failure, exceeding the target probability of failure at year 7. The first and the second pipeline segments exceed the target probability of failure at year 18 and 12 respectively.

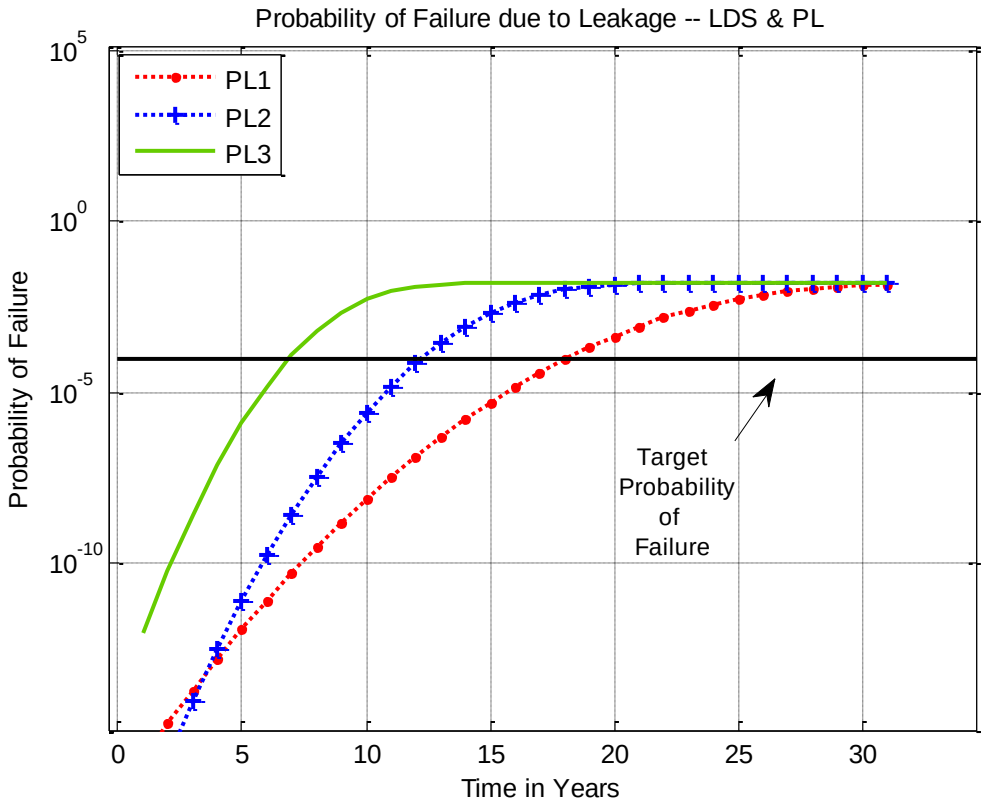

Figure 7-4: Pipelines Probability of Leakage Failure

Figure 7.5 illustrates the burst probability of failure for the three pipeline segments. The figure indicates that the third pipeline segment has the worst probability of failure exceeding the target probability of failure at year 4. The other pipeline segments, segments 1 and 2 exceed the target probability of failure at year 11.5 and 7.9 respectively.

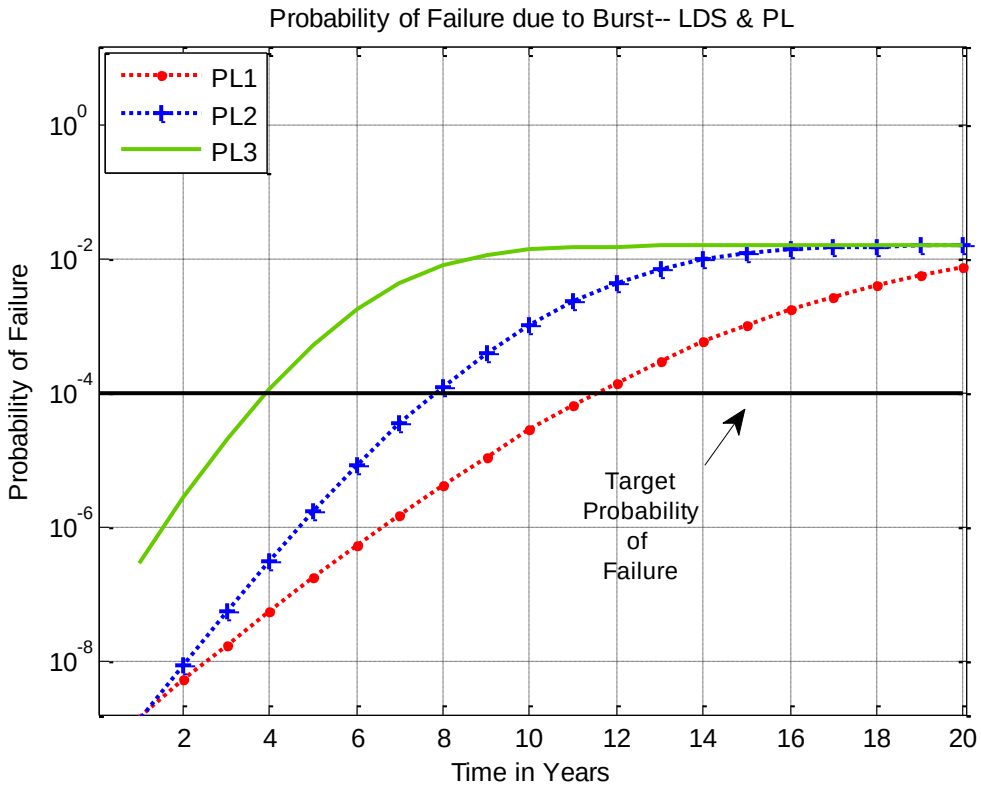

Figure 7-5: Pipelines Probability of Burst Failure

The estimated leak rate for the three Pipeline segments can be calculated using Equation 7.17 to yield the results indicated in Figure 7.6. The figure illustrates the expected leak rate for every year that could occur as result of pipeline failure with the assumption that the

corrosion flaw stayed without being repaired. The figure indicates that the third pipeline segment has the highest expected leak rate due to the fact that this segment has the highest corrosion growth rate and has the highest initial corrosion length. The second pipeline segment has the lowest expected leak rate as this segment has the lowest initial corrosion length.

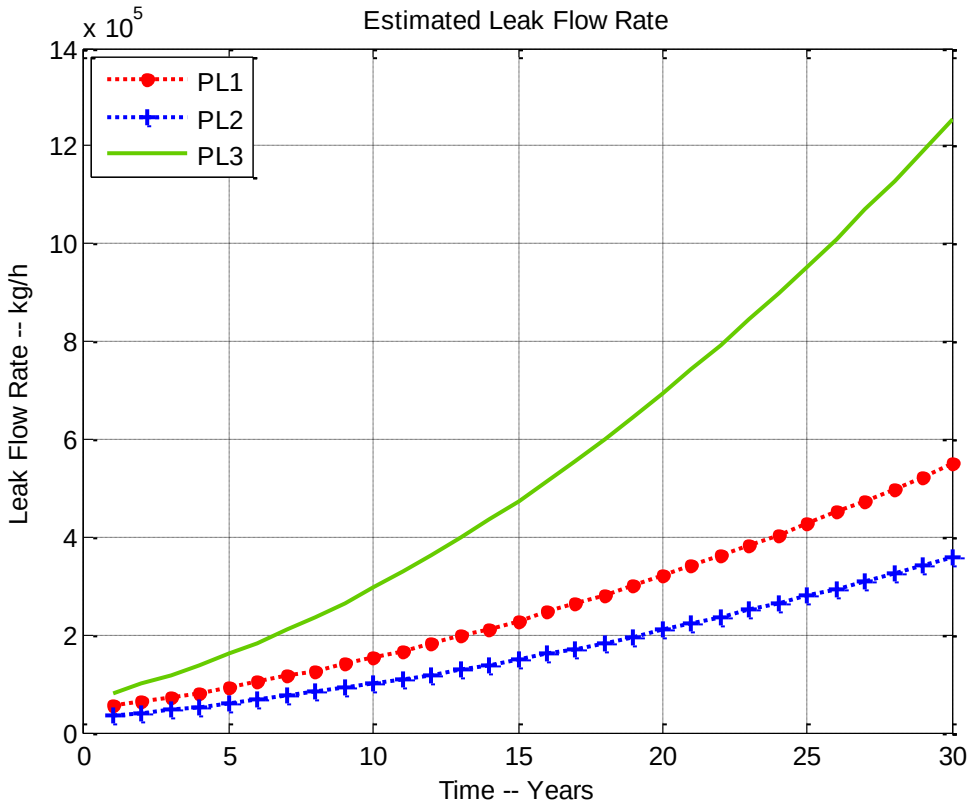

Figure 7-6: Estimated Leak Rate

Using Equation 7.22 the target risk is estimated to be 10,000 Dollars. Figure 7.7 illustrates the expected risk as a result of leakage failure over time for the three pipeline segments. The Figure reveals that the 1st pipeline segment exceeds the target risk at year 17, the second segment at year 12.25 and the third pipeline at year 6.8.

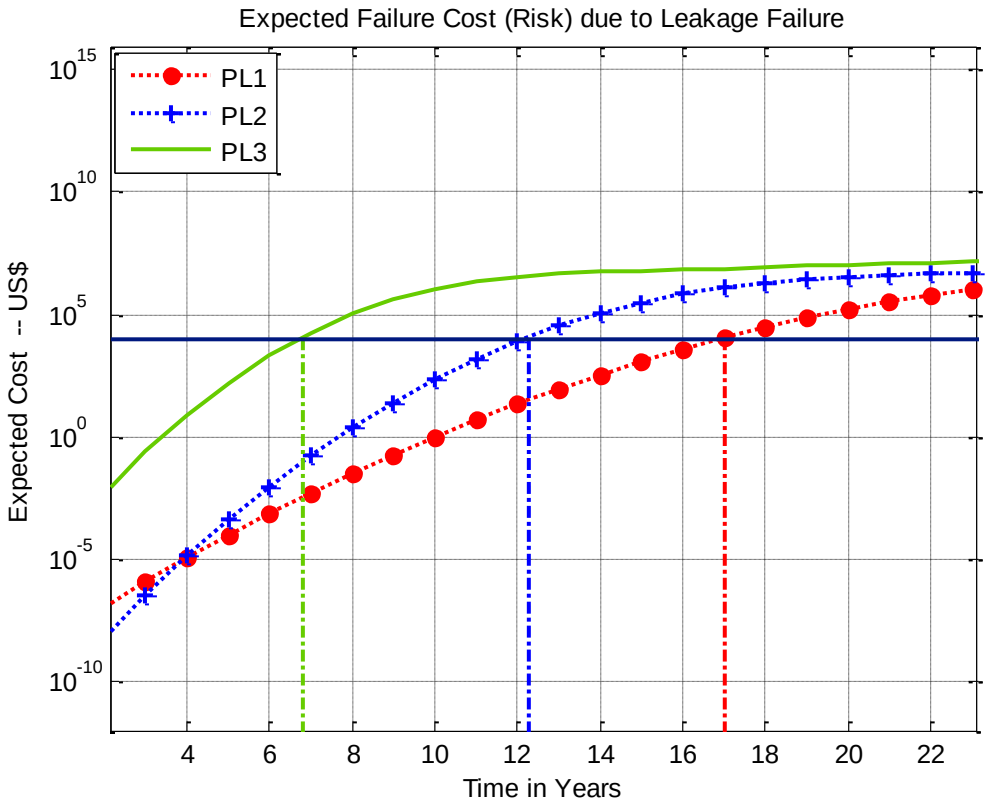

Figure 7-7: Expected Financial Losses Due to Leakage Failure

Figure 7.8 illustrates the expected risk due to burst failure over time for the three pipeline segments. The Figure reveals that the 1st pipeline segment exceeds the target risk at the year 11, the second segment at year 8 and the third pipeline at year 4.

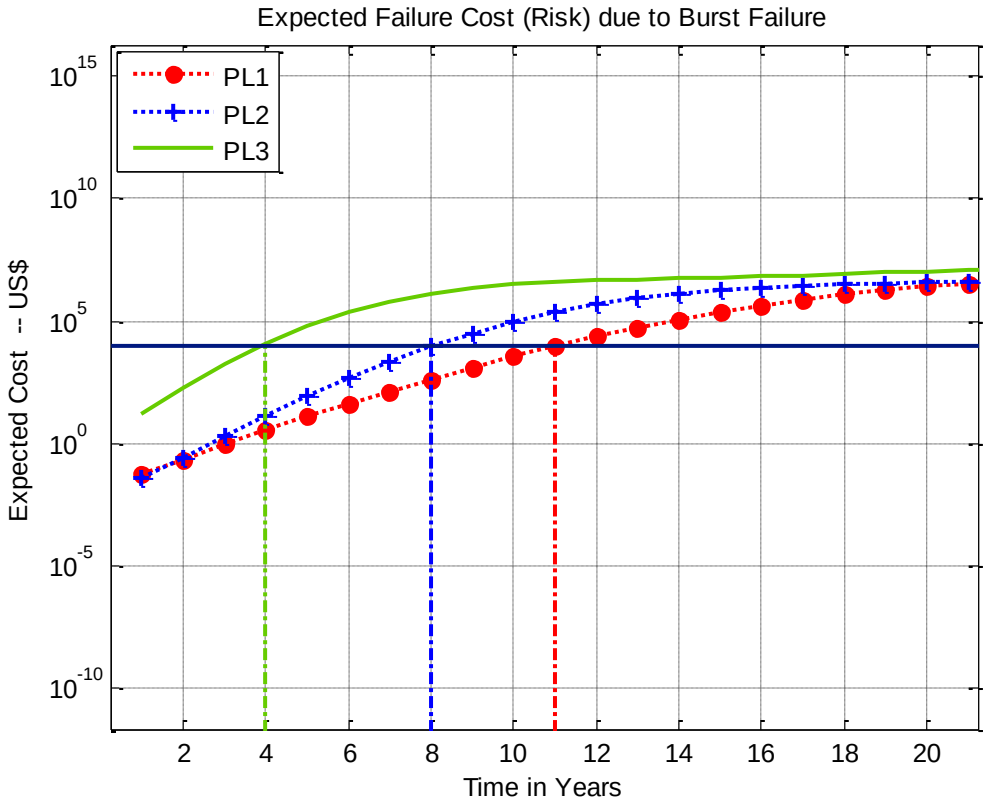

Figure 7-8: Expected Financial Losses Due to Burst Failure

Table 7.2 provides the critical failure and critical risk years for the three pipeline segments. The critical failure year is the year that the pipeline segment exceeds the target probability of failure. While the critical risk year is year that the pipeline exceeds target risk due to leakage or burst failure. Obviously, the third pipeline segment is the fastest to exceed the

target risk and is the worst among the three segments in terms of the expected financial losses due to either leakage or burst failure.

Table 7-2: Critical Years for the Three Pipeline Segments

Pipeline Segments	*Leakage Failure*		*Burst Failure*		*Critical Year*
	Critical Failure Year	*Critical Risk Year*	*Critical Failure Year*	*Critical Risk Year*	
PL1	*18*	*17*	*11.8*	*11*	*11*
PL2	*12*	*12.25*	*8*	*8*	*8*
PL3	*7*	*6.8*	*4*	*4*	*4*

As per the information presented in the table, it is recommended that the third pipeline segment should be replaced at year 4, while the first and the second segments should be replaced at years 11 and 8 respectively.

7.7 SUMMARY

Risk assessment methodology for offshore pipelines has been presented. The methodology has been used to determine the level of risk or the expected financial losses as a result of pipeline and LDS joint failures. Furthermore, the methodology has been applied to determine the critical failure and the critical risk years, from which the critical year for the asset being evaluated can be determined.

CHAPTER 8
SUMMARY AND CONCLUDING REMARKS

An integrated probabilistic assessment framework for assessing oil and gas transport systems and their condition monitoring systems has been developed. The focus of the research was on a fiber-optic-based leak detection system (LDS). Four major tasks were undertaken to accomplish the objectives of the research: 1) formulation of the probability of detection and false detection for a fiber-optic-based LDS, 2) development of a probabilistic performance assessment scheme for a fiber-optic-based LDS, 3) application of probabilistic methods for assessing the integrity and determining the probability of failure as well as the remaining life of an oil and gas transport component (i.e., the pipeline), and 4) development of a risk-based assessment methodology to determine the risk associated with the simultaneous failure of the LDS and the oil and gas pipeline.

The last task resulted in a joint probabilistic assessment approach for corroded pipelines and the LDS to provide a thorough and accurate assessment of the integrity of the pipeline and the performance of the LDS. The joint probability of failure for both the pipeline and the LDS encompasses both the failure of the pipeline and the failure of the detection system. The overall probability of failure for the LDS consists mainly of two failures; namely, detection failure and false detection. Probability of false detection was evaluated

separately as its consequences are different from those associated with detection failure. The consequences of false detection only include the deployment of equipment and personnel to the site thought to be affected; however, such consequences have insignificant financial losses and thus can be neglected. The consequences of detection failure take place only when an actual leak occurs and causes environmental damage; the effect of the ensuing production losses is very significant.

Under this research, a probability-based assessment approach was adopted as it is the best suited to deal with uncertainty. This research used probabilistic methods to quantify the magnitude of uncertainty and variability inherent in the parameters that govern the performance of the systems that are under study. It is evident from the analysis, that using probabilistic methods provided results that are more certain and accurate. Sometimes, systems might be so complex and have significant uncertainties inherent in the governing variables. To tackle such a problem is to use probabilistic methods in conjunction with Monte Carlo simulation. These methods can provide all possible outcomes of the problem being analyzed. Furthermore, they allow researchers to explore and predict the behavior of the system more easily. Using deterministic methods may not provide accurate results because they considers only one point estimate of the parameters that are under study.

A summary and concluding remarks for each research topic are discussed in the following sections.

8.1. Leak Detection Systems' Probability of Detection and False Detection

The PD and the PFA were formulated for a fiber-optic-based LDS. These parameters form the fundamental building blocks for assessing the performance of the LDS. The analysis revealed that as the SNR increases, the PD and PFA also increase. The simultaneous increase of the PD and the PFA presents a great challenge when designing or specifying the system. Furthermore, the analysis showed a direct relationship between the parameters; in other words, the PD increases with the increase of PFA. To address this challenge, an acceptable PFA should first be selected from which a satisfactory threshold can be determined. Once the threshold is established, the PD can be immediately determined.

Missed detection and false detection are detrimental to the system performance, and the consequences of their occurrence cost time and money. The question is which one is more costly; obviously, the consequences of missed detection will result in a greater financial burden than the consequences of false detection. Therefore, the initial step in designing such systems is to determine the magnitude of risk that the operators can accept and tolerate in the event a missed detection takes place. Once this step has been accomplished, the performance parameters can easily be established.

8.2 Probabilistic Performance Assessment of Fiber Optic Leak Detection Systems

A probabilistic performance assessment scheme based on limit state approach for the entire fiber optic LDS has been developed. The probabilistic assessment outcome includes the probability of failure for the entire LDS along the pipeline. In addition, the response time for the entire LDS along the pipeline was provided as part of the assessment. Essentially, this topic demonstrated how the limit state approach can be used to calculate the probability of failure (probability of missed detection) for fiber-optic-based LDS.

Monte Carlo simulation technique was applied to calculate the probability of failures using sample statistics and counting methods. Matlab codes were developed and used to implement the methodology and run the simulations.

The consequences of LDS detection failure are different than those of false detection, and therefore they are calculated separately. The latter causes oil spills that require the mobilization of full crew and equipment and other required resources required for cleanup and repair. The false detection only requires the mobilization of the crew to the site and no work is required as there is no actual leak or oil spill. Knowing the probability of failures beforehand will assist operators to prepare in advance and allocate the required resources

for such incidents. Having prior knowledge about what could happen in the case of a failure will minimize downtime and enhance production during these situations.

The limit state equations were formulated on the assumption that the capacity and load are probabilistic as they are affected by varying operational demands and environmental conditions. We found that the sample statistics technique and the counting method for calculating the probability of failure almost produce the same results.

8.3 Application of Probabilistic Methods for Assessing the Integrity of Offshore Pipelines

A methodology for determining the probability of failure and the remaining life of aging pipelines has been developed. The assessment was conducted using limit state approach to calculate the probability of failure. Two limit state functions (LSF) were formulated. The first defines the difference between the critical corrosion depth and the measured corrosion depth at a given point in time. The second expresses the pressure change, which is the difference between the two pressures (burst pressure and operating pressure). Monte Carlo simulation technique was applied to calculate the probability of failures and determine the remaining life of the pipeline. Matlab codes were developed and used to implement the methodology and run the simulations. The methodology adopted the models presented in DNV-RP-F101/BS-7910 and ASME-B31G. The results indicated that the difference in the estimated remaining life is fairly close. The analysis showed that the estimated remaining

life based on the corrosion LSF and the DNV/BS failure pressure LSF are similar. Moreover, the combined failure probability analysis indicated that ASME modified method is less conservative than the DNV approach. From the study it was concluded that the ASME B31G effective area method is the most conservative method.

The differences in these models are attributed mainly to the different approaches for calculating the area of flaw or defect shapes, the diameter of the pipe considered, and whether tensile strength or yield strength is used. For example, DNV-RP-F101 Part B and BS-7910 models consider the nominal diameter (D-t) while the ASME model considers the outer diameter (D). DNV-RP-F101 Part B, BS-7910, and ASME B31G effective area method use a rectangular shape for the flaw (dL) while the modified ASME B31G model uses 0.85(dL); where d is the flaw depth and L is the flaw length. DNV-RP-F101 Part B and BS-7910 use ultimate strength while ASME uses yield strength. In short, the difference arises from the usage of different models in these standards.

8.4 Risk Assessment of Offshore Crude Oil Pipeline Failure

Risk assessment methodology for offshore pipelines has been presented. The methodology is used to determine the level of risk or the expected financial losses due to the joint failure of the pipelines and the LDS. Chapters 6 and 7 were dedicated to discussing this topic. Chapter 6 presented a methodology to assess risk due to LDS failure and pipeline rupture

failure only, while chapter 7 presented a methodology to assess risk due to LDS failure and pipeline rupture and leakage failures. Time dependent degradation mechanism, such as corrosion, is one of the main causes of pipeline failure; it weakens the pipeline leading to two possible failure events, leak or rupture. When corrosion penetrates the entire thickness of the pipeline wall, a leak failure occurs. The operating pressure exceeds the maximum allowed pressure or the burst pressure at the corrosion flaw point, which causes a burst or large leak failure.

Limit state approach was used to determine the probability of failure due to corrosion, which was derived as the difference between the critical corrosion depth and the measured corrosion depth at time *T*. Likewise, limit state approach was used to determine the probability of failure due to burst pressure.

The LDS probability of failure was derived in terms of probability of false alarm. It was assumed as part of the LDS specification that either the probability of false alarm or the threshold is a given parameter. From the threshold the probability of false alarm can be determined and from this value the probability of detection and missed detection can be determined. Detection failure takes place only when there is an actual leak happening and the LDS fails to detect it (and the leak is assumed to be an independent failure event from that of the pipeline). The joint probability of failure, which encompasses the pipeline failure and the detection failure, was used to determine the overall probability of failure.

Risk was defined as the product of the joint probability and consequences of failure for the LDS and pipeline. Failure consequences, consist of economic and environmental damages estimated in monetary value. The economic consequences comprise the repair cost and the financial losses due to lost and deferred oil production. The environmental consequences comprise socioeconomic consequences, oil spill cleanup, and environmental damage repair. It is of great interest for oil and gas operators to know in advance the expected level of risk in the event the system fails so that they can be better prepared to deal with such failure incidents. Furthermore, having prior knowledge of the expected level of risk enables financial planners to allocate the required capital and resources to cover the costs associated with the consequences of failure. Examples were presented that illustrated the application of the methodology.

CHAPTER 9
CONTRIBUTIONS AND RECOMMENDATIONS FOR FUTURE RESEARCH

The developed assessment framework is a very useful tool to assess and predict the integrity of oil and gas transport components, i.e., pipelines, and the reliability of the LDS. Moreover, the assessment provides an estimate of the level of risk associated with the failure of these systems.

This framework can be considered as one of the key elements of the oil and gas asset integrity management system. It can be easily implemented by integrating it with the periodic or preventive maintenance programs to assess the integrity of the systems and determine what courses of action are necessary to enhance the performance of the evaluated systems.

The focus of this research was on the oil and gas transport component and the leak detection system, which can be extended to include pressure equipment, vessels, tanks, and other components of oil and gas infrastructure. Moreover, this research can be extended to include active components such as pumps, compressors, etc. Section 9.1 summarize the contributions of this research and section 9.2 recommends avenues for future research.

9.1 CONTRIBUTIONS

9.1.1 Performance Assessment of Fiber-Optic-Based LDS

9.1.1.1 Probability of detection and false detection

There is a need to have a reliable and effective condition monitoring system, such as LDS, to provide assurances that the monitored pipeline is safe and functioning as per operating conditions. Hence, the behavior of the monitoring system should be assessed frequently and the assessment should take into consideration the probabilistic nature of the system. Moreover, there is no established method for evaluating the PD and PFA for fiber-optic-based LDS. The missed detection and false detection are both detrimental to system performance, and thus it is essential to know these two parameters beforehand to be better prepared to deal with failure situations and able to minimize the impact of the failure. As a result, this research was undertaken in order to formulate these two parameters to establish the framework for assessing the performance of the LDS, which was addressed in the chapter 3 (first research topic) and chapter 4 (second research topic). Undoubtedly, knowing how the system behaves will assist operators in implementing the most appropriate course of action that might be required to enhance system reliability and ensure better preparedness to minimize the consequences of its failure. The research outcomes include mathematical models to calculate:

- Probability of detection
- Probability of missed detection
- Probability of false alarm
- Minimum detectable temperature change

9.1.1.2 Probabilistic Performance Assessment of Fiber-Optic-Based Leak Detection Systems

Chapter 4 extended the limit state approach, which is traditionally applied to structural assessment, to instrumentation, i.e., LDS, to determine the probability of detection failure for a fiber-optic-based LDS. Detection failure combines two failure events, missed detection and delayed detection. The assessment established a probabilistic scheme incorporating the randomness and variability inherent in the performance parameters. In essence, the outcome of the assessment provided the overall probability of failure for the entire LDS along the pipeline as well as response time and accuracy. The research outcomes include mathematical models based on limit state approach to calculate:

- Probability of detection failure for the entire LDS along the pipeline
- Probability of false alarm from the entire LDS along the pipeline
- Response time

9.1.2 Application of Probabilistic Methods for Assessing the Integrity of Offshore Pipelines

Uncertainty in the data pertaining to pipeline geometry, pipeline material properties, pipeline inspection, and operating characteristics present a great challenge to the analysis. Moreover, the codes and standards used for assessing pipeline integrity follow a deterministic approach for calculating the different parameters. Considering these challenges, efforts have been undertaken by this research to develop and introduce a probability-based assessment approach to deal with the aforementioned challenges and to determine the probability of failure for the pipeline (chapter 5). The pipeline probability of failure can be used as a measure to determine the fitness of the pipeline for service and determine its remaining life when compared against a target probability of failure. The research outcomes include:

- A probabilistic model for determining the annual probability of failure and assessing the remnant life of aging subsea pipelines. This model can be used to determine the allowable life extension without compromising safety and reliability.

- Comparative study of the remnant assessment models (using corrosion and burst pressure) as presented in selected codes and standards, i.e., ASME, DNV, and BS.

- Uncertainty and variability in the input data and model are reduced through Monte Carlo simulation and probabilistic methods.

9.1.3 Risk-Based Methodology for Assessing Offshore Pipeline Condition Monitoring Systems

The failure of the LDS to detect hydrocarbon releases from an offshore pipeline can have devastating effects on the operation and environment. Moreover, the failure consequences may bring about excessive financial losses and could threaten the survivability of the operating company in the market.

It is therefore crucial that operating companies continually conduct risk-based assessments of the integrity and operability of their pipeline network to ensure they do not pose any threat to the continuity of oil flow.

In light of the above, an integrated risk-based assessment approach for offshore pipelines and LDS was developed in this research. This approach can be used to predict and quantify the future financial impact in the event a pipeline or condition monitoring system (i.e., LDS) fails. The assessment provides the expected level of risk expressed in monetary value. Knowing the level of risk beforehand enables operating companies to allocate the required financial resources to cover the unexpected future financial losses that may result from the failure of a process component. The research outcomes include:

- A probabilistic model for determining the annual probability of failure of the pipeline based on thinning (corrosion) damage.

- The overall risk in terms of the probability and consequences of failure.
- An economic-based risk assessment.

9.2 FUTURE RESEARCH

9.2.1 Probability of Detection and False Detection for Fiber-Optic-Based LDS

This research was limited to fiber-optic-based LDS. Future research should be extended to include other types of LDS, such as negative pressure, pressure point, volume balance, and real time transient methods. In addition, fiber-optic-based LDS that use other sensing techniques, such as Raman, can be investigated in future research. Performing experimental work in a lab setting would provide different approaches to the development of the probability of detection and false detection models. Furthermore, the experimentally developed models can be compared against the theoretically developed models, which can provide a deep and thoughtful understanding of the probability of detection and false detection.

9.2.2 Probabilistic Performance Assessment of Fiber-Optic–Based LDS

This research developed a probabilistic performance assessment scheme based on limit state approach for the entire fiber-optic LDS. Similarity may exist between this research topic and the previous research topic, but they address two different subjects. The first topic

provided the formulation of the PD and the PFA, and this topic tries to determine these two parameters using the limit state approach. Essentially, this topic demonstrates how the limit state approach can be used to calculate the probability of failure (probability of missed detection) for fiber-optic-based LDS. Furthermore, the LDS response time and probability of delayed detection were developed. This research was limited to fiber-optic-based LDS used for monitoring pipelines; investigating the detection of hydrocarbon leakage from vessels and tanks in addition to pipelines would open the door for a wider spectrum of applications.

9.2.3 Application of Probabilistic Methods for Assessing the Integrity of Offshore Pipelines

Under this research topic, a probabilistic methodology was developed to assess the integrity of a pipeline and determine its probability of failure as well as its remaining life. The study considered only one damage mechanism which s corrosion, future research can extend this work to include other damage mechanism such cracks and other time-independent mechanisms such as third-party inference, geo-hazards, and operational as well as construction errors. Moreover, future research can extend this work to perform level III analysis using the Finite Element Method to obtain more insight and understanding of the failure models. This will enable practitioners to determine the most accurate model that needs to be considered in the evaluation.

9.2.4 Risk Assessment of Offshore Crude Oil Pipeline Failure Due to Rupture

A methodology was developed to assess the risk associated with the simultaneous failure of the LDS and offshore pipelines. The focus was on the failure due to rupture only, which occurs as a result of corrosion. Future research could be extended to include rupture failure resulting from accidental impact with foreign objects hitting the pipelines.

9.2.5 Risk Assessment of Offshore Pipeline Rupture and Leakage Failure

A methodology was developed to assess the risk associated with the simultaneous failure of the LDS and offshore pipelines, with a focus on failure due to rupture and leakage that may occur as a result of corrosion. Future research can be extended to include failures resulting from third-party interference, sabotage, or geo-hazard incidents. Moreover, extension of this work to include assessment of onshore as well as arctic pipelines is recommended.

REFERENCES

Agrawal, G. P. (2001). *Nonlinear fiber optics* (3rd ed.). Oxford, U.K.: Academic Press.

Ahmmed, M. (1998). Probabilistic estimation of remaining life of a pipeline in the presence of active corrosion defects. *International Journal of Pressure Vessels and Piping*, *75*, 321–329.

Akib, A., Saad, N., & Asirvadam, V. (2011). Pressure point analysis for early detection system. In *Proceedings of IEEE 7th International Colloquium on Signal Processing and Its Applications*, Penang, Malaysia, 4–6 March 2011, 103–107.

Alaska Department of Environmental Conservation. (1999). *Technical review of leak detection technologies volume 1: Crude oil transmission pipelines*. Retrieved from https://dec.alaska.gov/spar/ipp/docs/ldetect1.pdf

Aljaroudi, A., Khan, F., Akinturk, A., Haddara, M., & Thodi, P. (2014b). Formulation and analysis of probability of detection and false detection for subsea leak detection systems. *Proceedings of the 10th International Pipeline Conference, IPC2014*, September 29–October 3, 2014, Calgary, Alberta, Canada.

Aljaroudi, A., Thodi, P., Akinturk, A., Khan, F., & Paulin, M. (2014a). Application of probabilistic methods for predicting the remaining life of offshore pipelines. *Proceedings of the 10th International Pipeline Conference, IPC2014*, September 29–October 3, 2014, Calgary, Alberta, Canada.

American Bureau of Shipping (ABS). 2006. Guide for Building and Classing Subsea Pipeline Systems. Houston, TX, USA.

Andersen, T., & Misund, A. (1983). Pipeline reliability: An investigation of pipeline failure characteristics and analysis of pipeline failure rates for submarine and cross-country pipelines. *Journal of Petroleum Technology*, *35*(4). http://dx.doi.org/10.2118/10467-PA

API Publication 1155. (1995). *Evaluation methodology for software based leak detection systems*. Washington, DC: American Petroleum Institute.

API 1130. (2002). *Computational pipeline monitoring for liquid pipelines* (2nd ed.). Washington, DC: American Petroleum Institute.

API-579-1/ASME FFS-1. (2007). *Fitness-for-service, American Society of Mechanical Engineers (ASME)/American Petroleum Institute (API).* Washington, DC, USA.

ASME-B31G. (2012). *Manual for determining the remaining strength of corroded pipelines: A supplement to ASME B31 for Pressure Piping*. New York, NY, USA.

Ayyub, B. M. (2014). *Risk analysis in engineering and economics* (2nd ed.). Boca Raton, FL, USA: CRC Press.

Bai, Y., & Mustapha, M. (2010). Risk & reliability based fitness for service (FFS) assessment for subsea pipelines. *Proceedings of the ASME 29th International Conference on Ocean, Offshore and Arctic Engineering OMAE2010,* Shanghai, China.

Bao, X., & Chen, L. (2012). Recent progress in distributed fiber optic sensors. *Sensors 2012*, *12*, 8601–8639. doi: 10.3390/s 120708601.

Bao, X., DeMerchant, M., Brown, A., & Bremner, T. (2001) Tensile and compressive strain measurement in the lab and field with the distributed Brillouin scattering sensor. *Journal of Lightwave Technology*, *19*(11), 1698–1704.

Bao, X., Dhliwayo, J., Heron, N., Webb, D. J., & Jackson, D. (1995). Experimental and theoretical studies on distributed temperature sensor based on Brillouin scattering. *Journal of Lightwave Technology*. *13*(7), 1340–1347.

Bao, X., Webb, D. J., & Jackson, D. (1993). A 32-km distributed temperature sensor based on Brillouin loss in optical fiber. *Optics Letters*, *18*(18), 1561–1563.

Barkat, M. (2005). *Signal detection and estimation*. Norwood, MA, USA: Artech House.

Barnoski, M. K., Rourke, M. D., Jensen, S. M., & Melville, R. T. (1977). Optical time domain reflectometer. *Applied Optics*, *16*, 2375–2379.

Belal, M. (2011). *Development of a high spatial resolution temperature compensated distributed strain sensor* (PhD dissertation, Physical and Applied Science Optoelectronics Research Center, University of Southampton, Southampton, U.K.).

Bevilacqua, M., & Braglia, M. (2000). The analytical hierarchy process applied to maintenance strategy selection. *Reliability Engineering & System Safety, 70,* 71–83.

Brown, K. A. S. (2006). *Improvement of a Brillouin scattering based distributed fiber optic sensor* (PhD thesis, University of New Brunswick, NB, Canada).

BS-7910. (2005). *Guide to methods for assessing the acceptability of flaws in metallic structures*. British Standards, London, U.K.

Caleyo, F., Gonzalez, J., and Hallen, J. (2002). A study on the reliability assessment methodology for pipelines with active corrosion defects. *International Journal of Pressure and Piping*, *79*, 77–86.

Daneti, M. (2010). A model based approach for pipeline monitoring and leak locating. *September 2009 SPE Projects, Facilities & Construction* IEEE.

Damzen, M., Vlad, V. I., Babin, V., & Mocofanescu, A. (2003). *Stimulated Brillouin scattering: Fundamentals and applications*. London, U.K.: Institute of Physics Publishing.

Dey, P. K. (2001). A risk-based model for inspection and maintenance of cross-country petroleum pipeline. *Journal of Quality in Maintenance Engineering*, *7*(1), 25–41.

Dong, Y., Chen, L., & Bao, X. (2012). Extending the sensing range of Brillouin optical time domain analysis combining frequency-division multiplexing and in-line EDFAs. *Journal of Lightwave Technology*, *30*, 1161–1167.

DNV – Infrastructure. (2015). *Managing risk/corrosion and material degradation*. Retrieved from http://www.dnvusa.com/focus/corrosion_materials_degradation/infrastructure

DNV-RP-G101. (2010). *Risk based inspection of offshore topsides static mechanical equipment*. Oslo, Norway: Det Norske Veritas.

DNV-RP-F101. (2010). *Recommended practice for corroded pipelines*. Oslo, Norway: Det Norske Veritas.

Ebeling, C. E. (1997). *Reliability and maintainability engineering*. McGraw-Hill, New York, USA.

EGIG. (2011). *8th report of the European Gas Pipeline Incident Data Group*. Doc. Number EGIG 11.R.0402 (Version 2).

Eickhoff, W., & Ulrich, R. (1981). Optical frequency domain reflectometry in single-mode fiber. *Applied Physics Letters, 39,* 693–695.

Eisler, B. (2011). Leak detection and challenges for Arctic subsea pipelines. *Offshore Technology Conference*, *OTC-22134*, Houston, Texas, USA.

Eisler, B., & Lanan, G. (2012). Fiber optic leak detection systems for subsea pipelines. *Offshore Technology Conference, OTC 23070*, Houston, Texas, USA.

Faber, M. H. (2007). *Risk and safety in civil engineering*. [Lecture Notes]. Swiss Federal Institute of Technology, Zurich.

Francis, A., Gardiner, M., & McCallum, M. (2002). Life extension of a high pressure transmission pipeline using structural reliability analysis. *Proceedings of the 4th International Pipeline Conference*, Calgary, Alberta, Canada, IPC 2002-27159, 800–818.

Geiger, I. G. (2008). *Principles of leak detection.* The Netherlands: KROHNE Oil & Gas.

Ge, C., Wang, G., & Ye, H. (2008). Analysis of the smallest detectable leakage flow rate of negative pressure wave-based leak detection systems for liquid pipelines. *Computers & Chemical Engineering*, *32*, 1669–1680.

Ghazali, M. F. (2012). *Leak detection using instantaneous frequency analysis* (PhD thesis, University of Sheffield, U.K).

Green, D. M., & Swets, J. A. (1998). *Signal detection theory and psychophysics.* Los Altos, California: Peninsula Publishing.

Haldar, A., & Mahadevan, S. (2000). *Probability, reliability and statistical methods in engineering design*. New York: John Wiley and Sons.

Hallen, J., Caleyo, F., & González, J. (2003). Probabilistic condition assessment of corroding pipelines in Mexico. *Pan-American conference for non-destructive testing (PANNDT)*, Rio de Janeiro, Brazil.

Hauge, E., Aamo, O., Godhavn, J. (2009). Model based pipeline monitoring with leak detection. *September 2009 SPE Projects, Facilities & Construction.*

Hines, W. W., Montgomery, W., Douglas, C., Goldsman, D. M., & Borror, C. M. (2003). *Probability and statistics in engineering* (4th ed.). Hoboken, New Jersey, USA: Wiley & Sons.

Höbel, M., Ricka, J., Wüthrich, J. M., & Binkert, T. (1995). High-resolution distributed temperature sensing with the multi photon-timing technique. *Applied Optics*, *34*, 2955–2967.

Horiguchi, T., Kurashima, T., & Koyamada, Y. (1992). Measurement of temperature and strain distribution by Brillouin frequency shift in silica optical fibers. *Proceedings SPIE Distributed and Multiplexed Fiber Optic Sensors II*. 1797. doi:10.1117/12.141280

Horiguchi, T., & Tateda, M. (1989). Optical-fiber-attenuation investigation using stimulated Brillouin scattering between a pulse and a continuous wave. *Optics Letters*, *14*(8), 408–410. doi:10.1364/OL.14.000408

Horrocks, P., Mansfield, D., Thomson, J., Parker, K., & Winter, P. (2010). *Aging plant study phase 1 report.* Prepared for ESR Technology Limited for HSE U.K. Retrieved from http://www.hse.gov.uk/research/rrpdf/rr823.pdf

HSE. (2009). Key Programme 3 – Asset integrity: A review of industry's progress. *Health & Safety Executive*, U.K.

HSE U.K. (2011). *Offshore safety statistics bulletin*. Retrieved from http://www.hse.gov.uk/offshore/statistics/stat1011.htm

HSE U.K. (2014). *Offshore safety statistics bulletin 2011/2012*. Retrieved from http://www.hse.gov.uk/offshore/statistics/stat1011.htm

ISO/TS 12747. (2011). *Petroleum and Natural Gas Industries – Pipeline Transportation Systems*. Recommended Practice for Pipeline Life Extension, Geneva, Switzerland.

Kay, S. M. (1993). *Fundamentals of statistical signal processing vol. I: Estimation theory*. Upper Saddle River, NJ, USA: Prentice Hall.

Kay, S. M. (1998). *Fundamentals of statistical signal processing vol. II: Detection theory*. Upper Saddle River, NJ, USA: Prentice Hall.

Khan, F. I., Haddara, M. R., & Bhattacharya, S. K. (2006). Risk based integrity and inspection modeling (RBIM) of process components/system. *Risk Analysis*, *26*(1), 203–221.

Khan, F. I., Sadiq, R., & Haddara, M. M. (2004). Risk-based inspection and maintenance (RBIM): Multi-attribute decision-making with aggregative risk analysis. *Process Safety and Environmental Protection, 82*(6), 398–411.

Kiefner J. F., & Vieth P. H. (1990). New method corrects criterion for evaluating corroded Pipe. *Oil and Gas Journal,* 88-32.

Kim, Y., Miyazaki, K., & Tsukamoto, H. (2008). Leak detection in pipe using transient flow and genetic algorithm. *Journal of Mechanical Science and Technology*, *22*, 1930–1936.

Kontovas, C. A, & Psaraftis, H. N. (2008). Marine environment risk assessment: A survey on the disutility cost of oil spills. *2nd International Symposium on Ship Operations, Management and Economics*, Athens, Greece, 275–287.

Kontovas, C., Psaraftis, H., & Ventikos, N. (2010). An empirical analysis of IOPCF oil spill cost data. *Marine Pollution Bulletin*, *60,* 1455–1466.

Lay-Ekuakille, A., Trotta, A., Vendramin, G., &Vanderbemdem, P. (2009). FFT-based algorithm improvements for detecting leakage in pipelines. *2009 – 6th International Multi-Conference on Systems, Signals and Devices,* 1–4. Doi: 10.1109/SSD.2009.4956691

Lay-Ekuakille, A., Vendramin, G., & Trotta, A. (2009). Spectral analysis of leak detection in a zigzag pipeline: A filter diagonalization method-based algorithm application. *Measurement, 42*, 358–367. Retrieved from www.elsevier.com/locate/measurement

Li, W., Bao, X., Li, Y., & Chen, L. (2008). Differential pulse-width pair BOTDA for high spatial resolution sensing. *Optics Express*, *16*(26), 21616–21625. doi: 10.1364/OE.16.021616

Lindley, D. V. (1982). Scoring rules and the inevitability of probability. *International Statistical Review*, *50*, 1–26.

Liu, X., & Wirtz, K. W. (2006). Total oil spill costs and compensations. *Maritime Policy and Management*, *33*(1), 460–469.

Liu, Z., Ferrier, G., Bao, X., Zeng, X., Yu, Q., & Kim, A. (2003). Brillouin scattering based distributed fiber optic temperature sensing for fire detection. *Fire and Safety Science – Proceedings of the 7th International Symposium on Fire Safety Conference*, Worcester, U.S.A, 221–232.

Mahar, S. B. (2008). *Spontaneous Brillouin scattering quench diagnostics for large superconducting magnets* (PhD thesis, Massachusetts Institute of Technology, USA).

Martins, J., & Seleghim, P. (2010). Assessment of the performance of acoustic and mass balance methods for leak detection in pipelines for transporting liquids. *ASME Journal of Fluids Engineering, 132*(1). doi:10.1115/1.4000736

Milton, S., & Arnold, J. (2003). *Introduction to probability and statistics: Principles and applications for engineering and the computing sciences* (4th ed.). USA: McGraw-Hill Higher Education.

Mpesha, W., Chaudhry, M. H., Kahn, I. B., & Gassman, S. L. (2002). Leak detection in pipes by frequency response method using a step excitation. *Journal of Hydraulic Research, 40*(1).

Muhammed, A., & Speck, J. (2002). Probabilistic remnant life assessment of corroding pipelines within a risk-based framework. Cambridge, U.K.: TWI.

Nikles, M. (2009). Long-distance fiber optic sensing solutions for pipeline leakage, intrusion and ground movement detection. *Proceedings of SPIE, 7316*. doi: 10.1117/12.818021

Nowak, A., & Collins, K. (2000). *Reliability of structures*. New York, NY, USA: McGraw-Hill.

Ogwude, D. (2003). Integrated instrumentation system strategy for deepwater asset management. *Offshore Technology Conference,* Houston, Texas, U.S.A., 5–8 May 2003.

OZ Optics. (2013). Fiber optic distributed strain and temperature sensors. (USA Patent #: 7499151 and 7599047). Retrieved from www.ozoptics.com

Parker, T., Farhadiroushan, M., Feced, R., Handerek, V., & Rogers, A. (1998). Simultaneous distributed measurement of strain and temperature from noise-initiated Brillouin scattering in optical fibers. *IEEE Journal of Quantum Electronics*, *34*(4) 645–659.

Park, J., Bolognini, G., Lee, D., Kim, P., Cho, P., Pasquale, F., & Park, N. (2006). Raman-based distributed temperature sensor with simplex coding and link optimization. *IEEE Photonics Technology Letters*, *18*(17), 1879–1881.

PHMSA. (2014). *Pipeline safety statistics report.* Retrieved from http://primis.phmsa.dot.gov/comm/Index.htm?nocache=3213.

Rangel-Ramírez, J. and Sørensen, J. (2012). Risk-based inspection planning optimization of offshore wind turbines. *Structure and Infrastructure Engineering, 8*(5)*,* 473–481.

Ravet, F. (2011). Distributed Brillouin sensors application to structural failure detection. Mukhopadhyay, S. C. (Ed.). *New Developments in Sensing Technology for SHM, LNEE, 96*, 93–136. Retrieved from Springerlink.com

Saudi Aramco in the spotlight. (2011). *Pipelines International*. Retrieved from http://pipelinesinternational.com/news/saudi_aramco_in_the_spotlight/055350

Singh, M., & Markeset, T. (2009). A methodology for risk-based inspection planning of oil and gas pipes based on fuzzy logic framework. *Engineering Failure Analysis, 16*(7), 2098–2113.

Shimizu, K., Horiguchi, T., Koyamada, Y., & Kurashima, T. (1993). Coherent self-heterodyne detection of spontaneously Brillouin-scattered light waves in a single-mode fiber. *Optics Letters*, *18*(3), 185–187. doi: 10.1364/OL.18.000185

Smith, J. R. (1999a). *Characterization of the Brillouin loss spectrum for simultaneous distributed sensing of strain and temperature* (MSc. thesis). Department of Physics, University of New Brunswick, NB, Canada.

Smith, J., Brown, A., DeMarchant, M., & Bao, X. (1999b). Simultaneous distributed and temperature measurement. *Applied Optics, 38*(25), 5382–5388. doi: 10.1364/AO.38.005372

Song, K. Y., Zou, W., He, Z., & Hotate, K. (2008). All-optical dynamic grating generation based on Brillouin scattering in polarization-maintaining fiber. *Optics Letters*, *33*(9), 926–928.

Soto, M. A., Bolognini, G., & Pasquale, F. D. (2011). Long-range simplex-coded BOTDA sensor over 120km distance employing optical pre-amplification. *Optics Letters*, *36*(2), 232–234.

Straub, D., & Faber, M. (2005). Risk based inspection planning for structural systems. *Structural Safety, 27*, 335–355.

Tang, W. H. (1973). Probabilistic updating of flaw information. *Journal of Test Evaluation, 1*(6), 459–467.

Thodi, P., Khan, F., & Haddara, M. (2009). The selection of corrosion prior distributions for risk based integrity modeling. *Stochastic Environmental Research Risk Assessment*, *23*(6), 793–809.

Thodi, P., Khan F., & Haddara, M. (2013). Risk based integrity modeling of offshore process components suffering stochastic degradation. *Journal of Quality in Maintenance Engineering*, *19*(2), 157–180.

Ulrich, H. F., & Lehrmann, E. P. (2008). *Telecommunications Research Trends.* New York, NY, USA: Nova Science Publishers Inc.

U.S. Department of Transportation – Pipeline & Hazardous Materials Safety Administration (PHMSA). (2014). Retrieved from http://primis.phmsa.dot.gov/comm/Index.htm?nocache=3213

Wait, P. C., & Newson, T. P. (1996). Landau placzek ratio applied to distributed fiber sensing. *Optics Communications*, *122*(4–6), 141–146.

Walk, T., & Frings, J. (2010). Fiber optic sensing can help reduce third-party threats. *Oil & Gas Journal*. Retrieved from http://www.ilf.com/fileadmin/user_upload/publikationen/OGJ_Sept-06-10_Walk_Frings

Wang, J., Simpson, A. R., & Lambert, M. F. (2006). An analytical solution for the transients in a pipeline with a variable boundary condition: Leak detection in pipe networks using coded transients. *8th Annual Water Distribution Systems Analysis Symposium,* Cincinnati, Ohio, USA, August 27–30, 2006.

Wan, J., Yu, Y., Wu Y., Feng, R., & Yu, N. (2012). Hierarchical leak detection and localization method in natural gas pipeline monitoring sensor networks. *Sensors 2012, 12,* 189–214. doi: 10.3390/S120100189.

Wernli, R. (2000). *AUV Commercialization – Who's leading the pack?* San Diego, CA, USA: SPAWAR Systems Center. Retrieved from http://citeseerx.ist.psu.edu/viewdoc/download?doi=10.1.1.32.7577&rep=rep1&type=pdf

Wickens, T. D. (2002). *Elementary signal detection theory*. New York, NY, USA: Oxford University Press.

Xiang, X., Fang, Z., & Lu, C. (2011). Experimental study on detection and location of pipeline leakage based on acoustic emission technique. *ICPTT*, 645–652. doi: 10.1061/41202(423)70

Xiaoyi, B., & Liang, C. (2012). Recent progress in distributed fiber optic sensors. *Sensors 2012*, *12*, 8601–8639. doi:10.3390/s120708601

Xu, D., Liu, J., Yang, J., Liu, G., Wang, J., Jenkinson, I., & Ren, J. (2007). Inference and learning methodology of belief-rule-based expert system for pipeline leak detection. *Expert Systems with Applications, 32*(1), 103–113. doi:10.1016/j.eswa.2005.11.015

Zhaoyang, T., Jianfeng, L., Zongzhi, W., Jianhu, Z., & Weifeng, H. (2011). An evaluation of maintenance strategy using risk based inspection. *Safety Science, 49*(6), 852–860.